THALAMOSTRIATAL NEURONS AND PARKINSONISM

By

Sheila Vijay Kusnoor

Dissertation

Submitted to the Faculty of the

Graduate School of Vanderbilt University

in partial fulfillment of the requirements

for the degree of

DOCTOR OF PHILOSOPHY

in

Neuroscience

May, 2010

Nashville, Tennessee

Approved:

Professor Ariel Y. Deutch

Professor Roger J. Colbran

Professor Maureen A. Gannon

Professor Danny G. Winder

To my parents,

Drs. Vijay and Rita Kusnoor

ACKNOWLEDGEMENTS

TABLE OF CONTENTS

LIST OF TABLES

LIST OF FIGURES

LIST OF ABBREVIATIONS

6-OHDA	6-hydroxydopamine
BDA	Biotinylated dextran amine
Cbln1	Cerebellin1
CeM	Central medial thalamic nucleus
CL	Central lateral thalamic nucleus
CM	Centromedian thalamic nucleus
CTB	Cholera toxin B
D_1	Dopamine D_1 receptor
D_5	Dopamine D_5 receptor
DAB	3,3$'$-diaminobenzidine
DAT	Dopamine transporter
DBH	Dopamine β-hydroxylase
DBS	Deep brain stimulation
FG	FluoroGold
FJC	Fluoro Jade-C
GABA	γ-aminobutyric acid
Glu	Glutamate
GP	Globus pallidus
GPCR	G-protein coupled receptor
HPLC-EC	High pressure liquid chromatography-electrochemical detection
LY	Lucifer yellow

MD	Mediodorsal thalamic nucleus
MFB	Median forebrain bundle
MPTP	1-methyl-4-phenyl-1,2,3,6-tetrahydropyridine
MSN	Medium spiny neuron
NHS	Normal horse serum
PB	Phosphate buffer
PC	Paracentral thalamic nucleus
PD	Parkinson's disease
PF	Parafascicular nucleus
PVT	Paraventricular thalamic nucleus
PSD	Postsynaptic density
RT-PCR	Real-time polymerase chain reaction
SN	Substantia nigra
STN	Subthalamic nucleus
TAN	Tonically active neuron
TBS	Tris-buffered saline
TH	Tyrosine hydroxylase
VA	Ventral anterior thalamic nucleus
VGluT1	Vesicular glutamate transporter 1
VGluT2	Vesicular glutamate transporter 2
VL	Ventrolateral thalamic nucleus
VTA	Ventral tegmental area

CHAPTER I

THE STRIATUM

The corpus striatum was first described by the physician Thomas Willis in 1664 in his monumental work *Cerebri Anatome.* Willis hypothesized that "animal spirits" in the striatum moved throughout the brain and flowed through the medulla oblongata, spinal cord, peripheral nerves, and muscle to ultimately cause muscle contraction (see Sarikcioglu et al., 2008). Today, the striatum is still thought to have a role in the control of motor movement, although not in the way Willis imagined. Striatal projection neurons are now known to release the inhibitory neurotransmitter γ-aminobutyric acid (GABA) instead of releasing animal spirits. Through its projections to the globus pallidus (GP) and substantia nigra (SN), and thence the thalamus and cortex, the striatum induces purposeful movements while suppressing other movements (Kawaguchi 1997).

Organization of the striatum

The term "striatum" means striated in Latin, and refers to the striped appearance of the structure. These "stripes" are aggregates of myelinated axons of cortical cells that traverse the gray matter of the striatum. In higher order vertebrates, including primates, the internal capsule divides the striatum into the "caudate nucleus," and "putamen" (Tepper et al., 2007). However, in rodents the striatum is one nucleus. The striatum is one of four structures, along with the GP, SN, and subthalamic nucleus (STN), which are commonly designated as the basal ganglia (Tepper et al., 2007).

The striatum can be divided into dorsal and ventral sectors. The ventral striatum is comprised of the nucleus accumbens and olfactory tubercle, and receives dopaminergic projections that originate primarily from the ventral tegmental area (VTA; Voorn et al., 2004). By contrast, the SN is the main source of the dopaminergic innervation of the dorsal striatum (caudatoputamen).

<center>Striatal Neurons</center>

The striatum is composed of different types of neurons, including both interneurons and medium spiny neurons (MSNs), which are the projection neurons of the striatum. The main function of striatal interneurons is to modulate the activity of MSNs. Several types of interneurons, including cholinergic and GABAergic interneurons, are found in the striatum and can be distinguished by their anatomical and electrophysiological properties.

Cholinergic interneurons

Cholinergic interneurons have large cell bodies, often greater than 40 μm in diameter, and smooth or sparsely spiny dendrites (Wilson et al., 1990). Because they fire tonically (but irregularly) at 2-10 Hz in response to excitatory synaptic inputs, they have been referred to as tonically active interneurons (TANs; Wilson et al., 1990; Bennett and Wilson 1999).

Cholinergic interneurons receive dopaminergic inputs from the substantia nigra, glutamatergic projections from the thalamus, and GABAergic inputs from medium spiny neurons (Lapper and Bolam 1992; Reynolds and Wickens 2004). They express

<center>2</center>

dopamine D_2 and D_5 receptors and are activated by signaling through D_5 receptors and inhibited through the activation of D_2 receptors (Bergson et al., 1995; Rivera et al., 2002; Berlanga et al., 2005; Bertolli and Consolo 1990; Hersi et al., 2000). Cholinergic neurons can also be excited directly by glutamatergic axons of thalamostriatal neurons, and inhibited disynaptically through thalamic activation of MSNs that send GABAergic axonal collaterals which synapse with cholinergic neurons (Zackheim and Abercrombie 2005).

Signaling through cholinergic interneurons is thought to alter the firing patterns of medium spiny neurons. Thus, release of acetylcholine stabilizes the activity of projection neurons at either a depolarized or hyperpolarized state by acting through muscarinic receptors (Wang et al., 2006).

GABAergic interneurons

There are three subpopulations of GABAergic interneurons, which can be distinguished based on their anatomical structure, co-localization with other proteins, and electrophysiological properties. Parvalbumin interneurons have a cell soma 16-18 μm in diameter, aspiny dendrites, and axons which collaterize extensively near their dendritic fields. They are often referred to as fast-spiking interneurons because they fire phasically and at high frequency after cortical stimulation (Kawaguchi 1993). Parvalbumin interneurons are innervated by cholinergic interneurons as well as MSNs, and by corticostriatal glutamatergic neurons, thalamostriatal glutamatergic neurons, and pallidal parvalbumin-containing neurons (see Tepper and Bolam 2004). These neurons also

express D_5 receptors and are directly excited by dopamine (Bracci et al., 2002; Centonze et al., 2003).

A second population of GABAergic interneurons contain neuropeptide Y, somatostatin, nitric oxide synthase, and NADPH diaphorase. These cells have the least dense axonal arborization of the striatal interneurons (Tepper and Bolam 2004). Their resting membrane potentials are close to spike threshold, and have been referred to as persistent and low-threshold spike (PLTS) neurons, based on their characteristic firing pattern (Tepper and Bolam 2004). They receive inputs from cholinergic interneurons and from the three major striatal afferents: cortical and thalamic glutamatergic and nigral dopaminergic neurons (Kawaguchi et al., 1995; Sidibé and Smith 1999; Tepper and Bolam 2004). Like cholinergic neurons, these neurons also express dopamine D_5 receptors, which was shown using immunohistochemistry (Centonze et al., 2003).

Calretinin-immunoreactive cells are a third class of GABAergic interneurons (Kawaguchi et al., 1995). They are medium-sized, and in rats are primarily found in the rostral aspects of the medial striatum (Bennett and Bolam 1993). Their connectivity and electrophysiological properties are still unknown (Kawaguchi et al., 1995).

Medium spiny neurons

The medium spiny neuron (MSN) is the most common neuronal type and accounts for approximately 90-95% of striatal neurons (Kemp 1968; see Gerfen 1992). The name MSN was coined by Janet Kemp in 1968, based on her studies of the striatum in the cat. Kemp was interested in determining where the axonal terminations of striatal afferents occur. Contemporary scientists had shown that deafferentation results in

diminished Golgi staining of the target neuron (Kemp 1968). Thus, she realized that she would first need to characterize the normal morphology of these neurons in order to be able to determine where the afferent terminations occur.

Kemp observed that MSNs have a medium-sized cell body, ranging approximately from 9-18 μm in diameter. She and her colleague T.P.S. Powell observed that these dendrites extend radially for greater than 250 μm, branch extensively, and are densely studded with dendritic spines (Fig. 1; Kemp, 1968; Kemp and Powell, 1971). In addition, Kemp and Powell (1971) found that spine density varies in a consistent fashion as a function of distance from the cell soma. Proximal dendrites (at a distance less than 20 μm from the cell soma) tend to be spine free. Spine density then increases and peaks at a distance 60-80 μm from the cell soma, and then begins to decline along distal dendrites (Kemp and Powell, 1971).

Glutamatergic cortical and thalamic axons are the major source of excitatory synaptic input onto MSN dendrites. Normally, MSNs are hyperpolarized, with their membrane potential near -85 mV (the "down-state"). However, in response to strong cortical and/or thalamic stimulation, they can enter the "up-state," in which their membrane potential approaches spike threshold (~ −60 mV; Wilson 1993; Surmeier et al., 2007). Striatal GABAergic interneurons can also inhibit the firing of MSNs (Tepper and Bolam 2004). The activity of MSNs is also modulated by synaptic contacts made with the axon collaterals of neighboring MSNs (Tunstall et al., 2002).
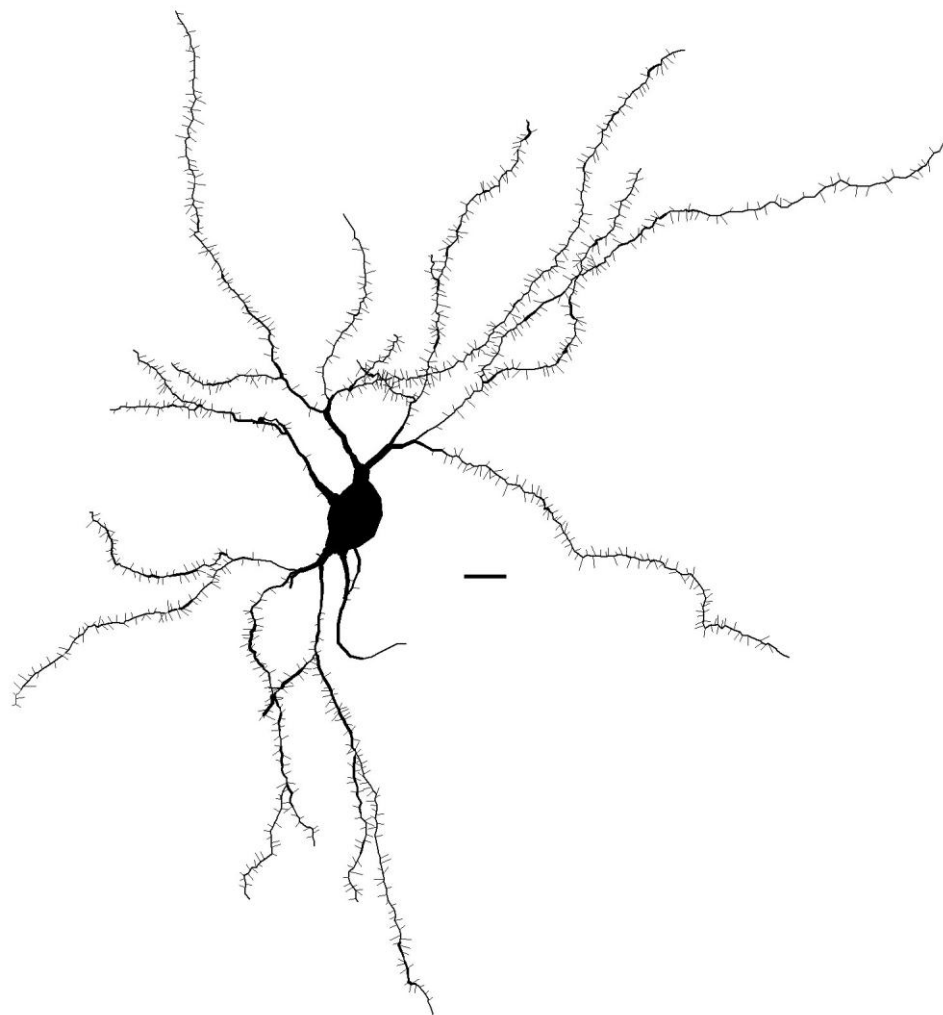
Figure 1. A Neurolucida-aided reconstruction of a Golgi-impregnated striatal medium spiny neuron. Scale bar, 10 µm.

<u>Populations of medium spiny neurons</u>

Medium spiny neurons are not a homogeneous group of cells. Although all medium spiny neurons are GABAergic, several different subtypes can be distinguished based on morphology, projection target, neurotransmitters, or receptors.

Morphology

Chang and colleagues (1982) grouped MSNs into five populations based on morphological features. Type I MSNs, which are the most common, have spine-free cell somata and proximal dendrites, but densely spiny distal dendrites. Type II MSNs have somatic spines, but fewer dendritic spines than the Type I MSNs. Type III, IV, and V MSNs have aspiny somata and dendrites that are sparsely spiny and can be distinguished based on their branching pattern: type III MSNs have poorly branched dendrites, type IV have profusely branched dendrites, and type V have varicose dendrites.

Projection targets

With the aid of neuroanatomical tract tracers, MSNs have been classified into two groups based on their axonal projection targets. Some MSNs project densely to the substantia nigra (SN), whereas others project heavily to the globus pallidus (GP), where they synapse with pallidal cells that project to the SN. The latter projection pattern has been called the "indirect" pathway, with the MSN projections that route to the SN but avoid the GP forming the "direct" pathway (Grofova 1975; Somogyi and Smith 1979; Preston et al., 1980; Wilson and Groves 1980; Chang et al., 1981).

More recent data suggest that the distinction between MSNs based on their projection target is an oversimplification. Early studies identified two populations of MSNs by injecting retrograde tracers into the SN and GP (Grofova 1975; Somogyi and Smith 1979). However, in areas with a small axonal plexus, so little tracer may have accumulated that the cell cannot be identified as retrogradely-labeled. Using juxtacellular iontophoretic deposits of biotin dextran amine to label single MSNs in their entirety, Parent and colleagues found that MSN axons collateralize extensively and typically innervate more than one structure, but with major differences in the size of the terminal axonal arbor (Wu et al., 2000; Lévesque and Parent, 2005). For example, they showed that some MSNs innervate both the GP (indirect pathway) and SN (direct pathway), with a profuse terminal arbor in one of the two sites but a very restricted axonal plexus in the other target. In the rat, they found that there are three groups of MSNs: 1) MSNs that innervate the GP, 2) MSNs that project to the GP and SN, and 3) MSNs that innervate the GP, SN, and entopeduncular nucleus (Wu et al., 2000). They calculated that approximately 36.4% of MSN axons project exclusively to the GP, where they arborize extensively, 26% collateralize en passant in the GP before reaching the SN, and 37.6 % emit a few collaterals in both the GP and the entopeduncular nucleus before arborizing extensively in the SN (Wu et al., 2000).

Neurotransmitters and Receptors

Medium spiny neurons can also be distinguished by their expression of certain peptide co-transmitters and by the type of dopamine receptor they express. Striatopallidal neurons contain enkephalin and express dopamine D_2 receptors, and

striatonigral neurons contain substance P and dynorphin in addition to GABA and express the D_1 receptor (Hong et al., 1977; Finley et al., 1981; Gerfen and Young 1988; Gerfen et al., 1990).

The exact degree to which dopamine receptor expression is segregated in direct and indirect pathway neurons is somewhat unclear. Meador-Woodruff et al., (1991) studied the distribution of D_1 and D_2 transcripts in MSNs in the rat striatum using *in situ* hybridization histochemistry with ^{35}S-labeled cRNA probes. They found that most MSNs contained either the D_1 or the D_2 receptor transcript, but that about a third expressed both receptors. Le Moine and Bloch (1995) used a similar approach but found that D_1 mRNA was mainly localized to substance P-containing MSNs, while the D_2 receptor was present in enkephalin-containing MSNs, with only a very small minority (~5%) of MSNs expressing both D_1 and D_2 receptors.

Surmeier and colleagues (1996) studied the distribution of dopamine receptors in dissociated striatal neurons prepared from adult rats using single cell real-time polymerase chain reaction (RT-PCR). They reported that nearly 50% of MSNs expressed both D_1 and D_2 mRNAs and additionally found that nearly half of neurons containing both substance P and D_1 mRNA co-expressed D_3 or D_4 mRNA. However, subsequent RT-PCR experiments by the same group found that in BAC transgenic mice, in which D_1- or D_2- containing neurons are fluorescently-labeled, expression of D_1 and D_2 receptors is largely restricted to separate populations of MSNs (Day et al., 2006).

A consensus opinion is that a minority of MSNs express both D_1 and D_2 receptors, with most MSNs having either D_1 or D_2 receptors. By contrast, the levels of D_3 and D_4 receptors are much lower in abundance, but are generally higher in MSNs

containing D_1 rather than D_2 receptors (Surmeier et al., 1996). Striatal MSNs do not express D_5 receptors.

Despite the fact that individual MSNs mainly project to more than one downstream target and thus don't follow the direct and indirect pathway dichotomy, functional studies suggest that there are indeed two populations of MSNs: one group expressing enkephalin and D_2 receptors that terminate in the globus pallidus, and the other expressing substance P and D_1 receptors that terminates in the SN. Selective dopamine receptor drugs independently regulate one of the two distinct MSN populations (as seen by co-transmitter gene induction), consistent with two functional sets of MSNs that correspond to the direct and indirect pathways (see Gerfen 2000; Table 1).

Synaptic targets of MSN afferents

The primary extrinsic afferents to MSNs in the dorsal striatum arise from the cortex, thalamus, and SN. In the 1970's, scientists began to ask which subcellular structures these afferents targeted. In 1971, Kemp and Powell lesioned the cortex, thalamus, or SN, and then used electron microscopy to determine where on striatal cells degenerating axonal profiles were found. They found that most synaptic contacts occurred at dendritic spines; however, occasionally dendritic shafts were contacted. The termination of cortical inputs onto dendritic spine heads is now well-established (Dubé et al., 1988; Raju et al., 2006; Fig. 2), and quantitative ultrastructural studies have found that dopamine terminals typically synapse with the neck of dendritic spines (Bouyer et al., 1984; Freund et al., 1984). In contrast to the selective targeting of spines by cortical axons, thalamostriatal neurons synapse on both MSN dendritic spines and shafts (Smith

Table 1. Summary of key differences between MSNs of the direct and indirect pathways in the rodent.

	Direct Pathway	**Indirect Pathway**
Major projection target	Substantia Nigra	Globus Pallidus
Neuropeptide co-transmitter	Substance P, Dynorphin	Enkephalin
Dopamine receptor	D_1	D_2
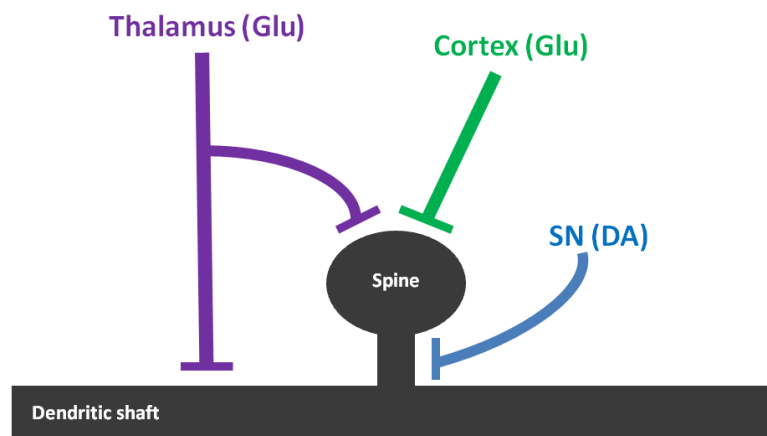
Figure 2. Schematic depiction of a medium spiny neuron dendritic segment and its synaptic contacts with substantia nigra (SN), cortical, and thalamic axons. Dopaminergic (DA) axons from the SN preferentially terminate on spine necks. Glutamatergic (Glu) cortical axons synapse onto dendritic spine heads. Thalamic axons synapse onto both the dendritic shafts and spine heads of MSNs.

et al., 2004; Raju et al., 2006; Lacey et al., 2007; see Chapter 2). Based on the arrangement of synaptic inputs onto MSNs, it has been suggested that dopamine modulates excitatory drive onto dendritic spines incurred from glutamatergic axospinous signaling (Freund et al. 1984).

<p style="text-align:center;"><u>Dystrophic changes in MSN dendrites in Parkinson's disease</u></p>

Parkinson's disease (PD) is a neurological disorder involving the degeneration of nigrostriatal dopamine neurons (Fahn 2003). Clinical hallmarks of the disease include tremor, bradykinesia, and rigidity (Fahn 2003). In contrast to Huntington's disease, no loss of striatal neurons occurs in PD. However, MSNs show dystrophic changes, including a reduction in spine density and dendritic length (McNeill et al., 1988; Stephens et al., 2005; Zaja-Milatovic et al., 2005).

The primary treatment strategy for PD is dopamine replacement therapy, with the gold standard being treatment with the dopamine precursor levodopa. Levodopa typically works well in treating motor symptoms early in the course of PD (Schapira et al. 2009). However, as the disease progresses, the response to levodopa becomes shorter and more unpredictable (the "on-off" effect), and within a variable period of time (years), most patients develop abnormal involuntary movements (see Jancovic 2005; Schapira et al. 2009). Late in the course of the illness there appears to be a gradual reduction in the responsiveness to levodopa (Marsden and Parkes 1977; Rinne 1981; Clissold et al., 2006). Loss of dendritic spines, which are the sites where dopamine receptors are expressed, has been hypothesized to be the structural basis for the reduction in levodopa responsiveness (Deutch, 2006; Deutch et al., 2007).

Mechanisms underlying dendritic spine loss

Loss of striatal dopamine instigates spine loss

Over the past twenty years, the mechanisms underlying the loss of dendritic spines in Parkinson's disease have been slowly unraveled. The proximate cause of MSN spine loss in PD is the loss of striatal dopamine. Ingham and colleagues (1989) found that 6-OHDA-induced lesions of SN dopamine neurons in rats cause a reduction in MSN dendritic spine density. These changes in spine density are progressive: a loss in spine density occurs as early as 12 days and persists until at least 13.5 months after the lesion (Ingham et al., 1993). A loss in dendritic spine density is seen in multiple models of parkinsonism, including reserpine-treated mice and 1-methyl-4-phenyl-1,2,3,6-tetrahydropyridine (MPTP)-treated primates (Day et al., 2006; Villalba et al., 2009). In addition, MSN dendritic spine loss has been observed in organotypic slice cultures of the cortex, striatum, and ventral midbrain that are treated with the dopaminergic toxin 1-methyl-4-phenylpyridinium MPP^+ or in which the ventral midbrain has been ablated (Neely et al., 2007). By contrast, animals treated chronically with psychostimulants, which increase striatal dopamine levels, show an increase in MSN spine density (Li et al., 2003; Meyer et al., 2008). Thus, through numerous studies manipulating striatal dopamine levels, the role of dopamine in regulating dendritic morphology has become well-established.

Subpopulation specific changes in spine density

Rodent studies have suggested that nigrostriatal dopamine depletion preferentially affects those MSNs that project to the GP. For example, MSNs of rats treated chronically with the D_2 receptor antagonist haloperidol suffer a loss of dendritic spines (Kelley et al., 1997). Day and colleagues (2006) found that in rodents in which striatal dopamine stores were depleted, MSNs that expressed D_2 but not D_1 receptors suffered dendritic spine loss at 4 weeks after the dopamine lesion. In contrast, a more recent primate study reported that MPTP treatment results in spine loss in both direct and indirect MSNs at 6-18 months after the last MPTP treatment (Villalba et al., 2009). These data suggest that nigrostriatal dopamine depletion may initially affect MSNs of the indirect pathway, but over time involve the direct pathway. This hypothesis remains to be tested.

Glutamatergic regulation of MSN dendrites

In PD and animal models of parkinsonism, the density of perforated synapses, which are thought to represent synapses with enhanced glutamatergic activity, is increased in the striatum (Anglade et al., 1996; Meshul et al., 1999). Medium spiny neurons of dopamine-depleted rodents are also hyperexcitable, which may be the result of enhanced glutamatergic signaling at corticostriatal synapses (Florio et al. 1993; Cepeda et al., 2001; Day et al., 2006). Normally, dopamine inhibits glutamate release by acting at D_2 receptors on corticostriatal axon terminals. However, in the dopamine-depleted striatum, this source of tonic inhibition is removed, which results in enhanced glutamatergic signaling at corticostriatal synapses (Bamford et al., 2004).

Recent studies have shown that reducing cortico-striatal excitatory drive onto MSNs prevents striatal dopamine depletion-induced changes in spine density. Using organotypic slice co-cultures of the cortex, striatum, and ventral mesencephalon (including the dopamine neurons of the SN), Neely and colleagues (2007) reported that cortical deafferentation prevents spine loss from occurring in dopamine-depleted cultures. Treatment with a metabotropic mGluR2/3 agonist, which blocks glutamatergic transmission by acting at release modulating autoreceptors on corticostriatal glutamate terminals (Testa et al., 1998), similarly abolishes spine loss (Garcia et al., 2010). Garcia and colleagues (2010) further showed that decortication reverses dopamine denervation-induced dendritic spine loss *in vivo*.

Just as deafferentation of cortical glutamate inputs protects MSN dendrites against dopamine-denervation-induced spine loss, could the removal of thalamostriatal neurons similarly protect MSN dendrites? This topic is of particular relevance because thalamostriatal neurons degenerate in Parkinson's disease (Henderson et al., 2000). The next chapter will provide an overview of the thalamostriatal projection and a description of the pathological changes that occur in these neurons in Parkinson's disease.

CHAPTER II

ALTERATIONS IN THALAMOSTRIATAL NEURONS IN PARKINSONISM

Discovery of the thalamus

Interest in the structure and function of the thalamus dates back to writings by the

Greek physician Galen in the second century AD (see Jones 2007b). Galen thought the

thalamus was the reservoir of a spirit which travelled through the optic nerve to

subsequently enter the eye. He therefore gave it the name "thalamos," which means

structure room or storeroom. Because of the lack of illustrations, it is unclear if Galen's

thalamos refers to the structure we call the thalamus today or the lateral ventricle. The

term "thalamus" later appeared in works by anatomists in the seventeenth century, most

notably by the English physician Thomas Willis, and was used to describe the large

structure of the diencephalon, that today bears the same name (see Jones 2007b). It was

not until the late 1800s that individual thalamic nuclei were identified and named, largely

through the contributions of the German professor Franz Nissl (1889), using the cell

staining method he discovered.

The thalamostriatal projection

While Nissl was distinguishing the boundaries of thalamic nuclear groups,

scientists began using the technique of lesion-induced retrograde degeneration to identify

the projection targets of brain regions (see Jones 2007a). As suggested by the name, the

technique relies on the principle that damage to the terminal fields of an axon results in

the retrograde degeneration of the neuron. However, this technique has certain

limitations (Jones 1999, 2007a). First, neurons in some brain structures do not undergo retrograde degeneration. Second, damage to some axons can cause degeneration of the parent neuron (primary degeneration) as well as degeneration of the neuron that innervates the primary neuron (secondary degeneration).

Because of the lack of alternative methods available at the time, Powell and Cowan applied this technique to study the targets of thalamic neurons in the 1950's. They discovered that when they lesioned the striatum of rats, several thalamic nuclei, most notably the intralaminar thalamic nuclei, degenerated (Powell and Cowan 1954; Cowan and Powell 1956). The thalamostriatal projection has since been confirmed using both anterograde and retrograde neuroanatomical tract tracers (Berendse and Groenewegen 1990; Elena Erro et al., 2002; Smith et al., 2004).

The name "intralaminar" is derived from the location of the nuclei relative to the internal medullary lamina (see Jones 2007b). The nuclei have been further subdivided into rostral and caudal groups. The rostral group includes the central medial (CeM), paracentral (PC), and central lateral (CL) nuclei, which are bordered by the internal medullary lamina (Fig. 3; Smith et al., 2004). The caudal group consists of the parafasicular (PF) nucleus, which is located at the posterior end of the internal medullary lamina, and the centromedian (CM) nucleus, which extends laterally from the PF (Smith et al., 2004; Jones 2007b). Rodents lack a clearly defined CM. The medial PF is thought to correspond to the primate CM, with the lateral PF more closely resembling the primate PF based on connectivity (Fig. 3; Smith et al., 2004).

Figure 3. Expression of the neuronal marker NeuN in the rostral and caudal intralaminar thalamic nuclei. Immunohistochemistry was used to evaluate NeuN expression in coronal sections through the thalamus of a rat brain. The boundaries of the intralaminar nuclear groups are outlined in white. *A)* The rostral intralaminar nuclear group is composed of the central medial, paracentral, and central lateral nulcei. *B)* The parafascicular nucleus comprises the caudal intralaminar nuclear group. Abbreviations: CeM, central medial nucleus; CL, central lateral nucleus; fr, fasciculus retroflexus; PC, paracentral nucleus; PF, parafascicular thalamic nucleus. Scale bars: 400 μm.

The thalamostriatal projection is topographically organized. In primates, the CM preferentially innervates the caudate, and the PF innervates the putamen (Sadikot et al., 1992). In rodents, the lateral PF targets the lateral striatum, and the medial PF projects to the medial striatum (Smith et al., 2004; Berendse and Groenewegen, 1990). The projection from the anterior intralaminar thalamic nuclei is similarly organized, with the CeM targeting the medial striatum and the PC and CL targeting the central striatum (Smith et al., 2004).

Within the striatum, CM-PF axons synapse with both striatal medium spiny neurons (MSNs) and interneurons (Dubé et al., 1988; Berendse and Groenewegen, 1990; Lapper and Bolam, 1992; Smith et al., 2004). In rats, PF axons typically innervate both striatopallidal and striatonigral MSNs (Dubé et al., 1988; Castle et al., 2005). However, in primates, CM-PF neurons appear to synapse mainly with striatonigral MSNs (Sidibé and Smith 1996; Sidibé and Smith 1999).

The striatum also receives some inputs from the midline nuclei, including the paraventricular (PVT), parataenial, interanteromedial, intermediodorsal, rhomboid, and reuniens nuclei (Smith et al., 2004). The midline nuclei primarily target the ventral striatum, but also project to the medial aspect of the dorsal striatum (Berendse and Groenewegen 1990; Smith et al., 2004). Small numbers of neurons in the ventral, lateral, and posterior thalamic groups also innervate the striatum (Elena Erro et al., 2002; Smith et al., 2004).

Dendritic targets of thalamostriatal neurons on MSNs

In 1977, Chung and colleagues discovered that small lesions confined to the posterior intralaminar nuclei resulted in degenerating axon profiles that primarily contacted the dendritic shafts of MSNs. This observation was confirmed by Dubé and colleagues (1988), whose ultrastructural studies of anterogradely-labeled PF axons revealed that these axons formed asymmetric synapses with dendritic shafts. Thus, axons of the PF nucleus were initially thought to contact exclusively the dendritic shafts of MSNs.

Nearly twenty years later, Raju and colleagues (2006) re-evaluated the dendritic targets of thalamostriatal inputs in rodents, using the vesicular glutamate transporter VGluT2 as a marker of thalamic axons. Their data indicated that most thalamic axons targeted dendritic spines. Using anterograde tract tracers, they suggested that PF thalamostriatal axons nearly exclusively targeted dendritic shafts, but that other thalamostriatal axons primarily formed axospinous synapses.

Recent data indicate that PF axons target both dendritic spines and shafts. Lacey and colleagues (2007) labeled single PF neurons of the rat, and observed that the axons of some PF cells exclusively target dendritic shafts or spines, while others target both spines and shafts (Sadikot et al., 1992; Lacey et al., 2007). There is a similar heterogeneity in the synaptic contacts of CM-PF neurons in the primate: most axon terminals of CM-PF neurons contact dendritic shafts, but approximately 10-30% contact dendritic spines (Sadikot et al., 1992; Smith et al., 1994).

Collateralization of thalamostriatal neurons to innervate the cortex

In addition to projecting to the striatum, the anterior and caudal intralaminar nuclei also innervate the cortex (Berendse and Groenewegen 1991). These projections were initially thought to be "diffuse" and "non-specific," but it is now evident that like the thalamostriatal projection, the intralaminar thalamocortical projections are also topographically organized and target discrete cortical areas (Berendse and Groenewegen 1991).

In rodents, this projection arises primarily from axon collaterals of thalamostriatal neurons. Deschênes and colleagues (1995) observed that CL axons emit long, varicose axon collaterals that arborize sparsely in the striatum, but form dense patches of terminals in the cortex. By contrast, PF axons form dense clusters of terminations within the striatum but sparsely collateralize in the cortex (Deschênes et al., 1995, 1996). A study by Parent and Parent (2005) showed that some CM-PF neurons of the primate exclusively target either the striatum or the cortex, while others targeted both structures.

Parafascicular afferents

The most exhaustive study of the rodent thalamostriatal inputs was by Cornwall and Phillipson (1988), who used retrograde transport of wheat germ agglutinin to determine PF afferents. After tracer deposits into the PF, they observed retrogradely-labeled cells in the cortex, thalamic reticular nucleus, zona incerta, striatum, entopeduncular nucleus, mesencephalic reticular formation, and pretectum. They also observed cells in the laterodorsal tegmental nucleus, pedunculopontine nucleus, dorsal and ventral parabrachial nuclei, and in the vestibular nuclei and cerebellar lateral cervical,

medial and interpositus nuclei. Based on these findings, they proposed that the PF helps regulate motor movement by connecting the reticular activating system with the motor system.

<u>Thalamic pathology in Parkinson's disease</u>

Lewy bodies and Lewy neurites

The appearance of Lewy bodies in the SN is considered the pathological hallmark of Parkinson's disease (Rub et al., 2002). These inclusion bodies consist primarily of α-synuclein and are concentrated in the surviving dopamine neurons of the SN. In addition, Lewy neurites (α-synuclein-positive processes) have been observed across a large number of extra-nigral brain structures, including the thalamus (Rub et al., 2002).

Based on an exhaustive study in which α-synuclein deposits were evaluated in over 100 autopsy cases, Braak and colleagues (2002, 2003) hypothesized that the PD-related pathology develops in a characteristic, six-stage pattern. In stages 1 and 2, the pathology is restricted to the olfactory bulb and the dorsal motor nucleus of the vagal nerve. Surprisingly, the SN is not involved until stage 3 (Braak et al., 2003). Motor symptoms appear in stage 4, at which point the pathology in the SN worsens and the thalamus also becomes affected (Braak et al., 2002; Braak et al., 2003). In stage 5, the inclusion pathology appears in the temporal mesocortex. Finally, by stage 6 the pathology extends to involve almost the entire neocortex (Braak et al., 2003).

The density of Lewy neurites in the thalamus of PD subjects is variable, but the PF and anterior intralaminar nuclei are among the most severely affected (Rub et al.

2002). A high density of Lewy neurites has also been observed in other thalamic sites, including the limitans-suprageniculate complex, PVT, and reunions nucleus (Rub et al., 2002). Lewy neurites are much less prevalent in the CM, and are nearly absent in the mediodorsal nucleus (Henderson et al., 2000; Rub et al., 2002). The severity of the Lewy neurite pathology in the thalamus does not correlate with gender, the age at death, or the Hoehn and Yahr stage of PD (Rub et al., 2002), and the functional significance of Lewy neurites is unclear.

Thalamic degeneration

It is evident that the presence of Lewy neurites does not correspond with neuronal loss. Recent data indicate a loss of cells in certain thalamic nuclei in PD (Henderson et al., 2000). Approximately 30-40% of neurons in the CM-PF nuclei degenerate in Parkinson's disease (Henderson et al., 2000). The neurons of the motor thalamus, which includes the ventral anterior (VA), ventrolateral (VL), and ventrolateral posterior nuclei, do not degenerate (Halliday et al., 2005).

It is unclear if thalamic degeneration in PD occurs before or after the degeneration of SN dopamine neurons. The loss of CM-PF neurons does not correlate with the age of onset, duration, or severity of PD (Henderson et al., 2000). As noted earlier, the inclusion pathology in the SN precedes that of the thalamus (Rub et al. 2002). However, the presence of α-synuclein deposits does not indicate cell loss.

Several recent studies suggest that dopamine depletion may result in thalamostriatal cell death in rodents (Freyaldenhoven et al., 1997; Ghorayeb et al., 2002; Aymerich et al., 2006; Sedaghat et al., 2009). The number of retrogradely-labeled PF

thalamostriatal neurons is reduced in rats with 6-OHDA-median forebrain bundle (MFB) lesions at five weeks after the lesion (Aymerich et al., 2006). This study, however, did not evaluate whether the change in retrograde labeling was the result of a loss of PF neurons. Recently, Sedaghat and colleagues (2009) used 6-OHDA to lesion the SN of rats and reported that PF cells had degenerated within one month post-lesion based on a qualitative assessment of Nissl stained sections through the thalamus. There is also a study of the effects of administration of a very high dose (50 mg/kg) of MPTP to mice maintained at a low temperature (6^oC) environment that showed loss of neurons in the midline and intralaminar nuclei as assessed using Fluorojade C, which is a marker of degenerating neurons (Freyaldenhoven et al., 1997).

These studies are inconsistent with data from Henderson and colleagues (2005), who reported that unilateral 6-OHDA MFB lesions in rats produce no significant change in the total number of PF neurons. Differences in the manner in which dopamine depletion was achieved or in the ways in which cell loss was quantified may underlie the discrepancies in the findings. Also, because the studies relied on catecholaminergic neurotoxins that may have also lesioned noradrenergic axons, it is difficult to conclude if loss of dopamine or norepinephrine causes a loss in PF cells.

<div align="center">Overview</div>

Does nigrostriatal dopamine depletion cause loss of thalamostriatal neurons?

To address these issues, this thesis will first discuss studies designed to determine if a transsynaptic degeneration of thalamostriatal neurons occurs secondary to dopamine

depletion. The SN has long been recognized as sending projections to the CM-PF, but from the pars reticulata rather than the pars compacta, where most dopamine neurons reside (Beckstead et al., 1979; François et al., 2002; Sidibé et al., 2002; Tsumori et al., 2002). It has recently become apparent that there is a more widespread dopaminergic innervation of the thalamus than hitherto appreciated, particularly in primates (Freeman et al., 2001; García-Cabezas et al., 2009). Accordingly, in Chapter III, we will evaluate the extent to which SN dopamine neurons innervate the anterior intralaminar complex and the PF in the rodent, and in Chapter IV we will determine if nigrostriatal dopamine depletion causes a loss of thalamostriatal neurons.

Does loss of Cbln1 alter MSN dendrites?

The second half of this thesis will evaluate how CM-PF degeneration alters MSN dendrites. Recent studies indicate that the glycoprotein Cerebellin1 (Cbln1) is enriched in both the primate CM-PF and the rodent PF (Miura et al., 2006; Murray et al., 2007; Wei et al., 2007). In the cerebellum, Cbln1 is released from granule cells and regulates the synaptic formation and maintenance of granule cell-Purkinje cell synapses (Hirai et al., 2005; Ito-Ishida et al., 2008). Based on these findings, we sought to characterize the distribution of Cbln1 in thalamostriatal neurons (Chapter V) and determine how the genetic deletion of *cbln1* alters MSN synapses (Chapter VI).

CHAPTER III

CHARACTERIZATION OF DOPAMINE AXONS IN THE PF

The SN has long been known to project to the PF (Beckstead et al., 1979);

however, this projection is generally thought to arise from the pars reticulata, which

primarily contains GABAergic neurons (François et al., 2002; Sidibé et al., 2002;

Tsumori et al., 2002). However, Gauthier and colleagues (1999) anterogradely-labeled

SN neurons in rodents and observed that axons of a few nigrostriatal neurons innervated

the anterior intralaminar thalamic nuclei and striatum (Gauthier et al. 1999). However,

they did not determine the neurochemical identity of the axons.

Freeman and colleagues (2001) deposited retrograde tracers into specific thalamic

nuclei and then used immunohistochemistry to determine whether the retrogradely-

labeled neurons in the SN were dopaminergic. They found that both dopaminergic and

non-dopaminergic neurons in the SN project to the ventral anterior and ventral lateral

(motor) thalamic nuclei, and that these dopaminergic projections were collaterals of

nigrostriatal dopamine axons. A dopaminergic projection to the ventral lateral thalamic

nucleus, which originates from dorsal tier pars compacta dopamine neurons in the SN has

also been demonstrated in the primate (Sánchez-González et al. 2005). Although these

studies are consistent with a relatively small DA projection to the motor thalamus, no

studies have evaluated whether the CM-PF receives an SN dopaminergic projection.

Initial attempts to evaluate the extent to which dopamine axons are present in the

thalamus used tyrosine hydroxylase (TH)-immunolabeling. This approach revealed a

27

widespread distribution of TH axons across the thalamus (Freeman et al. 2001).

However, TH is also expressed in norepinephrine axons, and thus the presence of TH

does not indicate that these axons are dopaminergic.

A second approach is to evaluate the expression of the dopamine transporter

(DAT) as a marker of dopamine neurons. In primates and rodents, the mediodorsal,

paraventricular, ventral medial, and ventral lateral nuclei, are among the thalamic nuclei

with the highest densities of DAT axons (Sánchez-González et al. 2005; García-Cabezas

et al. 2007; García-Cabezas et al. 2009). However, in rodents DAT fibers are much less

prevalent in the thalamus than in primates (García-Cabezas et al. 2009). Of the thalamic

nuclei that project to the striatum, DAT-ir is highest in the centrolateral nucleus (CL),

moderate in the PF, and low in the CM of primates (Sánchez-González et al. 2005;

García-Cabezas et al. 2007). In rodents, very few DAT-ir axons are present in the CL

and PF (García-Cabezas et al. 2009).

Since not all dopamine axons express DAT, evaluating immunolabeling for DAT

may underestimate the relative abundance of dopamine fibers. Notably, DAT-

immunonegative dopamine neurons are found in several brain regions, including the

supraoptic region and paraventricular nucleus of the hypothalamus, the rostral

periventricular region of the hypothalamus, the lateral hypothalamus, and the arcuate

nucleus of the hypothalamus and the adjacent periventricular region (see Sánchez-

González et al. 2005).

An alternative approach is to label dopamine axons using an antibody directed

against dopamine. Using this approach Groenewegen (1988) showed that the CeM and

CL nuclei contain a few dopamine fibers in rodents. Because he was primarily interested

in the mediodorsal nucleus, he did not evaluate dopamine-immunolabeling in the PF. In

primates, dopamine fibers are sparsely distributed in the PF and CeM nucleus and to a

lesser extent in the CM (Sánchez-González et al. 2005; García-Cabezas et al. 2007).

Dopamine receptors have been described in both the primate and rodent thalamus.

In primates, the thalamic intralaminar nuclei contain relatively high densities of $D_{2/3}$

receptors (Gurevich and Joyce 1999; Rieck et al. 2004), and in rodents, the PF expresses

D_5 receptor mRNA (Meador-Woodruff et al. 1992. In light of these findings, we

examined whether SN dopamine neurons project to the PF.

Methods

A combination of approaches was used to determine whether SN dopamine

neurons innervate the PF. To evaluate the SN projection to the PF, we deposited the

anterograde tracer biotinylated dextran amine (BDA) in the SN of rats and examined

BDA-ir axons in the thalamus. To determine if the nigrothalamic axons are

dopaminergic, we deposited a retrograde tracer into the PF and assessed if the

retrogradely-labeled neurons in the SN expressed TH-ir.

We next evaluated the abundance of dopamine fibers in the PF using two different

approaches. First, we used immunofluorescence to double-label axons with TH and

dopamine β-hydroxylase (DBH). This method provides a way to distinguish

dopaminergic from noradrenergic axons. Thus, axons that contain TH but not DBH are

dopaminergic, and axons that have both TH and DBH are noradrenergic. Second, we

directly immunolabeled dopamine axons using an antibody that recognizes a dopamine-

glutaraldehyde conjugate.

Animals. Adult male Sprague-Dawley rats (Harlan; Indianapolis, IN, USA) were group-housed, with *ad libitum* access to food and water, and placed on a 12 hour light-dark cycle with lights on at 6 A.M. All experiments were conducted in accordance with the National Institutes of Health's *Guide for the Care and Use of Laboratory Animals*.

Surgical procedures. For all surgical procedures, rats were first anesthetized with isoflurane. The anterograde tracer BDA (10,000 MW; 15% BDA in 0.1 M phosphate buffer; Invitrogen, Carlsbad, CA) was iontophoretically deposited into the SN, with a micropipette tip 18-25 μm in diameter, using a pulsed (7s on/off) positive current of 5 μA for 15-20 minutes. The animals were sacrificed 10 days after the surgical procedure, and immunohistochemistry was used to assess BDA and TH in the SN, and BDA fibers in the thalamus, as described below. Other animals received iontophoretic deposits of the retrograde tracer FluoroGold (FG; 3% in cacodylate buffer; Fluorochrome, LLC, Denver, CO) into the lateral PF, using pulsed (7s on/off) positive current of 1.0 μA, and were sacrificed 10 days later. To determine if retrogradely-labeled (FG-positive) neurons in the SN were dopaminergic, midbrain sections were immunohistochemically stained for TH and the presence of FG-positive-TH-ir neurons was charted.

Immunohistochemistry. Rats were perfused with phosphate-buffered saline followed by 4% paraformaldehyde in phosphate buffer. The brains were removed from the skull, postfixed in 4% paraformaldehyde, and cryoprotected in 30% sucrose. A freezing microtome was then used to cut 42 μm-thick coronal sections through the brain, and sections were processed using immunohistochemical methods as previously described (Bubser et al. 2000).

The following primary antibodies were used: mouse anti-TH (1:1000 or 1:3000; ImmunoStar, Inc., Hudson, WI), mouse anti-TH (1:10,000; Sigma-Aldrich, St. Louis, MO), sheep anti-TH (1:800 or 1:3000; Millipore, Billerica, MA), mouse anti-DBH (1:800 or 1:2000; Millipore), rabbit anti-FluoroGold (1:3000; Millipore), and mouse anti-NeuN (1:1000; Millipore).

An antibody generated against a dopamine-glutaraldehyde conjugate (Millipore) was used to detect dopamine fibers. The antibody recognizes dopamine with high affinity and specificity, as reported previously (Geffard et al., 1984; Chagnaud et al., 1987). In addition, preincubation with dopamine-BSA-glutaraldehyde conjugate abolishes immunostaining, as reported by Millipore. The antibody is specific for dopamine and does not label norepinephrine. Thus, repeated absorptions of the antiserum with noradrenaline coupled to BSA does not alter the staining pattern, as reported by Millipore.

A modified fixation protocol was followed for immunohistochemical detection of dopamine fibers. This involved the addition of glutaraldehyde in the fixative since the antibody recognizes a dopamine-glutaraldehyde conjugate. An acidic fixative was also used to prevent the degradation of dopamine. The antioxidant sodium metabisulfite was also added to the washing steps to prevent the oxidation of dopamine (McRae-Degueurce and Geffard, 1996).

Rats were rapidly perfused intracardially with 50 ml of 0.2% $NaNO_2$ in 0.9% NaCl followed by 400 ml of ice-cold 5% glutaraldehyde in 50 mM acetate, pH 4. The brains were then removed and immersed in the same fixative for 1 hour at $4^{o}C$ before cutting 50 μm-thick coronal sections through the thalamus and midbrain on a vibrating

microtome. Next, the sections were washed thoroughly in Tris-metabisulfite [1% sodium

metabisulfite (MBS) in 0.05M Tris-HCl, pH 7.2], blocked in Tris-MBS containing 0.5%

Triton-X-100 and 4% normal horse serum (NHS), and incubated overnight in an antibody

generated against a dopamine-glutaraldehyde conjugate at 1:1000 (Millipore).

The following day, the sections were again washed in Tris-MBS, immersed for 2

hours in donkey anti-rabbit serum (1:40 in the blocking solution), and rinsed in TBS.

After incubating the sections for 90 minutes in rabbit peroxidase-anti-peroxidase (1:200

in TBS containing 4% NHS and 0.5% Triton-x-100), they were developed for 20-30

minutes in 0.025% diaminobenzidine in TBS containing 1.5% nickel ammonium sulfate

and 0.15% cobalt chloride, with 0.0009% H_2O_2.

Chartings. The software program Neurolucida (MBF Bioscience; Williston, VT) was

used to chart BDA- and dopamine-ir fibers in the thalamus and retrogradely-labeled FG

neurons in the SN.

Results

Tract tracing studies. Although most of the BDA iontophoretic deposits into the

SN were confined to the pars reticulata, there was always some degree of involvement of

the pars compacta (Fig. 4). The BDA deposit also extended dorsally into the medial

leminiscus; however, these axons are unlikely to have taken up the tracer since we used

pulsed, low current iontophoresis. The density of BDA fibers was low in the CeM and

high in the PC and CL. Anterogradely-labeled BDA-ir fibers were sparsely distributed

across the PF, with a slightly higher density of BDA-ir fibers in the medial PF than in the

lateral PF (Fig. 4).
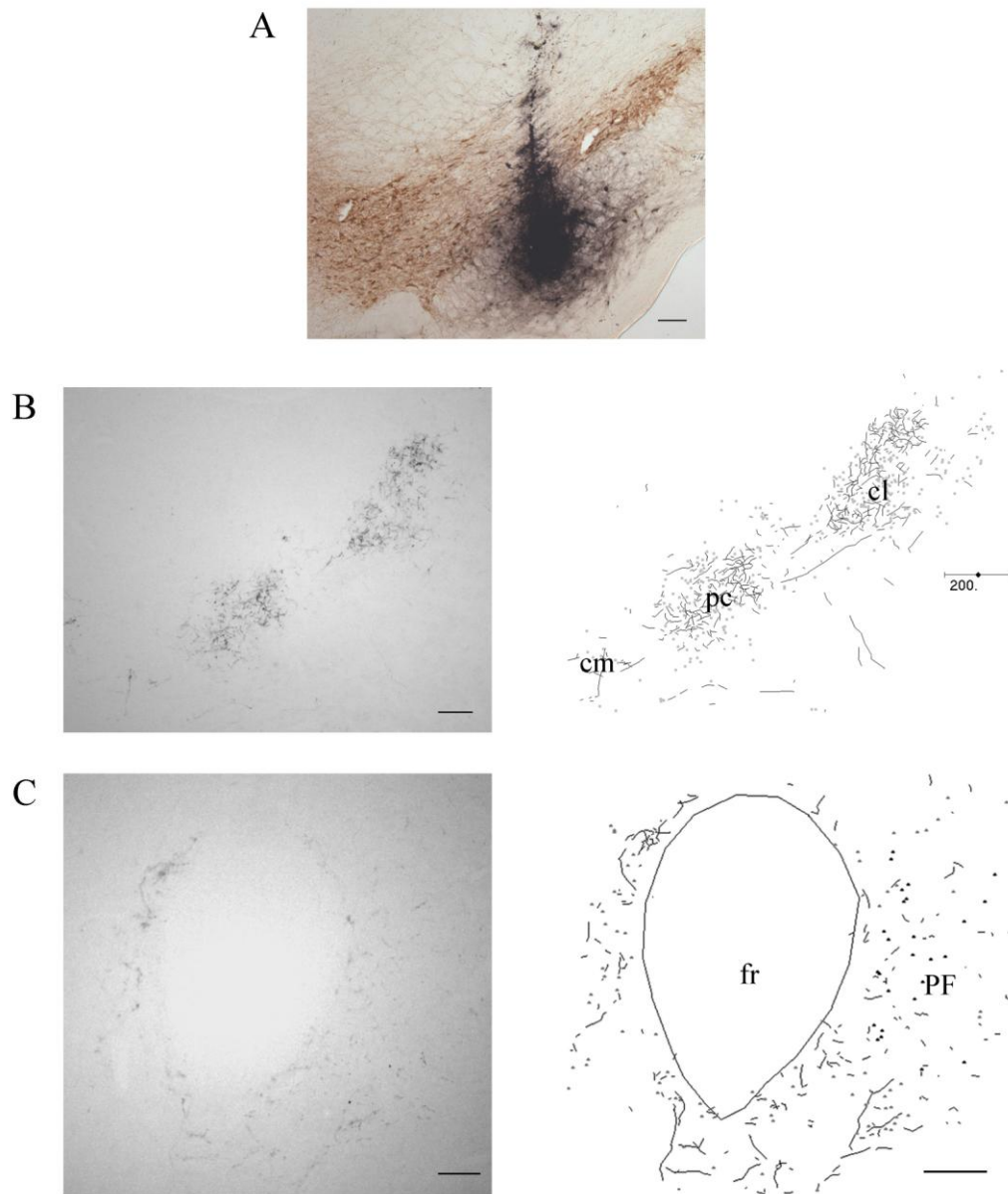
Figure 4. The substantia nigra projects to the anterior intralaminar thalamic nuclei and the PF. *A)* Immunohistochemistry for biotinylated dextran amine (BDA; black) and tyrosine hydroxylase (brown) in the substantia nigra. The BDA deposit is centered on the substantia nigra pars reticulata, but also encompasses the pars compacta. *B-C)* Photomicrographs (left) and chartings (right) of BDA-ir fibers in the central medial (cm), paracentral (pc), and central lateral nuclei (cl; panel B) and in the parafascicular nucleus (PF; panel C). Scale bars: photomicrographs, 100 μm; chartings, 200 μm.

33

We next deposited the retrograde tracer FG into the lateral PF of rats. Many FG-positive cells were seen in the SN, where they were mainly confined to the ventromedial sector of the pars reticulata (Fig. 5). A few FG-positive neurons were observed in the pars compacta. To determine whether the retrogradely-labeled neurons were dopaminergic, we assessed colocalization of FG with TH. None of the FG-positive neurons in the SN were TH-ir (Fig. 5), nor were double-labeled neurons observed in the ventral tegmental area (A10 cell group) or retrorubral field (A8 cell group).

TH/DBH-ir in the PF. It is possible that the SN projection to the PF is so sparse that it cannot be detected using retrograde labeling. We therefore evaluated the distribution of dopamine axons in the thalamus. To assess the presence of a dopamine innervation of the PF, we first examined if there were TH-positive/DBH-negative axons in the intralaminar nuclei. Dopaminergic axons were rarely observed in the PF, or CeM, PC, and CL nuclei. By contrast, there was a high density of double-labeled (noradrenergic) axons (Fig. 6). The morphology of both single and double-labeled axons was similar: long, thin, and varicose, consistent with previous reports on forebrain dopamine and norepinephrine axons (Moore and Bloom 1979; García-Cabezas et al. 2009).

Distribution of dopamine fibers. Within the dorsal thalamus, the highest density of dopamine-ir axons was observed in the paraventricular thalamic nucleus (PVT; Fig. 7). By contrast, the density of dopamine-ir axons was low in the PC and CL. In these nuclei, dopamine axons were seen to be of thin caliber and varicose (Fig. 7). The varicosities were generally spherical and irregularly spaced along the length of the axon.
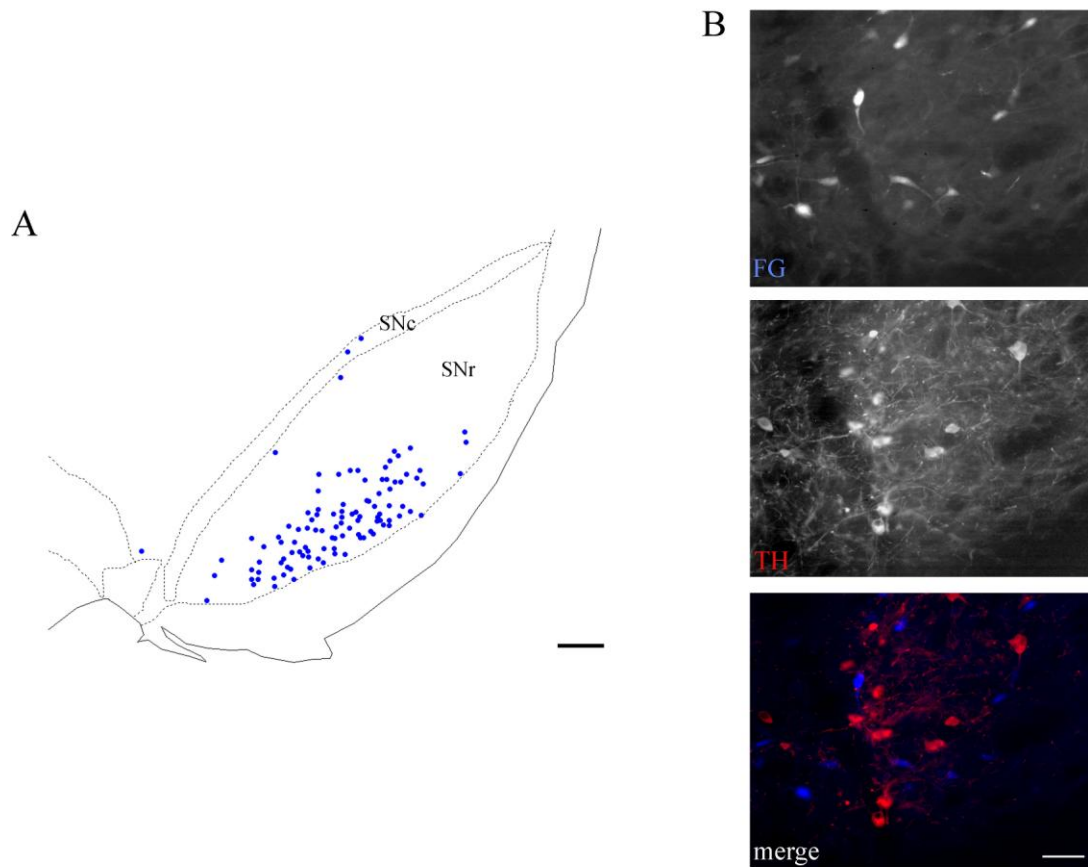
Figure 5. Non-dopaminergic neurons in the substantia nigra (SN) project to the parafascicular nucleus. Substantia nigra neurons were retrogradely-labeled from the lateral parafascicular nucleus with FluoroGold (FG). *A)* Charting of FG-positive neurons (blue) in the SN. Most retrogradely-labeled neurons were confined to the SN_r (substantia nigra pars reticulata); however a few FluoroGold-positive neurons were seen in the SN_c (substantia nigra pars compacta). *B)* FluoroGold-positive neurons (FG; blue) in the SN did not express tyrosine hydroxylase (TH; red). Scale bars: *A*, 200 μm; *B*, 50 μm.
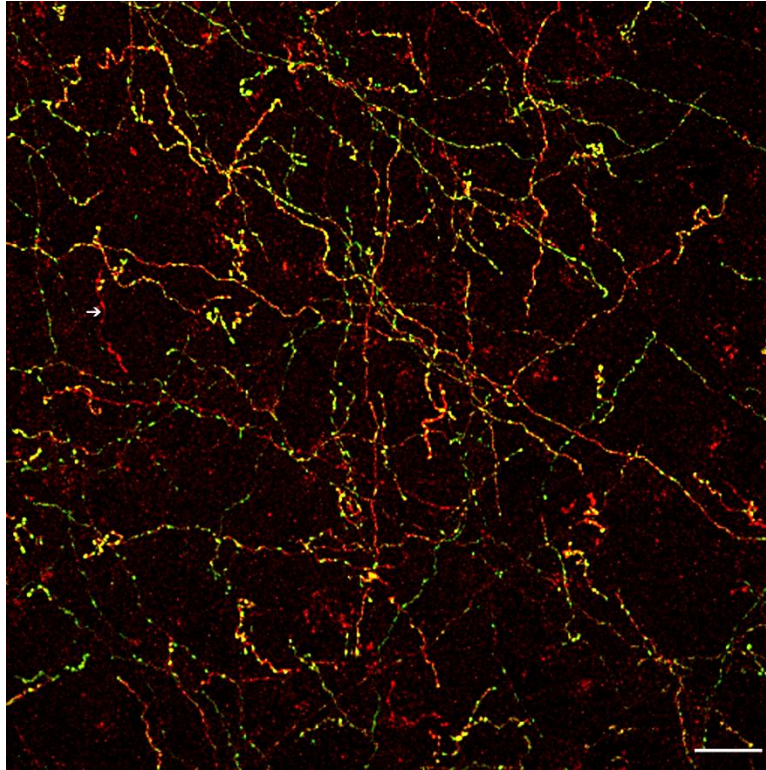
Figure 6. Immunolabeling for tyrosine hydroxylase- (TH; red) and dopamine β-hydroxylase- (DBH; green) ir axons in the parafascicular nucleus. Very few single labeled TH (dopaminergic) axons were observed (see arrow). Most fibers were double labeled and were therefore considered noradrenergic. Scale bar, 20 μm.
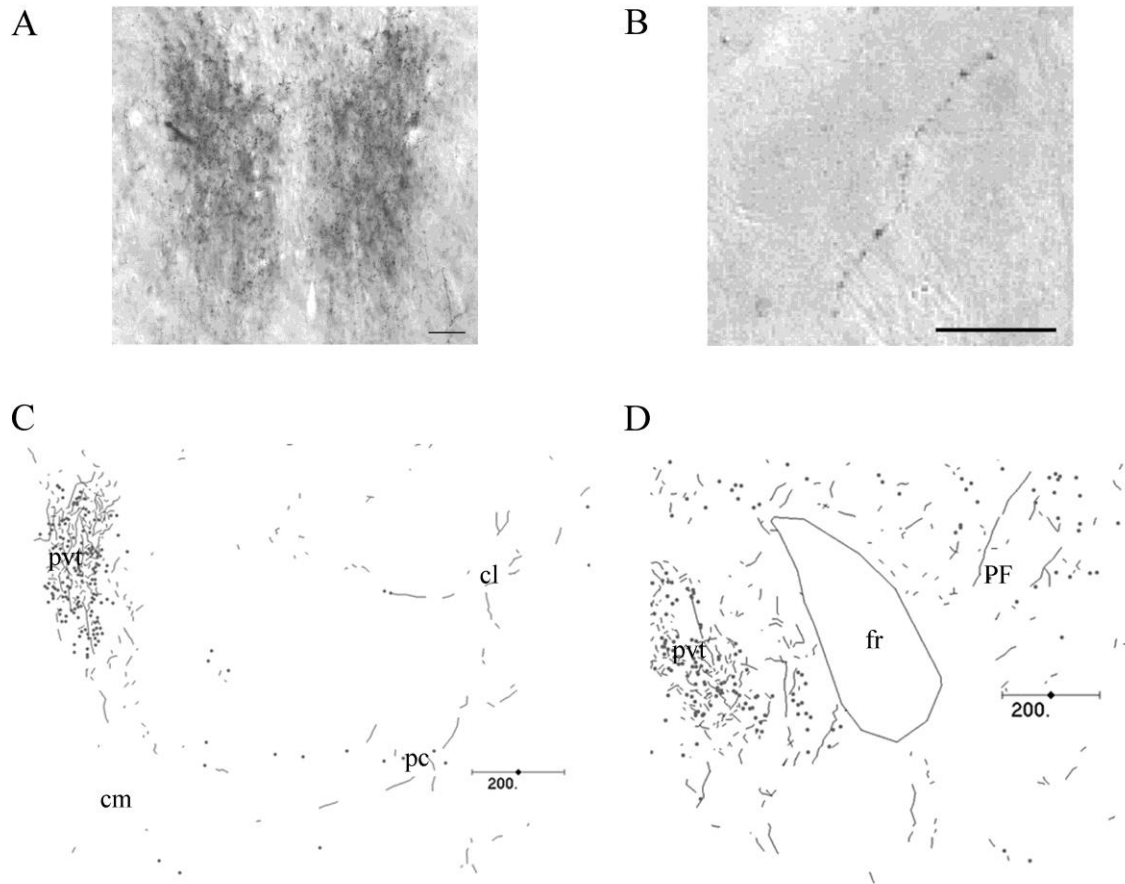
Figure 7. Distribution of dopamine-immunoreactive axons in the dorsomedial thalamus. *A-B)* Photomicrographs of dopamine immunolabeling in the paraventricular thalamic nucleus (panel A) and central lateral nucleus (panel B). *C-D)* Chartings of the distribution of dopamine fibers in the rostral (panel C) and caudal (panel D) intralaminar nuclei. Abbreviations: cm, central medial nucleus; cl, centrolateral nucleus; pc, paracentral nucleus; fr, fasciculus retroflexus; pvt, paraventricular thalamic nucleus; PF, parafascicular thalamic nucleus. Scale bars: *A*, 50 μm; *B,* 10 μm; *C-D,* 200 μm.

The thickness of the diameter of the varicosities also differed across the length of a given axon in an inconsistent fashion. The CeM was nearly devoid of dopamine axons.

The density of dopamine-ir axons varied across the medial and lateral PF, with the medial PF containing a slightly higher density of dopamine axons than the lateral PF. In the lateral PF, dopamine-ir axons were of thin caliber and resembled those seen in the PC and CL (Fig. 7). The dopamine-ir axons in the medial PF were of the same thickness in diameter in the PC, CL, and lateral PF.

Discussion

We first evaluated the SN projection to the PF using anterograde and retrograde tract tracing methods. Deposits of the anterograde tracer BDA into the SN revealed a moderate density of BDA-ir labeled axons in the rostral intralaminar nuclei, with somewhat fewer BDA-ir axons in the PF. However, our retrograde tracer deposits into the PF only labeled non-dopaminergic neurons in the SN. Most of the retrogradely-labeled neurons were found in the SN pars reticulata, which is primarily GABAergic. Thus, our data indicate that although there is a modest projection from the SN to the PF, this projection is non-dopaminergic. If there is a nigrothalamic dopamine projection to the PF, it is likely that this projection is very sparse.

Consistent with this inference, our immunohistochemical studies indicate that dopamine fibers are very sparsely distributed in both the anterior intralaminar nuclei and in the PF. We used two different approaches to evaluate dopamine axons: double immunolabeling for TH and DBH and dopamine immunohistochemistry. Both methods revealed similar results: that the anterior intralaminar nuclei and the PF only rarely contained dopamine axons. The relative density of dopamine-ir fibers in the anterior

intralaminar nuclei that we observed was consistent with that described in previous reports that used either an antibody generated against dopamine or DAT immunohistochemistry (Groenewegen 1988; García-Cabezas et al. 2009).

We found that the density of noradrenergic axons (TH-positive/DBH-positive axons) was much greater than that of dopamine axons in the PF. There is a modest noradrenergic innervation of the PF as indicated by DBH-immunohistochemistry (Swanson and Hartman 1975). The noradrenergic innervation of the PF appears to be derived from the locus coeruleus (LC; Krout et al. 2002), and PF neurons express α_{2B} adrenoceptor mRNA (Scheinin et al 1994).

There is neuronal loss in the LC in PD (German et al. 1992; Mann and Yates 1983; Rommelfanger and Weinshenker 2007). Animal studies have suggested that loss of LC neurons exacerbates MPTP-induced cell death of SN neurons (Rommelfanger and Weinshenker 2007). It is unclear if this occurs as a consequence of the loss of norepinephrine or the loss of other neurotransmitters, such as brain-derived neurotrophic factor or the neuropeptide galanin, that are co-released from the LC (Castren et al. 1995; Conner et al. 1997; Xu et al. 1998; Rommelfanger and Weinshenker 2007). Nevertheless, these studies suggest that disruptions of the noradrenergic innervation of the thalamus may also disrupt CM-PF function in PD. We will assess this possibility in the next chapter.

Overall, our data suggests that a direct nigral dopaminergic projection to thalamostriatal neurons does not exist. Recent studies have suggested that nigrostriatal dopamine depletion causes a loss of PF neurons and deficits in the retrograde labeling of PF thalamostriatal neurons (Aymerich et al. 2006; Sedaghat et al. 2009). Our data

indicate that the transsynaptic degeneration of nigrothalamic dopamine neurons cannot be

the mechanism by which nigrostriatal dopamine depletion alters the number and function

of PF thalamostriatal neurons.

CHAPTER IV

CATECHOLAMINERGIC REGULATION OF PF THALAMOSTRIATAL NEURONS

Although we found no indication of a significant dopamine innervation of the PF, previous data reported that 6-OHDA lesions of the MFB result in a decreased number of retrogradely-labeled PF, but not PC or CL, thalamostriatal neurons (Aymerich et al., 2006). One interpretation of this finding is that dopamine depletion results in the degeneration of PF neurons. Loss of PF neurons secondary to nigrostriatal dopamine depletion has been suggested to occur by Sedaghat and colleagues (2009), based on their qualitative assessment of Nissl stained PF neurons. Alternatively, the change in PF retrograde labeling observed by Aymerich et al. may simply indicate a functional effect of dopamine depletion on thalamostriatal neurons. To achieve retrograde labeling, the tracer must be taken up by axon terminals, transported to the cell soma, and then stored appropriately and protected from degradation. Given the lack of a dopaminergic innervation of the rodent PF, it was unclear how a lesion of nigrostriatal dopamine neurons could impact thalamostriatal neurons.

Aymerich and colleagues (2006) injected a large volume (4.0 µL) of 6-OHDA into the MFB, rather than the SN, of rats. The MFB contains both dopaminergic and noradrenergic axons. Because they did not pretreat the animals with a noradrenergic transporter blocker, their 6-OHDA injection would have lesioned noradrenergic as well as dopaminergic axons. In the previous chapter, we noted that the density of noradrenergic axons is much greater than that of dopaminergic axons in the PF,

suggesting that functional changes in thalamostriatal neurons may be the result of noradrenergic deafferentation. In this chapter, we determine whether a loss of dopamine or norepinephrine causes the degeneration of PF neurons. In addition we evaluate whether lesions of dopamine or norepinephrine neurons result in alterations in the number of PF neurons that can be retrogradely-labeled from the striatum.

Methods

We designed a series of experiments to address these issues. First, we determined if 6-OHDA lesions of the SN result in the degeneration of PF cells as reflected by accumulation of Fluoro-Jade C (FJC). Fluoro-Jade C is a reagent that selectively reveals neurons that are in the process of degenerating (Schmued et al., 2005). Although neuronal degeneration, as reflected by FJC accumulation, has previously been reported to occur by 2 days of the dopamine lesion (Freyaldenhoven et al., 1997), we extended the study to examine changes that occur between 2 and 42 days, which would potentially account for any transsynaptic or polysynaptic degeneration. Second, we evaluated whether 6-OHDA lesions of the SN result in a loss of PF neurons. Third, we determined if 6-OHDA lesions of the DNAB decrease the number of retrogradely-labeled thalamostriatal neurons in the PF and if a loss of PF neurons is seen. Finally, we attempted to replicate the data from Aymerich and colleagues (2006), by examining how lesions of the MFB alter the number of retrogradely-labeled thalamostriatal PF neurons.

Animals. Adult male Sprague-Dawley rats (Harlan; Indianapolis, IN, USA) were group-housed, with *ad libitum* access to food and water, and placed on a 12 hour light-dark

42

cycle with lights on at 6 A.M. All experiments were conducted in accordance with the National Institutes of Health's *Guide for the Care and Use of Laboratory Animals*.

Do 6-OHDA SN lesions cause PF cell death, as reflected by Fluoro-Jade C?   We first determined if 6-OHDA SN lesions result in PF degeneration as reflected by accumulation of Fluoro-Jade C (FJC). We infused 1.5 µL of 6-OHDA-HBr (6 µg/µL in 0.02% ascorbic acid) at coordinates AP: -5.2, ML: 2.4, DV: -8.4 over 15 minutes; a second 1.0 µL injection of the toxin was made at AP: -5.3, ML: 1.5, DV: -8.4 over 10 minutes. Control animals received sham surgeries. The rats were sacrificed at 2 days, 4 days, 7 days, or 42 days following the 6-OHDA lesion. The extent of the dopamine lesion was evaluated using TH immunohistochemistry, as described in Chapter II. Fluoro-Jade C staining was then used to reveal degenerating neurons in the thalamus and midbrain of 6-OHDA SN-lesioned animals, following the protocol of Schmued et al. (2005).

Do 6-OHDA lesions of the SN alter the number of PF neurons as determined by stereology? Animals were pretreated with the noradrenergic transporter blocker desipramine (20 mg/kg), and 6-OHDA was infused into the SN as described above. Six weeks after the lesion, the animals were sacrificed and 42 µm-thick sections through the thalamus were immunohistochemically stained (as described in Chapter III) for the neuronal marker NeuN using a mouse anti-NeuN (1:500; Millipore) antibody. An adjacent set of sections through the thalamus were Nissl stained with cresyl violet. Parafascicular neurons were visualized using a light microscope with a 63x 1.4 planApo objective. A digital camera coupled the microscope to the computer, and the image was digitally magnified by two. The number of neurons in the lateral PF of SN-lesioned and

sham-lesioned animals, as assessed by both Nissl staining and NeuN immunohistochemistry, was determined using the optical dissector method, with the aid of the software program Stereo Investigator (MBF Bioscience). Changes in the number of Nissl- and NeuN-stained neurons were analyzed using Student's t-tests.

Do 6-OHDA lesions of the SN alter the number of retrogradely-labeled thalamostriatal neurons in the PF? Rats were pretreated with despiramine and SN dopamine neurons were lesioned as described above. Approximately 4 weeks after the first surgery, FG (3% in 0.1M cacodylate, pH 3.3; Fluorochrome, Denver, CO) was bilaterally deposited into the dorsolateral striatum (at AP: 0.2, ML: 3.4, DV: -4.2) using a micropipette with a tip 20-30 μm in diameter, with pulsed (7s on/off) positive current of 5 μA for 15 minutes.

The animals were sacrificed ~14 days after the second surgery. Striatal sections were immunohistochemically stained for TH and FG to evaluate the FG deposit and assess the extent of striatal dopamine loss achieved by the lesions. An additional set of thalamic sections was immunohistochemically stained for FG to assess changes in the number of retrogradely-labeled thalamostriatal neurons. The slide-mounted sections were counterstained using cresyl violet. Retrogradely-labeled thalamostriatal neurons were counted in a 42 μm-thick section through the PF of SN- and sham-lesioned animals using Neurolucida (MBF Bioscience). The data was analyzed using a t-test.

Do 6-OHDA lesions of the DNAB alter the number of PF neurons? The noradrenergic innervation of the PF was lesioned by infusing 0.75 μL of 6-OHDA into the dorsal noradrenergic bundle (DNAB) at coordinates AP: -6.3, ML: 0.9, DV: -6.3. The animals were sacrificed ~42 days later. To determine the extent of thalamic noradrenergic

depletion, immunohistochemistry was used to reveal DBH axons. Changes in NeuN-ir and Nissl-stained neurons were evaluated using stereology.

Do 6-OHDA lesions of the DNAB alter the retrograde labeling of PF thalamostriatal neurons? The DNAB was lesioned with 6-OHDA and FG was deposited into the striatum 4 weeks later, as described above. The rats were sacrificed two weeks after the second surgery. Changes in the number of retrogradely-labeled PF neurons in the DNAB-lesioned animals relative to sham-lesioned animals were evaluated as described above.

Do 6-OHDA lesions of the MFB alter retrograde labeling of PF thalamostriatal neurons? The MFB was lesioned by infusing 1.5 µL of 6-OHDA at AP: -3.60; ML: +2.0; DV: -8.4. Four weeks later, FG was bilaterally deposited into the striatum, as described above. The rats were sacrificed approximately two weeks after the second surgery. Changes in the number of retrogradely-labeled PF neurons ipsilateral versus contralateral to the MFB lesion and relative to control-lesioned animals were evaluated as described above.

Results

Do 6-OHDA SN lesions cause PF cell death? A nearly complete loss of TH-ir neurons was observed ipsilateral to the lesion in the SN of 6-OHDA-lesioned animals (Fig. 8). We used FJC to qualitatively examine the presence of degenerating neurons in the PF at variable times after 6-ODHA lesions of the SN. Fluoro-Jade C labeled degenerating cell bodies in the pars compacta at two days post-operatively (Fig. 8). Four days after the
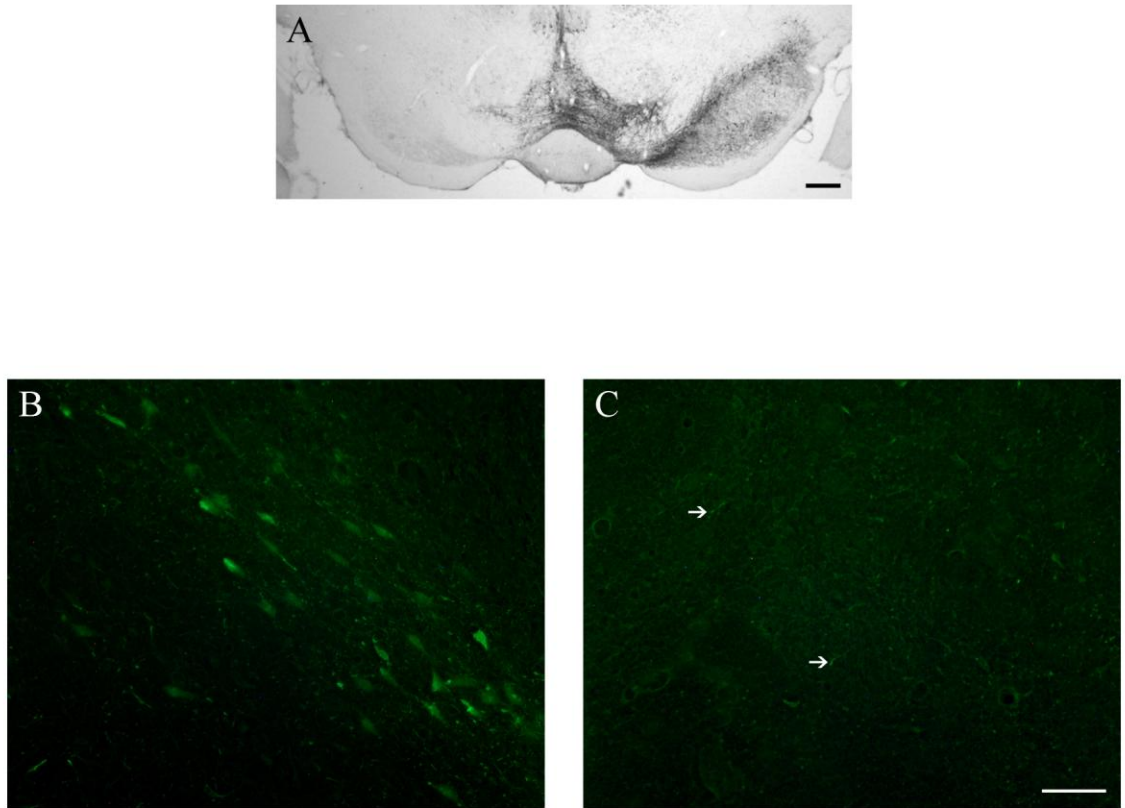
Figure 8. Fluoro-Jade C positive cell bodies are present in the substantia nigra (SN) but not the thalamus of 6-OHDA SN lesioned rats. *A)* The extent of the 6-OHDA SN lesion can be seen in TH-stained sections. There was an almost complete loss of SN dopamine neurons, with a considerable number of lateral dopamine ventral tegmental area dopamine cells also being involved. *B)* Fluoro-Jade-C (FJC) labels degenerating cell bodies in the SN at two days after the surgery. *C)* No degenerating cell bodies were seen in the thalamus at any of the time points assessed. A few FJC processes (arrows) were detected at four days post-operatively. Scale bars: *A*, 400 μm; *B-C*, 50 μm.

lesion, no FJC-positive cell bodies were seen in the thalamus, although a few

degenerating FJC profiles were observed in the CL and PF nuclei ipsilateral to the lesion

(Fig. 8). No FJC-positive cell bodies were observed in the thalamus at the later any of

the time points (7 days and 42 days).

Six weeks after the 6-OHDA lesion, stereological assessment revealed that the

number of Nissl stained PF cells did not differ between 6-OHDA-SN and sham-treated

animals (t_{10} = 0.31, NS; Fig. 9). Similarly, we observed no difference in the number of

NeuN-ir neurons in the PF of 6-OHDA-SN-lesioned animals relative to sham-treated

animals (t_{12} = 0.90, NS; Fig. 9).

Do 6-OHDA lesions of the SN alter the number of retrogradely-labeled thalamostriatal

neurons in the PF? The 6-OHDA SN-lesioned animals showed an extensive loss of

striatal TH-ir axons ipsilateral to the lesion (Fig. 10). The deposits of FG were confined

to the dorsolateral striatum. The retrograde tracer deposits resulted in the labeling of

many PF neurons, most in the dorsolateral PF (Fig. 10). The number of retrogradely-

labeled PF neurons did not differ between 6-OHDA SN- and sham-lesioned animals (t_{14}

= 0.32, NS; Fig. 11).

Do 6-OHDA lesions of the DNAB alter the number of PF neurons or result in changes

in the number of retrogradely-labeled PF neurons? The DNAB-lesioned group showed

an extensive loss of DBH-ir axons in the PF (Fig. 12). Stereological assessment revealed

that the number of Nissl-stained PF cells did not differ between 6-OHDA-SN and sham-

treated animals at 6 weeks post-lesion (t_{15} = 0.42, NS; Fig. 13). Similarly, we observed

no change in the number of NeuN-ir neurons in the PF of 6-OHDA-SN- lesioned animals
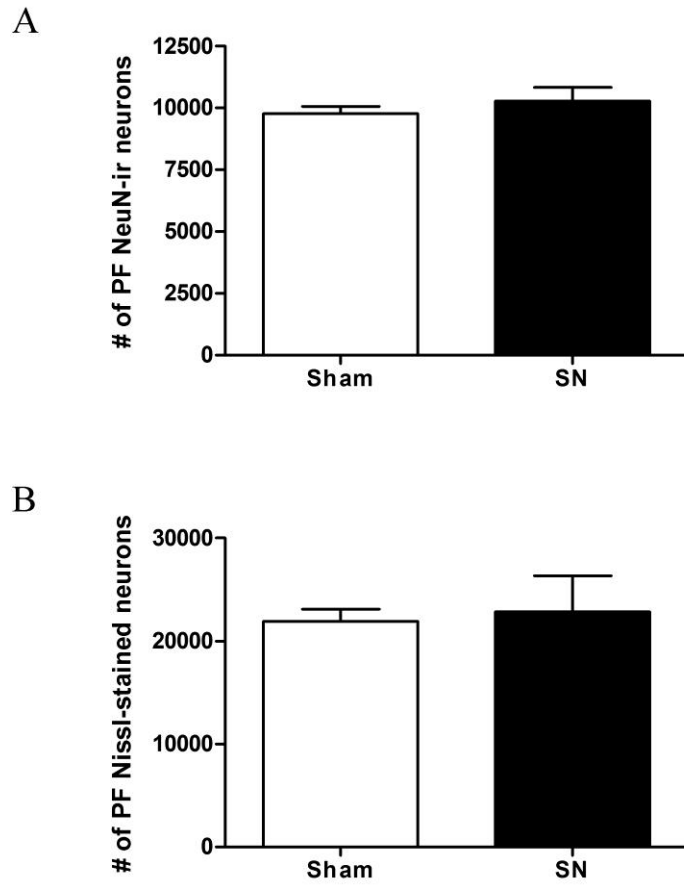
Figure 9. Substantia nigra (SN) 6-OHDA lesions do not alter the number of PF neurons. *A)* The number of PF NeuN-immunoreactive (-ir) neurons did not differ between sham- and 6-OHDA SN-lesioned animals. *B)* Similarly, we observed no change in the number of Nissl-stained PF neurons in the 6-OHDA-lesioned animals.
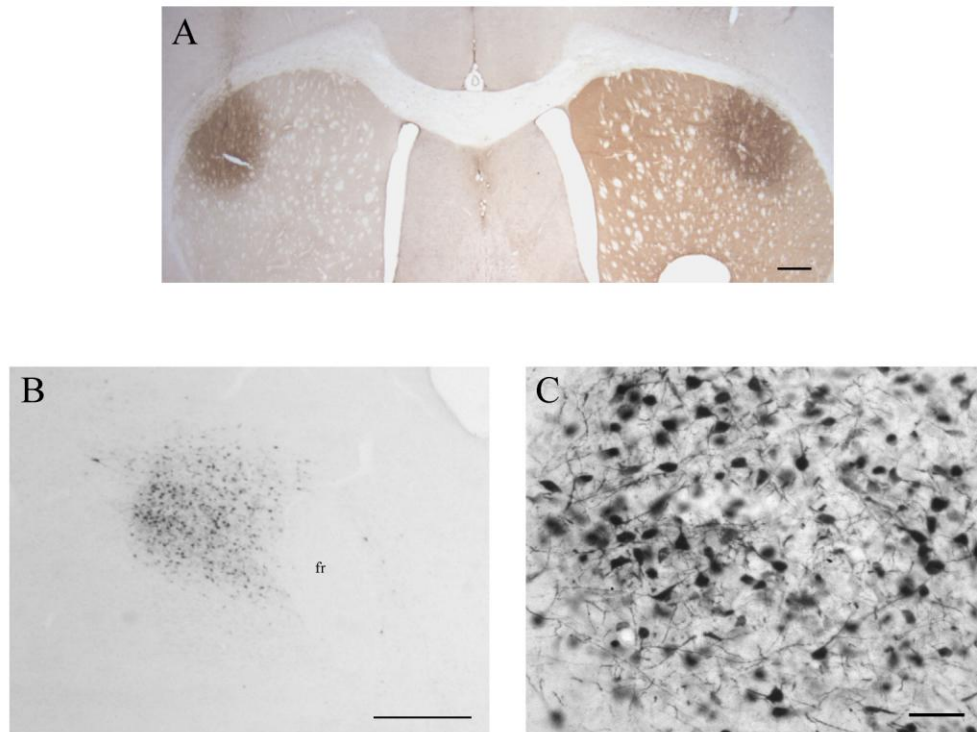
Figure 10. Retrograde labeling of thalamostriatal neurons with FluoroGold (FG). *A)* Immunohistochemistry for FG (black) and tyrosine hydroxylase (TH; brown) in the striatum of a 6-OHDA substantia nigra (SN)-lesioned animal. The FG deposit was confined to the dorsolateral striatum. A unilateral loss in striatal TH was seen ipsilateral to the 6-OHDA SN lesion. *B)* Retrogradely-labeled FG-ir neurons were primarily seen in the dorsolateral parafascicular nucleus (PF). *C)* FG-ir filled the cell bodies and proximal dendrites of PF neurons. Scale bars: *A-B*, 400 μm; *C*, 50 μm.
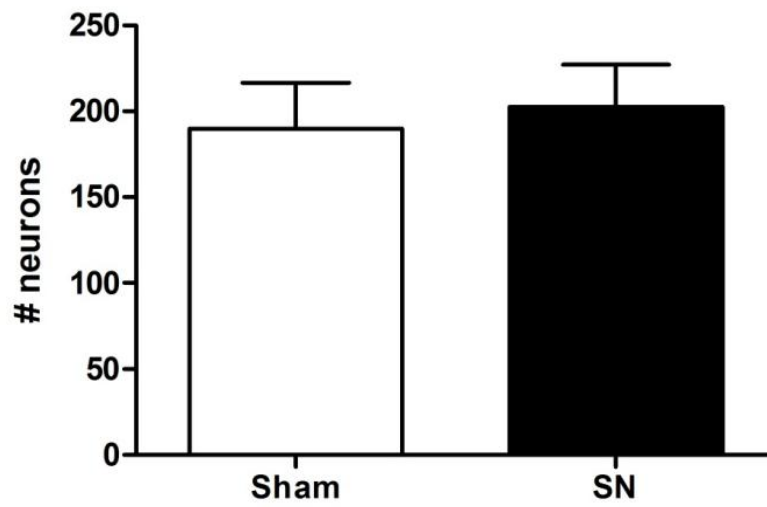
Figure 11. The number of retrogradely-labeled thalamostriatal neurons in the PF did not differ between 6-OHDA substantia nigra (SN) and sham-lesioned animals.
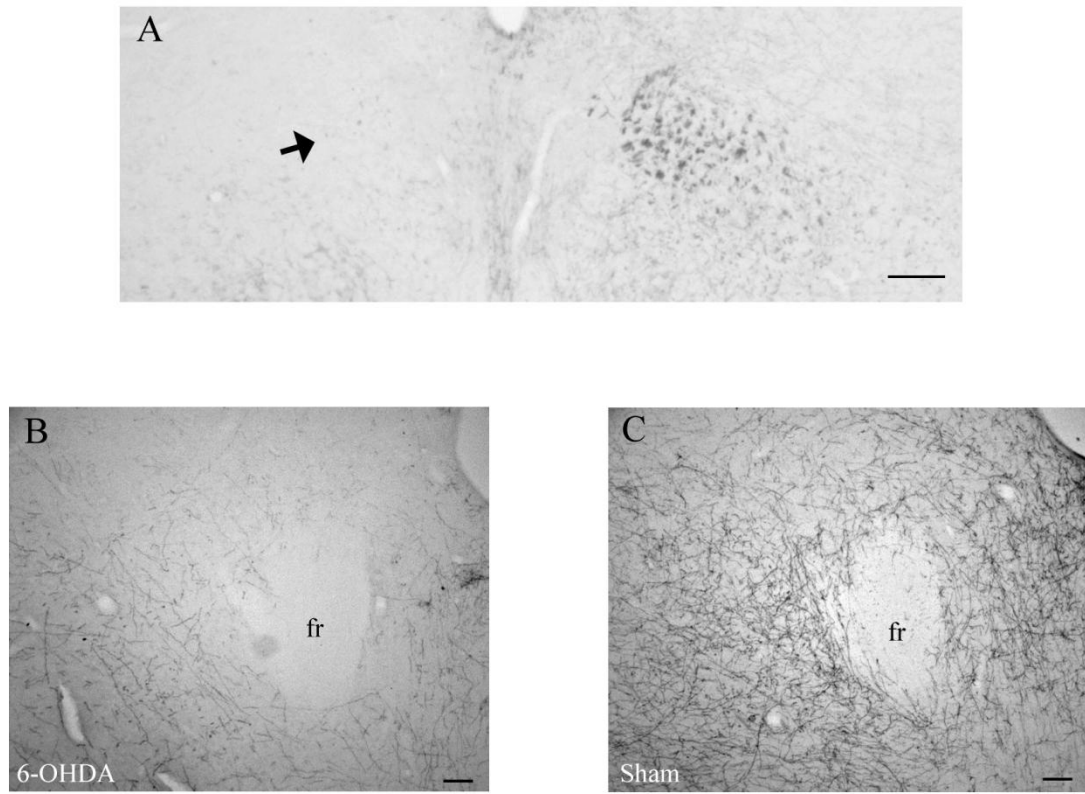
Figure 12. Characterization of the 6-OHDA DNAB lesion. *A)* Immunohistochemistry for dopamine β-hydroxylase (DBH) in the DNAB. 6-OHDA lesions of the DNAB resulted in a complete loss of DBH-ir axons (arrow) in the DNAB. *B)* The PF of a sham-lesioned animal is densely innervated by DBH-ir axons. *C)* An extensive loss of DBH-ir axons ipsilateral to the 6-OHDA lesion is seen in the PF of DNAB-lesioned animals. Scale bars: *A*, 400 μm; *B-C*, 100 μm.
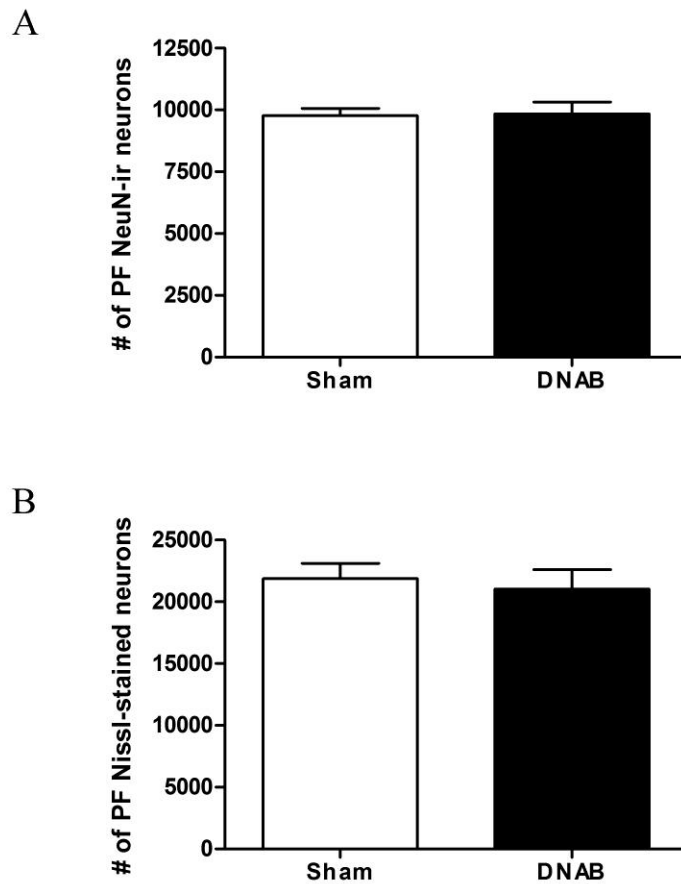
Figure 13. Dorsal noradrenergic bundle (DNAB) 6-OHDA lesions do not alter the number of PF neurons, as assessed using stereology. *A)* The number of PF NeuN-immunoreactive (-ir) neurons did not differ between sham- and 6-OHDA DNAB-lesioned animals. *B)* Similarly, we observed no change in the number of Nissl-stained PF neurons between sham- and 6-OHDA DNAB-lesioned animals.

relative to sham-treated animals ($t_{15} = 0.15$, NS; Fig. 13).

We next evaluated whether 6-OHDA DNAB lesions affect the retrograde labeling of PF thalamostriatal neurons. The FG deposit was confined to dorsolateral striatum, and the 6-OHDA DNAB lesion did not alter striatal TH-ir (Fig. 14). There was no significant decrease in the number of retrogradely-labeled PF neurons in the DNAB-lesioned animals relative to the sham-lesioned animals, although a trend-noted was noted ($t_{17} = 1.81$, $p = .0880$; Fig. 14).

Do 6-OHDA lesions of the MFB alter retrograde labeling of PF thalamostriatal neurons? The 6-OHDA MFB-lesioned animals showed a loss of striatal TH ipsilateral to the lesion (Fig. 15). We observed no change in the number of PF neurons of the MFB-lesioned animals relative to sham-lesioned animals ($t_{15} = 0.15$, NS; Fig. 15). Similarly, we observed no difference in the number of retrogradely-labeled PF neurons ipsilateral versus contralateral to the MFB lesion ($t_{12} = 0.11$, NS; Fig. 15).

Discussion

We found no evidence to support the hypothesis that dopaminergic or noradrenergic denervation causes the degeneration of PF neurons in rodents. Fluoro-Jade C staining did not reveal any dying neurons in the PF at time points ranging from 2 days to 42 days after the 6-OHDA lesions, and stereological analysis of the number of PF neurons revealed no differences between animals with 6-OHDA or sham-SN lesions. In addition, we did not observe a change in the number of retrogradely-labeled thalamostriatal PF neurons. Similarly, our 6-OHDA lesions of the median forebrain bundle caused no changes in retrograde labeling of PF neurons. We also found that
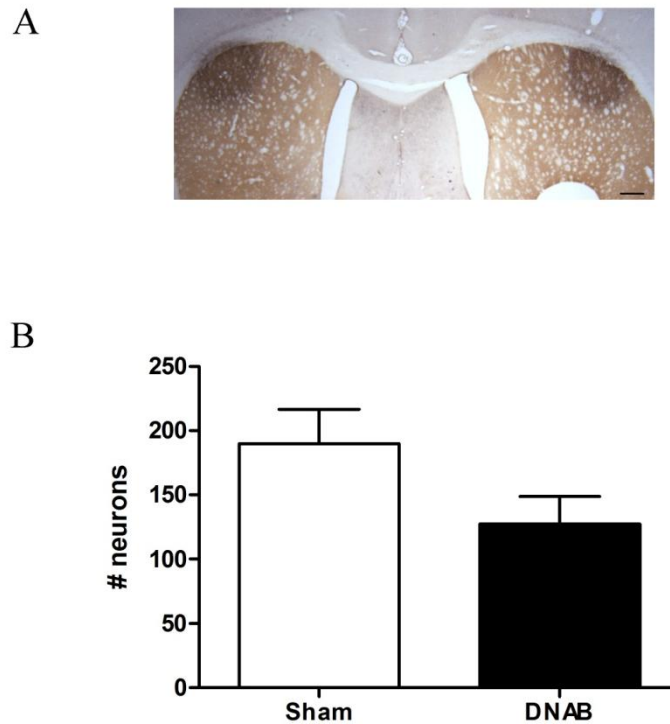
Figure 14. Dorsal noradrenergic bundle (DNAB) 6-OHDA lesions do not alter the number of retrogradely-labeled PF thalamostriatal neurons. *A)* FluoroGold (FG; black) injection of the striatum, counterstained with tyrosine hydroxylase (TH; brown). The 6-OHDA DNAB lesions did not change the density of the dopaminergic innervation of the striatum. The FG deposit was confined to the dorsolateral striatum and was bilaterally symmetrical. *B)* The number of retrogradely-labeled FG neurons in the PF did not differ significantly between 6-OHDA DNAB- and sham-lesioned animals. Scale bar: 400 μm.

A

B

C
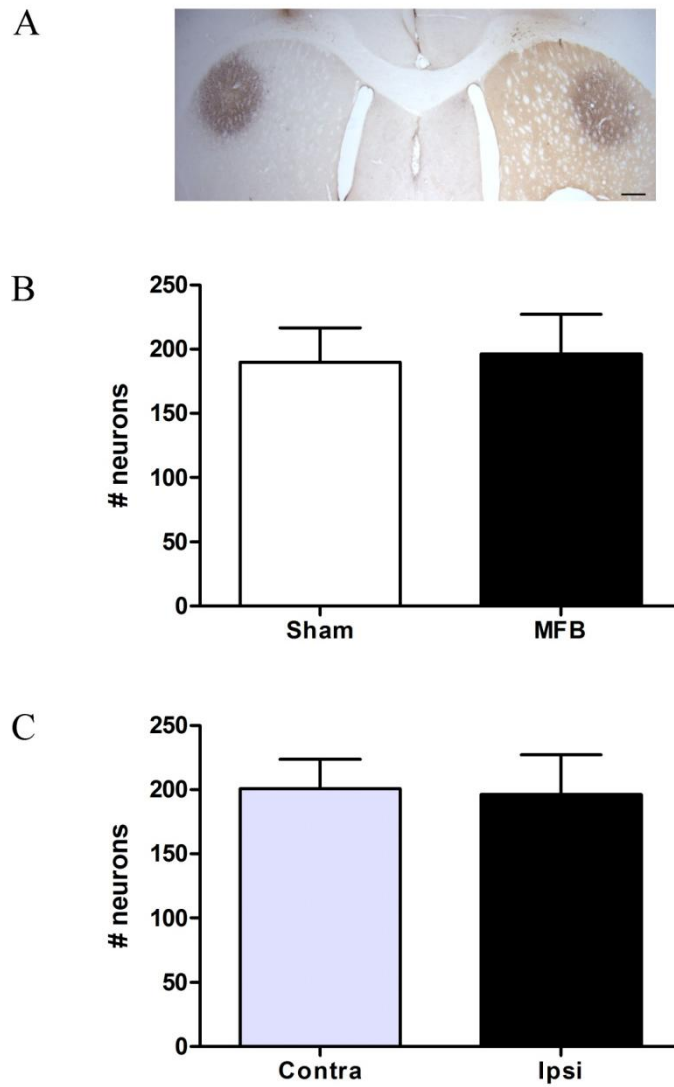
Figure 15. Median forebrain bundle (MFB) 6-OHDA lesions do not alter the number of retrogradely-labeled PF thalamostriatal neurons. *A)* Immunohistochemistry for FluoroGold (FG; black) and tyrosine hydroxylase (TH; brown) in the striatum of a 6-OHDA MFB-lesioned animal. The FG deposit was confined to the dorsolateral striatum, and a loss of striatal TH was seen ipsilateral to the 6-OHDA lesion. *B)* The number of retrogradely-labeled FG neurons in the PF ipsilateral to the lesion did not differ between 6-OHDA MFB- and sham-lesioned animals. *C)* Similarly, there was no difference in the number of retrogradely-labeled FG neurons in the PF ipsilateral to the lesion (ipsi) relative to the contralateral (contra) hemisphere. Scale bar: 400 μm.

thalamic noradrenergic denervation did not alter the number of PF neurons or have a statistically significant affect on the number of retrogradely-labeled thalamostriatal PF neurons.

We initially used FJC staining as a qualitative assessment of cell loss. Fluoro-Jade C has been shown to label neurons that degenerate in response to a variety of insults, including those involving excitotoxicity and the generation of oxidative free radicals (see Schmued et al., 1997). One of the advantages of the method is that it stains degenerating neurons and their processes with high contrast and is relatively resistant to fading (Schmued et al., 2005). However, there are limitations to using FJC as a marker of cell death. Among these is that FJC can only be used to mark neurons undergoing cell death, and thus is useful over a relatively short time window.

Because we did not know when thalamic cell death might occur, we examined FJC staining at a variety of time points. The two day time point was chosen based on a previous study, which showed that extremely high doses (50 mg/kg) of MPTP at low ambient temperature (6°C) result in FJC accumulation in neurons of the CeM and paraventricular thalamic nucleus by two days (Freyaldenhoven et al. 1996). However, we did not observe any FJC-positive neurons in the thalamus at any time after 6-OHDA SN lesions. The high dose of MPTP used in the previous study (Freyaldenhoven et al. 1996) may have caused cell death of the thalamic nuclei by a mechanism totally unrelated to the loss of dopamine. We observed sparse FJC axonal labeling in the CL and PF, which was maximal at 4 days post-operatively. Given the lack of a dopaminergic projection to the PF, it is likely that the FJC labeling of axons in the thalamus represents a non-specific (mechanical) damage to a small number of nigrothalamic neurons.

Because of the limitations of FJC labeling in determining cell death, we used stereology to quantify changes in the number of PF neurons. We assessed alterations in PF neurons at 6 weeks following the lesion because previous studies had suggested that PF degeneration, as evaluated by a qualitative assessment of Nissl-stained sections, has occured by this point (Sedaghat et al., 2009). We identified PF neurons on the basis of two different methods, NeuN-ir and Nissl staining. Our estimate of the number of NeuN-ir PF neurons was roughly half that of Nissl stained cells. This may be the result of failure of the NeuN antibody to penetrate the full thickness (42 μm) of the section. Nevertheless, both methods showed that the number of PF neurons was unaltered in rats with 6-OHDA SN lesions.

Although nigrostriatal dopamine depletion does not cause a loss of PF neurons, it is still possible that it may have a functional effect on PF neurons. To evaluate this possibility, we determined if 6-OHDA lesions result in a loss of retrogradely-labeled PF neurons. Our data showed that the number of retrogradely-labeled thalamostriatal PF neurons was unaltered by 6-OHDA lesions of the SN.

A previous study had reported that unilateral 6-OHDA lesions of the MFB result in a loss of PF neurons relative to the contralateral hemisphere (Aymerich et al., 2006). Both noradrenergic and dopaminergic axons ascend to forebrain targets in the MFB. Because Aymerich and colleagues did not pretreat the animals with a noradrenergic transporter blocker, their lesions likely resulted in thalamic noradrenergic denervation. We attempted to replicate their study by injecting 6-OHDA into the MFB. However, we found no change in the number of retrogradely-labeled PF neurons relative to the contralateral side or relative to sham-operated control animals. One reason why we may

have failed to see a difference is that we infused 1.5 µL of 6-OHDA to lesion the MFB whereas they injected 4.0 µL of the toxin. This volume almost certainly resulted in loss of the noradrenergic axons in the MFB, but may in addition have spread into the adjacent thalamus (unfortunately the report by Aymerich et al. did not indicate the coordinates in which they infused 6-OHDA). By using a smaller volume of 6-OHDA, we were able to restrict the spread of the toxin into adjacent brain regions. Our lesions of the MFB still resulted in substantial loss of striatal TH ipsilateral to the lesion.

We evaluated if 6-OHDA DNAB lesions cause the loss of PF neurons. We observed no change in the number of PF neurons. Thus, it is unlikely that the data of Aymerich et al. could be explained by a loss of PF thalamostriatal neurons secondary to forebrain noradrenergic denervation.

We next evaluated whether 6-OHDA DNAB lesions resulted in deficits in retrograde labeling of PF neurons. We found a slight but consistent decrease in the number of retrogradely-labeled PF neurons, but this did not reach statistical significance. A power analysis revealed that we would need to use 29 animals per group to achieve significant power to detect an effect at the .05 alpha level. This suggests that the effect of forebrain noradrenergic depletion on the retrograde labeling of PF thalamostriatal neurons is likely to be small. Thus, our data suggest that although there is a modest noradrenergic innervation of the PF, the loss of retrogradely-labeled PF neurons by Aymerich is probably not due to loss of norepinephrine.

It remains unclear why Aymerich et al. observed a loss of retrogradely-labeled PF neurons. We did not attempt to evaluate changes in the number of PF neurons secondary to large lesions of the MFB. However, a previous study by Henderson and colleagues

(2005) found that large 6-OHDA lesions (4.0 μL) of the MFB do not alter the number of PF neurons, as assessed using stereology. This bolsters the argument that the decrease in the number of retrogradely-labeled PF neurons observed by Aymerich et al. (2006) is not a result of PF degeneration.

It is possible that the 6-OHDA MFB lesions performed by Aymerich et al. caused a functional deficit in PF thalamostriatal neurons. One difference between our studies is that we allowed 15 minutes for iontophoretic deposition of the tracer in the striatum, whereas they only allowed 5 minutes. Thus, their deposits may not have labeled PF neurons with axons that sparsely innervate the striatum.

It has recently been suggested that the PF innervation of the striatum is altered by nigrostriatal dopamine depletion: in MPTP primates, the ratio of VGluT2-ir axospinous to axodendritic synapses is increased in striatal MSNs (Raju et al., 2008). The PF is the primary source of VGluT2-ir axodendritic synapses onto MSNs (Raju et al., 2006). Based on our data indicating that the number of PF neurons is unaltered in nigrostriatal dopamine-lesioned animals, this finding cannot be explained by the degeneration of PF neurons. A more likely explanation is that there is a reduction in the number of synaptic terminations onto the dendritic shaft that are formed by individual PF axons.

Could it be that PF neurons are functionally impacted by 6-OHDA SN lesions, but do not undergo degeneration? Parr-Brownlie and colleagues (2009) found that the number of spontaneously active PF cells was decreased at two weeks post-operatively. The firing rate of PF neurons is also thought to be altered by 6-OHDA SN lesions in a tri-phasic manner. Thus, electrophysiological data suggest a decrease in the firing rate of PF neurons at 1 week post-operatively, followed by recovery at 2 weeks, and an increase in

the firing rate at 5 weeks post-operatively (Ni et al., 2000; Yan et al., 2008). Changes in the firing rate of PF neurons have not been assessed beyond 5 weeks.

Interestingly, fluctuations in the firing rate of CM and CL neurons, as induced by MPTP treatment, correlate with the appearance of motor symptoms in cats. Thus, Schneider and Rothblat (1996) found a decrease in the number and firing rate of CM-CL neurons responsive to tactile stimulation of the face following MPTP treatment in cats at a time when motor deficits (including rigidity, akineasia, and lack of orienting responses) were detected. However, at six weeks post-MPTP treatment, when the motor deficits had resolved (as defined by an increase in spontaneous movements and the recovery of orienting responses to sensory stimuli), these functions returned to normal.

In summary, our findings indicate that nigrostriatal dopamine depletion does not cause the loss of PF thalamostriatal neurons nor does it cause a loss of retrogradely-labeled thalamostriatal neurons. Given the lack of a significant dopaminergic innervation of thalamostriatal neurons, it is likely that the functional changes in PF neurons in striatal dopamine-depleted rodents are a consequence of alterations in non-dopaminergic neurons that project to the thalamus, presumably the gabaergic neurons of the SN pars reticulata, NE neurons of the locus coeruleus, or glutamatergic neurons of the subthalamic nucleus and cortex.

CHAPTER V

CHARACTERIZATION OF CBLN1 EXPRESSION IN THALAMOSTRIATAL
NEURONS

We were intrigued by the possibility that CM-PF degeneration might lead to changes in MSN dendrites because these dendrites undergo dystrophic changes in PD (McNeill et al., 1988; Stephens et al., 2005; Zaja-Milatovic et al., 2005). In Chapter IV, we found that it is not possible to model thalamostriatal degeneration in rodents by simply lesioning SN dopamine neurons. One way to study the functional impact of the loss of thalamostriatal neurons on the intact or dopamine-denervated striatum is to lesion the thalamic nuclei that innervate the striatum and assess the consequences. Unfortunately, the geometry of these nuclei in the rat makes it difficult to lesion the PF without significantly damaging adjacent nuclei.

An alternative approach is to create discrete lesions of thalamostriatal neurons by identifying a protein that is selectively expressed in these neurons, and using this information to generate transgenic animals with molecular lesions of these neurons. Murray and colleagues (2007) examined the expression profile of the primate thalamus and identified a number of transcripts enriched in the thalamus. Among these was Cbln1 which was essentially restricted to the CM-PF in the thalamus. In this chapter, we evaluate the use of Cbln1 as a marker of thalamostriatal neurons.

The peptide cerebellin was discovered over twenty-five years ago, before its precursor had been identified, and was named for its expression in the cerebellum (Slemmon et al., 1984). It was initially hypothesized to function as a neurotransmitter

because it was found in synaptosomes (Slemmon et al., 1984) and its release could be evoked in a calcium-dependent manner by high potassium concentrations (Burnet et al., 1988). In 1994, Urade and colleagues discovered that cerebellin was produced from a larger protein, Cbln1, through proteolytic cleavage (Urade et al., 1994).

Cbln1 is the prototype of a subfamily (Cbln1-4) of the C1q/TNFα superfamily of proteins (Pang et al., 2000; Bao et al., 2005). Cbln family members have a conserved C-terminal C1q domain, which is thought to aid in complex formation with other family members (Pang et al., 2000; Bao et al., 2005). They are distinguished from other C1q/TNFα family members by the inclusion of a 16 amino acid "cerebellin" sequence.

Contrary to its name, Cbln1 has a widespread but heterogeneous distribution in the brain (Mugnaini and Morgan, 1987; Miura et al., 2006; Wei et al., 2007). Among the sites outside of the cerebellum with abundant central expression of *cbln1* mRNA and protein is the PF (Miura et al., 2006; Murray et al., 2007; Wei et al., 2007). In view of the high density of Cbln1 mRNA-expressing cells in the PF, we determined if Cbln1 was present in the thalamostriatal system.

Methods

We used immunohistochemistry to characterize the anatomical localization of Cbln1 in the thalamus and striatum. To determine if Cbln1 was expressed in striatal and PF neurons, we used dual-label immunohistochemistry to reveal Cbln1 and the neuronal marker NeuN. We next determined if thalamostriatal and thalamocortical PF neurons express Cbln1 by depositing retrograde tracers into the striatum and cortex of animals, and then determining if the retrogradely-labeled neurons in the PF expressed Cbln1-ir.

We next evaluated Cbln1-ir contacts onto striatal MSN dendrites by intracellularly filling MSNs with Lucifer yellow (LY) and then assessing at the light microscopic level Cbln1-ir appositions onto MSN dendrites. Finally, we used electron microscopy (EM) to evaluate Cbln1 expression in PF axon terminals.

Animals. *cbln1$^{-/-}$* mice and their wildtype littermates (Hirai et al., 2005), between 3 and 5 months of age, were group housed with food and water freely available. The *cbln1$^{-/-}$* mice were backcrossed to the C57Bl/6J strain for more than nine generations. Sprague-Dawley rats (Harlan Sprague-Dawley; Indianapolis, IN) were group housed with food and water available *ad libitum*. All studies were performed in accordance with the National Institutes of Health Guide for Care and Use of Laboratory Animals and under the oversight of the institutional Animal Care and Use Committee.

Immunohistochemistry. The basic methods follow those as described in Chapter III, with the exception that an antigen retrieval method was used to enhance Cbln1 staining. Free-floating sections were incubated in 10 mM sodium citrate buffer containing 0.05% Tween 20 (pH 6.0) at 80°C for 25-30 min, and then washed extensively before the tissue was processed for immunohistochemical localization of Cbln1, using a previously characterized (E3) antibody (see Bao et al., 2005; Wei et al., 2007).

The following primary antibodies were used: rabbit anti-Cbln1 (1:600 for immunofluorescence, 1:2000 for immunoperoxidase, 1:1000 for electron microscopy; obtained from James I. Morgan (see Bao et al., 2005 and Wei et al., 2007), goat anti-cholera toxin B subunit (1:5000; List Biological, Campbell, CA), and mouse anti-NeuN

(1:500; Millipore). A Zeiss LSM-510 confocal microscope was used to acquire fluorescent images.

Retrograde tracer studies. FluoroGold was iontophoretically deposited in the dorsolateral striatum of rats as described in Chapter IV. In addition, three animals received pressure injections of 200 nl of Cholera toxin B (1% CTB in H_2O; List Biological Laboratories; Campbell, CA) into somatomotor cortex of animals that also received striatal FG deposits. Animals were sacrificed 10 days later, and immunohistochemical methods were used to reveal retrogradely-labeled neurons that expressed Cbln1-ir.

Chartings. The software program Neurolucida (MBF Bioscience; Williston, VT) was used to chart the distribution of Cbln1-ir elements in the thalamus and striatum.

Intracellular injections of MSNs. Two adult, male Sprague-Dawley rats were rapidly perfused with 300 ml of 9.25% sucrose at 37° C, followed by 100-150 ml of 4% paraformaldehyde in phosphate buffer. The brains were then removed, postfixed at 4^oC for 30 minutes, and 150 μm-thick coronal sections were cut on a vibrating microtome. Striatal cells were iontophoretically filled with 8% LY (Sigma-Aldrich, St. Louis, MO) in 50 mM Tris, pH 7.4, using continuous +5.0 nA current for 3-5 minutes. Immunohistochemistry was subsequently used to localize Cbln1 in axons, as described above. The software program Imaris (Bitplane, Saint Paul, MN) was then used to analyze Cbln1 appositions with MSN dendrites.

Ultrastructural studies of striatal MSN dendrites. For electron microscopic localization of Cbln1-ir, animals were sacrificed and perfused with 4% paraformaldehyde, 0.2% glutaraldehyde, and 0.2% picric acid in PBS. The brains were blocked and postfixed in 4% paraformaldehyde for 4 hours.

Coronal 50 μm thick vibratome sections of the striatum were cut and stored frozen at -80°C in 15% sucrose until immunohistochemical experiments were performed. Single-label immunoperoxidase methods were performed as previously described (Muly et al., 2003), using the rabbit anti-Cbln1 antibody. Briefly, sections were thawed, incubated in blocking serum (3% normal goat serum, 1% bovine serum albumin, 0.1% glycine, 0.1% lysine in 0.01 M phosphate buffered saline, pH 7.4) for 1 hour and then placed in primary antiserum diluted in blocking serum. After 36 hours at 4°C, the sections were rinsed and placed in a 1:200 dilution of biotinylated goat anti-rabbit IgG (Jackson Immuno Research, West Grove, PA) for 1 hour at room temperature. The sections were then rinsed, placed in avidin-biotinylated peroxidase complex (ABC Elite, Vector, Burlingame, CA) for 1 hour at room temperature, and then processed to reveal peroxidase using 3,3$^{'}$-diaminobenzidine (DAB) as the chromagen. Sections were then post-fixed in osmium tetroxide, stained *en bloc* with uranyl acetate, dehydrated, and embedded in Durcupan resin (Electron Microscopy Sciences, Fort Washington, PA). Selected regions of the dorsal striatum were mounted on blocks, and ultrathin sections were collected onto pioloform-coated slot grids and counterstained with lead citrate. Control sections, processed as above except that the primary antiserum was admitted, did not contain DAB label upon electron microscopic examination.

Ultrathin sections were examined with a Zeiss EM10C electron microscope and immunoreactive elements were imaged using a Dualvision cooled CCD camera (1300 x 1030 pixels) and Digital Micrograph software (version 3.7.4, Gatan, Inc., Pleasanton, CA). The tissue was scanned and every labeled terminal was examined and if a synaptic contact was identified, the terminal and postsynaptic element were imaged.

<div align="center">Results</div>

Cbln1 in thalamostriatal neurons. Essentially all PF cells displayed dense Cbln1-immunoreactivity (Fig. 16 and 17). We did not observe any Cbln1-ir in the PF or any other brain site (data not shown) of *cbln1* knockout mice; however, Cbln1-ir was observed in the PF of *cbln2* and *cbln4* knockout mice, validating the specificity of the Cbln1 antibody (Fig. 18). Cbln1-ir in PF cells was characteristically punctate (Fig. 17), with the soma and most proximal dendrites being stained. In contrast to the PF, only rarely were Cbln1-ir cells observed in the centrolateral and paracentral nuclei (see Fig. 16). All Cbln1-ir cells in the PF expressed the neuronal marker NeuN (Fig. 17).

Virtually all PF cells that were retrogradely-labeled from the striatum showed Cbln1-ir (Fig. 19). Previous studies have shown that PF neurons also project to the cortex, and single PF neurons collateralize to innervate both the striatum and cortex (Deschênes et al., 1995, 1996). We therefore also examined several cases involving retrograde tracer deposits of FG into the lateral striatum and CTB into the somatomotor cortex. We found that PF neurons innervating the cortex showed Cbln1-ir (Fig. 20). Moreover, some neurons were triple-labeled for Cbln1, FG, and CTB, indicating that these PF cells collateralized to innervate both striatal and cortical projection fields of
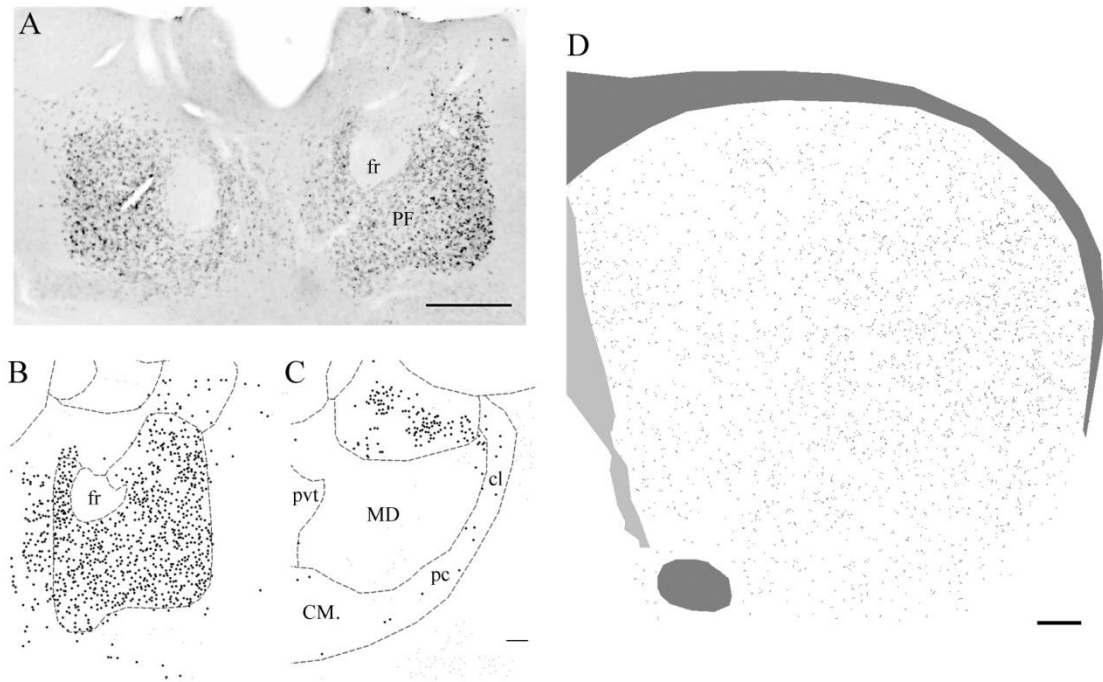
Figure 16. Distribution of Cbln1-immunoreactivity (-ir) in the thalamus and striatum. *A)* Cbln1-ir in cells of the PF. Cbln1-ir cells are seen throughout the PF. *B-C)* Chartings of the distribution of Cbln1-ir neurons in the PF (B) and in the CM complex (panel C). In contrast to the PF, only rare cells in the CM complex, including centrolateral, paracentral, and central medial nuclei, display Cbln1-ir. The cluster of Cbln1-ir cells dorsomedial to the centrolateral (CL) nucleus is in the lateral habenula. *D)* Charting of the distribution of Cbln1-ir axons in the striatum. Cbln1-ir axons are seen throughout the striatum, but with a clear mediolateral gradient in their density. Abbreviations: CM, central medial complex; cl, centrolateral division of CM; pc, paracentral division of CM; fr, fasciculus retroflexus; MD, mediodorsal nucleus of the thalamus; pvt, paraventricular thalamic nucleus. Scale bar panel *A,* 200 μm; *B, C* 100 μm; *D,* 100 μm.
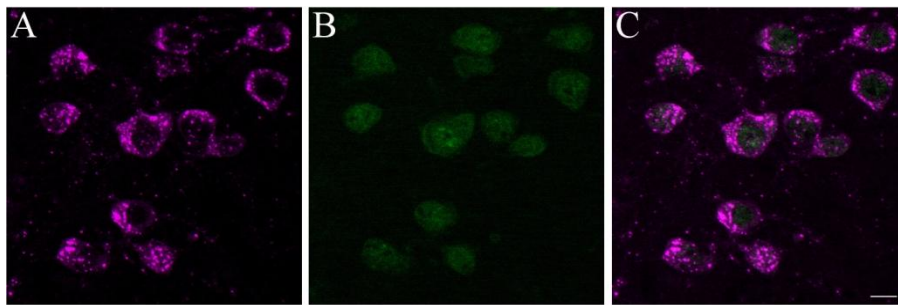
Figure 17. Cbln1 is expressed in PF neurons. *A-C)* Cbln1-ir cells (shown in magenta) in the PF (panel A) also express the neuronal marker NeuN (shown in green in panel B), with the merged image shown in C. Scale bar, 10 μm.
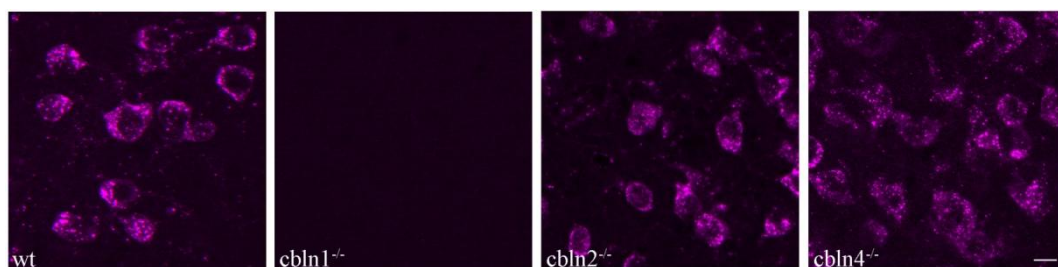
Figure 18. Cbln1-immunoreactivity (-ir) in the PF of wildtype (wt), *cbln1$^{-/-}$*, *cbln2$^{-/-}$, and cbln4$^{-/-}$* mice. No Cbln1-ir is seen in the PF of the *cbln1* knockout mouse. In the PF of *cbln2$^{-/-}$* and *cbln4$^{-/-}$* mice, Cbln1-ir appeared unaltered. Scale bar, 10 μm.
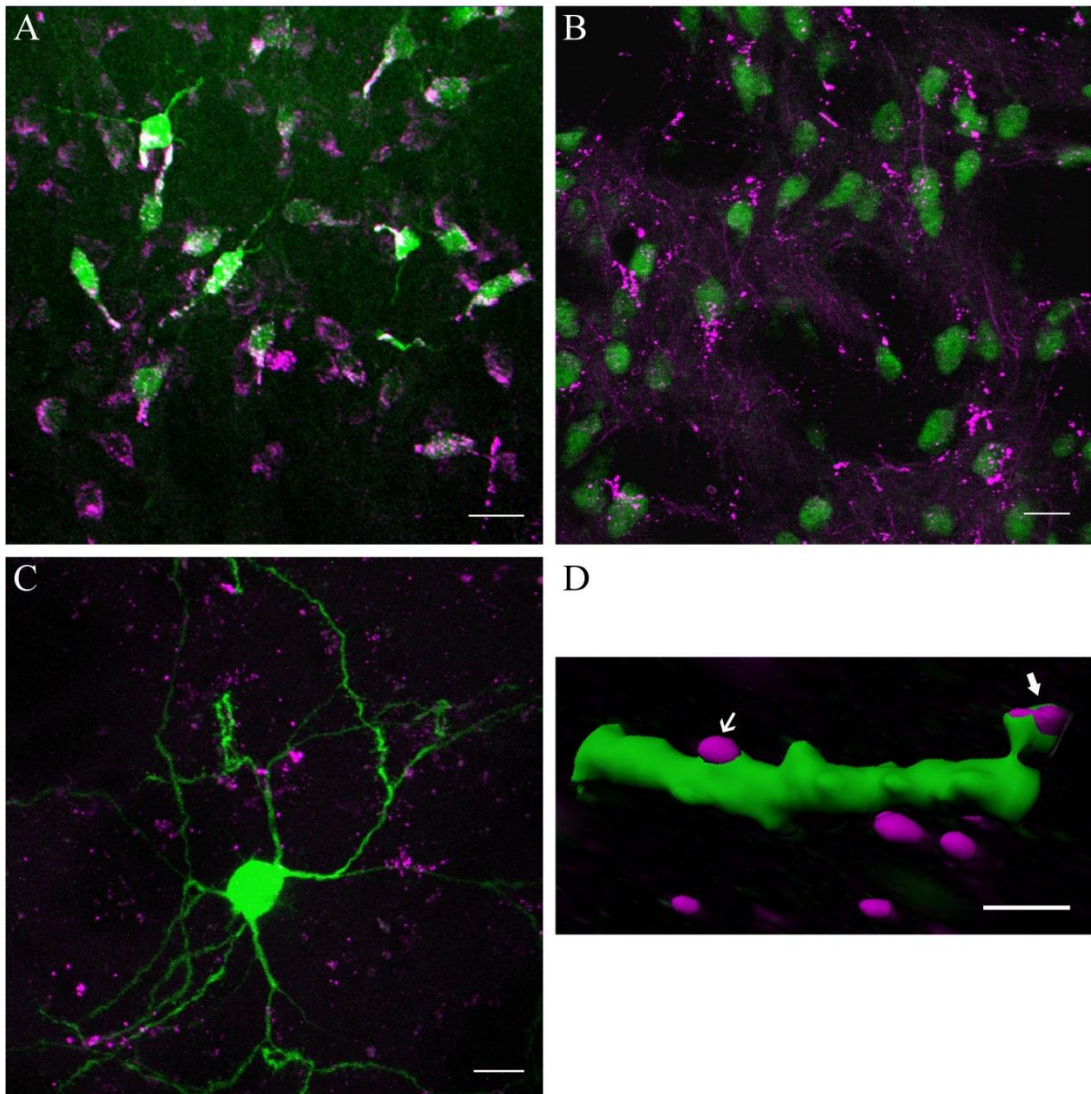
Figure 19. Cbln1 is expressed in PF thalamostriatal neurons and in striatal axons. *A)* PF neurons were retrogradely-labeled from the striatum with FluoroGold (green). All retrogradely-labeled FG cells expressed Cbln1 (magenta), although some Cbln1-ir cells, seen toward the bottom of the panel, were not retrogradely-labeled. *B)* Fine-caliber Cbln1-ir axons (magenta) are present in the striatum, with profuse terminal plexi that appear to be apposed to the dendrites and somata of striatal NeuN-ir neurons (green). *C-D)* Relationship of Cbln1-ir axons (magenta) to Lucifer Yellow-filled MSNs (green). In panel C a merged confocal image shows that Cbln1-ir axons are interspersed among the dendrites of MSNs. Panel D shows an Imaris reconstruction of a confocal image revealing Cbln1-ir appositions onto both a spine head and the dendritic shaft of a distal MSN dendrite. Scale bars: *A-B*, 20 μm; *C*,10 μm; *D*, 2.0 μm.
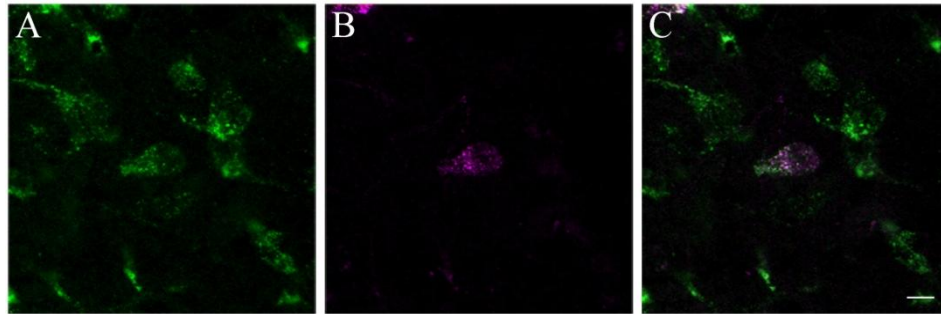
Figure 20. Thalamocortical PF neurons exhibit Cbln1 immunoreactivity. *A-C)* PF neurons were retrogradely-labeled from the somatomotor cortex with cholera toxin B (magenta) and then processed to reveal Cbln1-ir (green). PF cells that were retrogradely-labeled from the cortex expressed Cbln1-ir. Scale bar, 10 μm.

the PF.

Cbln1 in the striatum. Cbln1-ir processes were scattered throughout the striatum, with an

appreciably greater density in the lateral than medial striatum (Fig. 16). Occasionally,

fine-caliber non-varicose Cbln1-ir axons were seen to terminate in pericellular arrays

surrounding striatal neurons (Fig. 19), the great majority of which had a soma size (8-17

μm) that corresponds to that of MSNs. We also examined striatal cells that were injected

intracellularly with Lucifer Yellow and then processed to reveal Cbln1-ir. Using this

method, we confirmed that the major target of Cbln1-ir axons was the MSN, with image

analysis showing that Cbln1-ir axons were apposed to both dendritic spines and dendritic

shafts (Fig. 19). At the light microscopic level, Cbln1-ir was typically not observed in

NeuN-ir striatal neurons (Fig. 19), although rarely what appeared to be Cbln1-ir puncta

were seen in cell bodies.

In order to determine if areas other than the PF send Cbln1 projections to the

striatum, we deposited the retrograde tracer FG into the lateral striatum and then charted

the presence of double-labeled (FG-positive–Cbln1-ir) neurons in the cortex, SN, and

other areas. Although we observed a dense cluster of Cbln1-ir cells in the retrosplenial

cortex, none of these cells were retrogradely-labeled from the striatum. A significant

number of FG-positive cells that did not express Cbln1 were seen lateral to the

retrosplenial cortex (Fig. 21). In other areas of the cortex, Cbln1-ir was very rarely

observed. In the SN we observed a single Cbln1-ir neuron in the dorsal tier of the pars

compacta that was retrogradely-labeled from the lateral striatum (Fig. 21). A cluster of

Cbln1-ir cells was present in the SN pars lateralis, but these cells were not retrogradely

labeled. We did not see any double-labeled Cbln1-ir--PF-positive cells in the dorsal

72
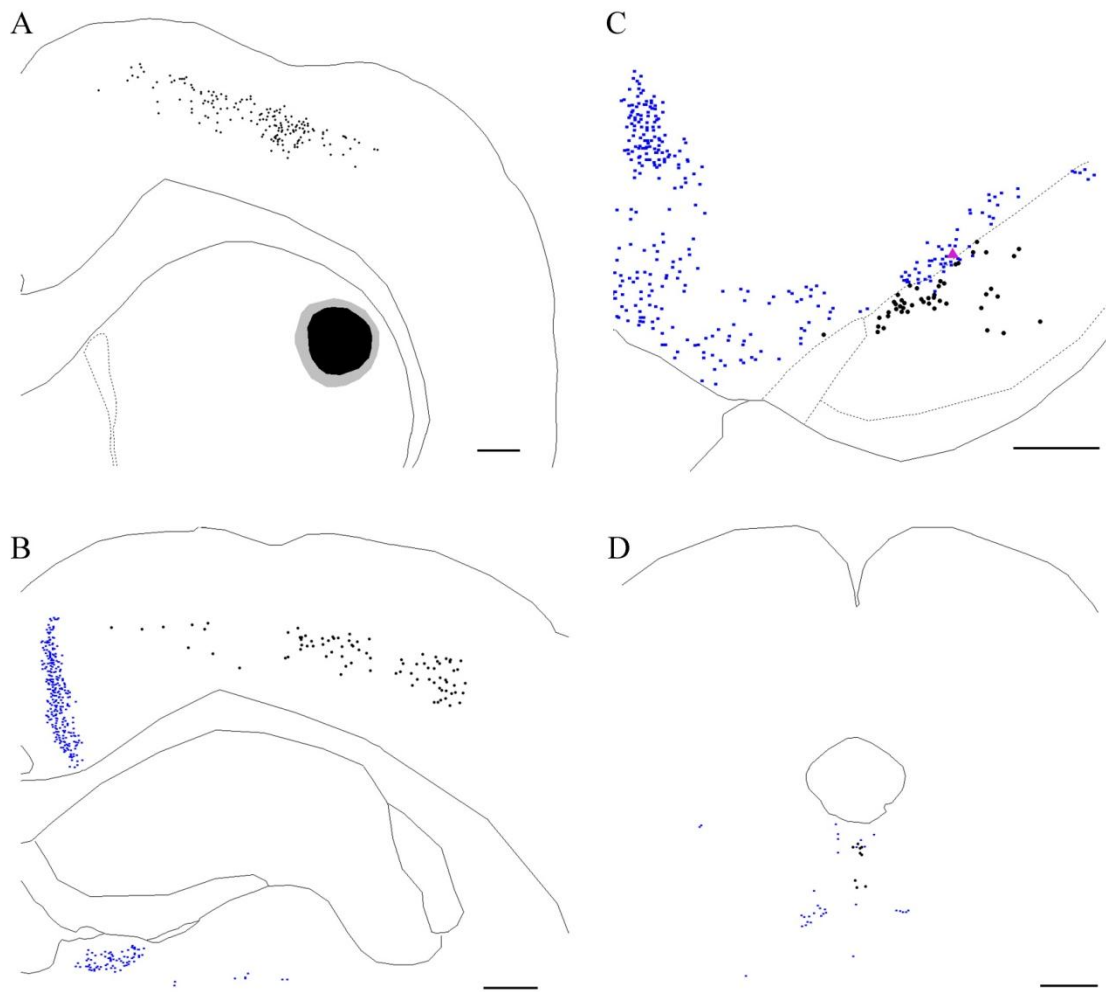
Figure 21. Cbln1-ir neurons in extra-thalamic regions of the brain do not innervate the striatum, as revealed by retrograde tract tracing with FluoroGold (FG). *A)* Charting of the FG deposit into the striatum, showing the dense core (black) and more lightly-labeled penumbra (gray). The presence of FG-positive retrogradely-labeled neurons (black) in the cingulate and motor cortices is seen, but no Cbln1-ir cells (blue) are present. *B)* In the retrosplenial cortex a dense aggregation of Cbln1-ir neurons (blue) are present. However, cells that are retrogradely-labeled (black) are found more laterally, in the motor and somatosensory regions. A cluster of Cbln1-ir neurons is also seen in the habenula. *C)* With the exception of one double-labeled cell (magenta) just above the dorsal tier of the substantia nigra pars compacta, no nigrostriatal cells exhibited Cbln1-ir. There is a relatively dense collection of Cbln1-ir cells dorsal to the pars compacta, and in the ventral tegmental area, including the nucleus linearis. *D)* No Cbln1-ir cells in the vicinity of the dorsal raphe were retrogradely-labeled after striatal FG deposits. Scale bars, 500 μm.

or median raphe (Fig. 21). In summary, these data suggest that virtually all of the Cbln1 innervation of the lateral striatum is derived from the PF.

Ultrastructural observations on Cbln1-ir in the striatum. Cbln1-ir in the striatum was observed in both pre-terminal axon segments and axon terminals (Fig. 22).   In addition, Cbln1-ir was occasionally seen in myelinated axons. Within pre-terminal axons cut in cross section, the reaction product was often found throughout the labeled profile. The immunoreactive product in larger terminals usually did not fill the entire profile; Cbln1-ir was seen close to the plasma membrane of the terminal, with DAB reaction product interspersed between the plasma membrane and synaptic vesicles. In some cases, the label was present between the plasma membrane and a mitochondrion in the terminal; these patches of immunoreactivity were on some occasions in close proximity to a presynaptic specialization.

In addition to the presynaptic localization of Cbln1-ir, we also observed some Cbln1-immunoreactivity in MSNs, both in dendritic shafts and spines (Fig. 22). In dendritic shafts, patches of DAB reaction product were associated with either the plasma membrane or internal membranous structures. In smaller dendritic spines, label sometimes filled the spine. More frequently, patches of label were observed, sometimes associated with the plasma membrane and occasionally associated with the spine apparatus. The postsynaptic densities (PSDs) of asymmetric synapses on spines and dendrites were frequently so dark they appeared to be labeled. In some cases, these dark PSDs were contiguous with patches of DAB label that extended laterally and/or internally, suggesting that at some synapses, Cbln1-ir was associated with the postsynaptic specialization. However, because the PSD is so electron dense, it is not
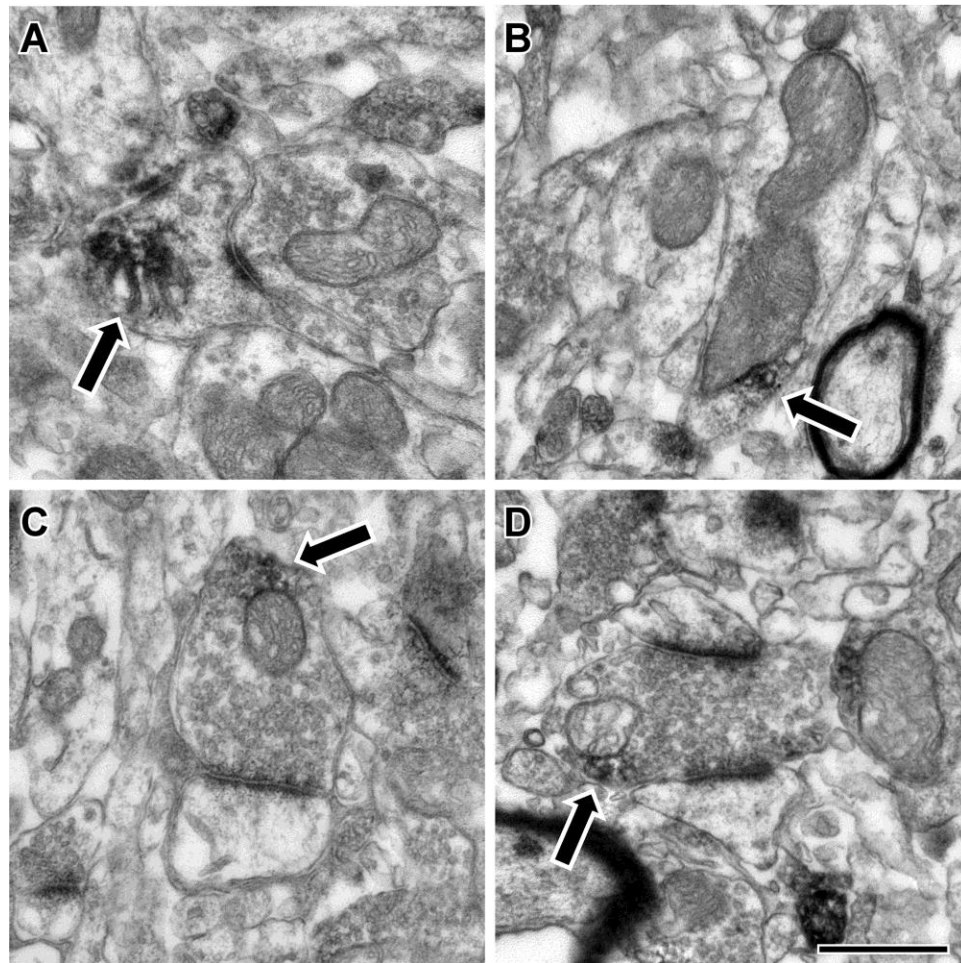
Figure 22. Electron microscopic localization of Cbln1 immunoreactivity in the rat striatum. Cbln1-ir (arrows) was found in many different subcellular compartments in the striatum, including axon terminals and dendrites. *A)* Within spines, Cbln1-ir was occasionally associated with the spine apparatus. *B)* In dendrites, Cbln1-ir was often observed adjacent to mitochondria, though other small vesicular structures were also seen nearby. *C-D)* Within axon terminals, Cbln1-ir was also often observed near mitochondria or vesicles in close proximity to the mitochondria. Synaptic contacts made by labeled terminals were always asymmetric and targeted both spines (panel C) and dendrites (panel D). Scale bar represents 500 nm in *A*, *C*, and *D*; and 600 nm in *B*.

possible to state with any certainty if Cbln1 is associated with the PSD.

Discussion

Cbln1 was localized to a subset of thalamostriatal projection neurons: thalamostriatal axons originating in the PF but not CeM, PC, or CL displayed Cbln1-ir. This distribution of Cbln1-ir is consistent with the distribution of *cbln1* mRNA-expressing cells in the rodent thalamus (Miura et al., 2006), but differs somewhat from that seen in primates, where Cbln1-ir is present across the intralaminar thalamic nuclei that innervate the striatum, including the CM and CeM nuclei as well as the PF (Murray et al., 2007; K. D. Murray, personal communication). Essentially all PF cells in both the mouse and rat express Cbln1. Because all Cbln1-ir cells in the PF also express NeuN-ir, Cbln1 is localized to neurons but not glia, consistent with the observations of Wei et al. (2007). Tracer deposits into the dorsolateral striatum revealed that all PF cells retrogradely-labeled from the striatum expressed Cbln1.

Cbln1-ir processes were seen across the entire striatum but with a clear lateral-to-medial gradient, a pattern consistent with the projection of PF neurons onto the striatum (Berendse and Groenewegen, 1990). *In situ* hybridization histochemistry studies have not observed Cbln1 mRNA in striatal neurons (Miura et al., 2006), suggesting that the Cbln1-ir in axonal plexuses in the striatum is derived from extra-striatal sites.

We did not observe retrograde labeling of Cbln1-ir cortical neurons after tracer deposits into the striatum, consistent with the lack of *cbln1* mRNA or Cbln1-ir in most cortical neurons (Miura et al., 2006; Wei et al., 2007). Although the retrosplenial cortex contains Cbln1-ir cells, our tracer injections into the dorsolateral striatum failed to label

cells in this cortical area, consistent with a projection of the retrosplenial cortex to the medial but not lateral striatum (McGeorge and Faull, 1989). Moreover, with the exception of a single Cbln1-ir neuron in the dorsal tier of the substantia nigra, we did not observe any double-labeled cells in the cortex, midbrain, or pons. Thus, it appears that lateral striatal Cbln1-ir afferents almost exclusively originate in the PF. We have not systematically examined the origin of Cbln1 axons in the medial striatum.

We saw very fine Cbln1-ir axons arborizing amidst the dendrites of striatal cells with a soma size characteristic of MSNs. Intracellular LY injections confirmed that MSNs were the primary target of Cbln1-ir inputs. The density of these Cbln1-ir axons is somewhat less than might be expected in light of the abundant expression of Cbln1 mRNA and protein in PF neurons. This may reflect rapid release of Cbln1 from striatal terminals of PF neurons. The storage compartment for release of Cbln1 remains unclear. Wei et al. (2007) found that Cbln1-ir is localized to lysosomes and late-stage endosomes, based on its colocalization with the lysosomal marker, cathepsin D.

Our light microscopic computer-aided reconstructions suggested that Cbln1-ir axons were apposed to both MSN dendritic spines and shafts. Consistent with these observations, our ultrastructural examination revealed that presynaptic Cbln1-ir terminals synapse predominantly but not exclusively with MSN spines. Lacey et al. (2007) showed that some PF neurons form both axospinous and axodendritic synapses with MSNs, while others predominantly make axospinous synapses.

Somewhat surprisingly, our ultrastructural studies also revealed that Cbln1-ir is relatively common in MSNs, particularly in dendritic spines. This finding stands in contrast to the lack of *cbln1* mRNA, as detected by *in situ* hybridization histochemistry or

77

RT-PCR in striatal neurons (Miura et al., 2006), although there are examples of various transcripts not being expressed under basal conditions that become apparent after an appropriate challenge (Deutch and Zahm, 1992). Our ultrastructural findings are consistent with recent data of Wei et al. (2009), who showed that Cbln1 is released from cerebellar granule cells and then accumulates in Purkinje cells, i.e., is accumulated by postsynaptic elements after release from Cbln1-containing terminals. Thus, it appears that Cbln1 from thalamostriatal neurons may influence MSNs either by interacting with an as yet un-identified receptor on MSNs, or by being incorporated by striatal cells and then exerting some effect. In the next chapter, we will discuss experiments to assess the functional impact of Cbln1 on striatal synapses using *cbln1$^{-/-}$* mice.

CHAPTER VI

GENETIC DELETION OF CBLN1 ALTERS MEDIUM SPINY NEURON DENDRITIC SPINE DENSITY AND SYNAPSES

In the cerebellum, Cbln1 is secreted as either a homo- or hetero-trimeric complex from granule cells (Pang et al., 2000; Bao et al., 2005, 2006; Wei et al., 2007) and binds to an unknown receptor on Purkinje cell dendrites (Matsuda et al., 2009). It has also been shown to be transported across granule cell-Purkinje cell synapses (Wei et al., 2009).

Cbln1 is essential for maintaining the structure and function of granule cell-Purkinje cell synapses (Hirai et al., 2005). *Cbln1* null mutant mice have a decreased number of granule cell-Purkinje cell synapses, with many Purkinje cell dendritic spines lacking a presynaptic partner (Hirai et al., 2005; Ito-Ishida et al., 2008). These morphological changes are associated with an absence of long-term depression at granule cell-Purkinje cell synapses and gross ataxia (Hirai et al., 2005). A recent report noted that the injection of recombinant Cbln1 into the subarachnoid space of *cbln1*$^{-/-}$ mice transiently restores synapse number in the cerebellar cortex (Ito-Ishida et al., 2008).

In the previous chapter, we discovered that the PF is the primary source of Cbln1 inputs to dorsolateral striatum. Based on studies indicating that Cbln1 regulates cerebellar synaptic function, we hypothesized that genetic deletion of Cbln1 would similarly alter MSN synapses.

Methods

We determined how genetic deletion of Cbln1 alters striatal synapses using two different approaches. First, we used the Golgi method to impregnate MSNs and allow the assessment of structural changes in MSN dendrites. Second, we evaluated whether the number of axospinous synapses, length of the postsynaptic density, or density of perforated axospinous synapses was altered in the *cbln1*-null mice using electron microscopy.

To begin to assess whether a change in PF neurons could account for the alterations in striatal synapse seen in the *cbln1*-null mouse, we also assessed if the number of PF cells was changed in the *cbln1$^{-/-}$* mouse. In addition, we evaluated if expression of VGluT2, a marker of thalamostriatal axons, was altered in immunoblots prepared from the dorsolateral striatum of *cbln1*-null mice and their wildtype littermates. Finally, we examined changes in striatal dopamine concentration in the *cbln1*-null mice relative to their wildtype littermates.

Animals. Adult *cbln1$^{-/-}$* mice and their wildtype littermates (Hirai et al., 2005), between 3 and 5 months of age, were group housed with food and water freely available. The *cbln1$^{-/-}$* mice were backcrossed to the C57Bl/6J strain for more than nine generations. Sprague-Dawley rats (Harlan Sprague-Dawley; Indianapolis, IN) were group housed with food and water available *ad libitum*. All studies were performed in accordance with the National Institutes of Health Guide for Care and Use of Laboratory Animals and under the oversight of the institutional Animal Care and Use Committee.

Golgi impregnation. *cbln1* null mutant mice and their wildtype littermates were perfused with 0.1 M phosphate buffer followed by a solution containing 2% paraformaldehyde--2.5% glutaraldehyde in 0.1M phosphate buffer. Coronal sections (150 μm) through the precommissural striatum were cut on a vibrating microtome. The sections were then incubated in 1% osmium tetroxide for 30 minutes and kept in 3.5% potassium dichromate overnight. The next day the sections were developed in 1% silver nitrate for 4-6 hours before being washed extensively, mounted, and coverslipped.

Dendritic analyses of MSNs. Golgi-stained striatal MSNs in the lateral striatum were reconstructed using Neurolucida. Dendritic spine density was determined on segments of secondary or tertiary dendrites at distances between 70 and 90 μm from the soma by an investigator blind to the treatment. Segments from three different dendrites per neuron and 5-6 neurons per animal were analyzed to compute an average dendritic spine density for a given animal. Total dendritic length was also determined.

The length of dendritic spines was measured in >50 spines/animal of *cbln1* knockout and wildtype mice by an investigator blind to the treatment. We also determined the shape of dendritic spines in *cbln1*^{-/-} mice, following the classification scheme of Peters and Kaiserman-Abramof (1970).

Ultrastructural studies of MSN synapses. Animals were perfused with 4% paraformaldehyde, 0.2% glutaraldehyde, and 0.2% picric acid in PBS. The brains were blocked and postfixed in 4% paraformaldehyde for 4 hours. For ultrastructural examination of synapses, 2 *cbln1* wildtype and 2 *cbln1* knockout mice were perfused.

Coronal 50 μm thick vibratome sections of the striatum were cut and stored frozen at -80°C in 15% sucrose. Ultrathin sections were examined with a Zeiss EM10C electron microscope and immunoreactive elements were imaged using a Dualvision cooled CCD camera (1300 x 1030 pixels) and Digital Micrograph software (version 3.7.4, Gatan, Inc., Pleasanton, CA). The tissue was scanned and every labeled terminal was examined and if a synaptic contact was identified the terminal and postsynaptic element were imaged.

Fifty images from each animal were examined, for a total of 1,108 um^2 for each genotype. Asymmetric synapses were identified and the postsynaptic element was identified as a spine or dendritic shaft; the density of axospinous synapses was calculated. In order to determine if differences in the size of postsynaptic densities contributed to observed differences in synaptic density, we measured the length of axospinous synaptic PSDs in each condition (N = 264 for wildtype and N = 292 for knockout).

Stereological evaluation of PF neuron number. The number of PF neurons in Nissl-stained coronal sections (42 μm) in *cbln1$^{-/-}$* mice was determined using the optical dissector method (Stereo Investigator; MBF Bioscience).

Immunoblot analyses. The dorsolateral striatum was rapidly dissected from 1.0-mm-thick coronal sections of *cbln1* null mutant mice (N=4) and their wildtype littermates (N=4) and then stored at -80°C. The frozen tissue was sonicated in 300 μL of 2% SDS containing a 1:10,000 dilution of a protease inhibitor cocktail (P8340; Sigma-Aldrich). The appropriate volume of sample buffer (4% SDS, 20% glycerol, 0.12M Tris, 0.01% bromophenol blue, pH 6.8) was added to the homogenates to adjust the protein concentration of each sample to 10 μg/15 μL. The samples were then stored at -80°C.

Striatal protein homogenates (10 μg total protein) were separated using SDS-PAGE and transferred to nitrocellulose membranes. The membranes were stained with 0.2 % Ponceau-S in 1% acetic acid and digitally scanned. The membranes were blocked in 4% milk (in PBS containing 0.2% Tween-20) and incubated in a rabbit anti-VGluT2 antibody (1:500; MAb Technologies, Stone Mountain, GA) overnight at 4^oC. The membrane was then rinsed in PBS and incubated in horseradish peroxidase-conjugated donkey anti-rabbit IgG (1:10,000; Jackson Immunoresearch; West Grove, MA) for 2 hours. The membrane was then rinsed in PBS and developed using enhanced chemiluminescence (Perkin Elmer; Waltham, MA). Multiple X-ray film exposures were obtained.

The films were digitally scanned, and the optical density of the bands was determined using ImageJ. The samples were normalized to the total protein loaded, as assessed by Ponceau S-staining (Aldridge et al., 2008). The mean normalized signal from the wildtype mice was set at 100%, and the $cbln1^{-/-}$ data was expressed relative to this value.

Dopamine concentration. The dorsolateral striatum was rapidly dissected from $cbln1^{-/-}$ mice and their wildtype littermates. Samples were stored at −80°C until assayed. Regional concentrations of dopamine were assessed by high pressure liquid chromatography-electrochemical detection (HPLC-EC) as described by Deutch and Cameron (1992).

Statistical analyses. Differences across genotypes in dendritic spine density and dendritic length were analyzed by t-tests. The proportions of different morphological types of spines were analyzed by a Kruskal-Wallis non-parametric ANOVA.

In the ultrastructural studies of MSN synaptic density in $cbln1^{-/-}$ mice, the densities of axospinous synapses for both wildtype and knockout mice were calculated. In order to determine if differences in the size of postsynaptic densities contributed to observed differences, we measured the length of axospinous synaptic PSDs in each condition and compared the means with t tests.

The stereological data, the mean values for striatal VGluT2 levels, and the mean values for striatal dopamine levels were also analyzed by comparing values from Cbln1 null mutant and wildtype mice using Student's t tests.

Results

Effects of genetic deletion of cbln1 on MSN dendritic spine density and length. We observed a significant (22%) increase in MSN dendritic spine density of $cbln1^{-/-}$ relative to wildtype littermate mice ($t_7 = 7.718$, $p = .0001$; Fig. 23). All MSN spines in $cbln1$ null mutants were < 4.0 µm in length, suggesting that they are not filopodia, and the frequency distributions of spine lengths in Cbln1 knockout and wildtype mice were almost identical (Fig. 23). There were no differences across genotypes in the proportions of total spines that were thin-, stubby-, or mushroom-shaped (Fig. 23). The total dendritic length of MSNs did not differ across genotypes (Fig. 23). Dendritic spine density was unaltered in $cbln2^{-/-}$ and $cbln4^{-/-}$ mice relative to their wildtype littermates (Fig. 24).
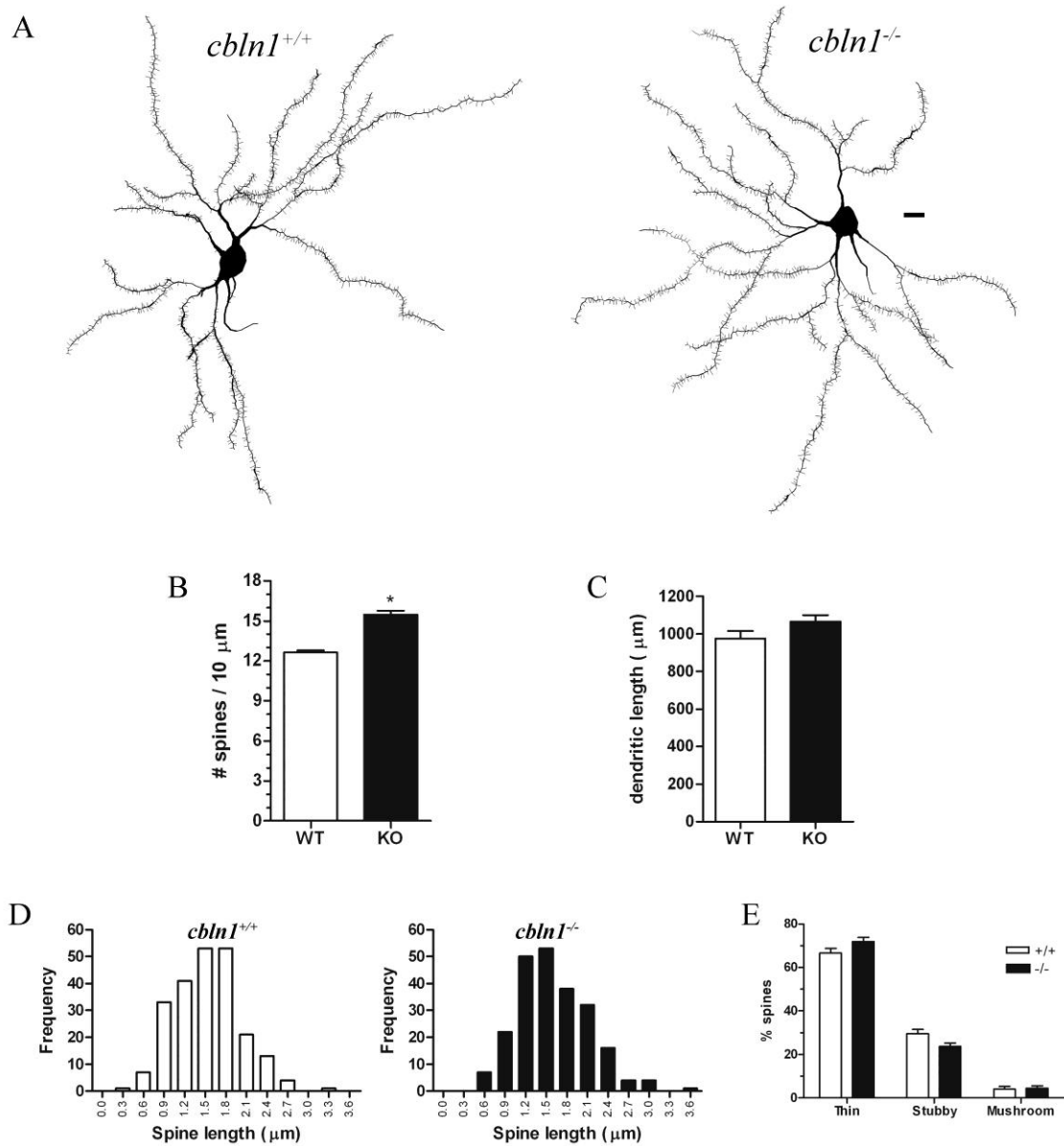
Figure 23. MSN dendritic spine density is increased in *cbln1^-/-* mice. *A)* Neurolucida reconstructions of Golgi-impregnated MSNs from *cbln1^+/+* (left) and *cbln1^-/-* (right) mice. Scale bar, 10 μm. *B)* Dendritic spine density is increased in the *cbln1* knockout (KO) relative to wildtype (WT) mice. *C)* Total dendritic length of MSNs does not differ across genotypes. *D)* The frequency distributions of the length of MSN spines are not significantly different across *cbln1^+/+* and cbln1^-/- mice. Moreover, none of the spines has a length corresponding to that of filopodia (> 4.5 μm). *E)* No differences in the proportions of thin, stubby, or mushroom-shaped MSN spines were observed across genotypes.
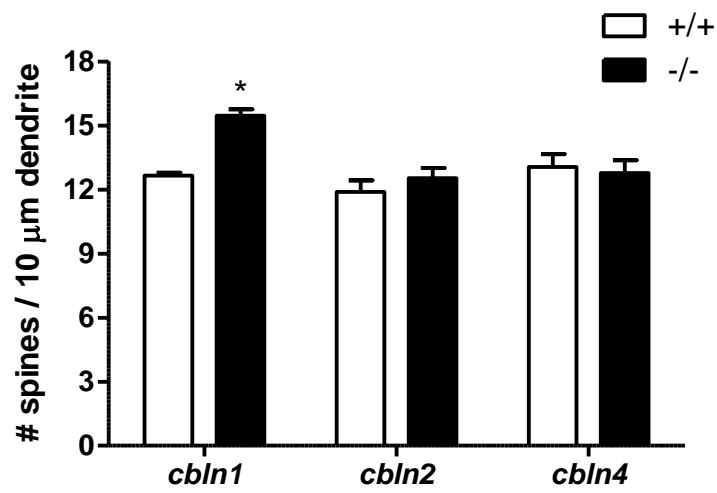
Figure 24. MSN dendritic spine density is increased in *cbln1*$^{-/-}$ mice, but is unaltered in *cbln2*$^{-/-}$ and *cbln4*$^{-/-}$ mice relative to their wildtype littermates.

Medium spiny neuron synaptic changes in cbln1 knockout mice. Consistent with the increase in spine density in the *cbln1*$^{-/-}$ mice, we observed a 21.7% increase in the frequency of axospinous synapses of *cbln1* knockout relative to wildtype mice (2.45 synapses/10 μm^2 for *cbln1*$^{-/-}$ versus 2.01 synapses/10 μm^2 for *cbln1*$^{+/+}$ mice). Thus, although MSN dendritic spine number was increased in *cbln1*$^{-/-}$ mice, these spines were not "naked" but had synaptic partners. Because we examined only two animals of each genotype these values were not statistically different, although a strong trend was uncovered (t=3.60; p=0.069). The relative difference in axospinous synapses across wildtype and *cbln1*$^{-/-}$ mice was not due to larger PSDs in the knockout mice, which would have rendered axospinous synapses more easily observed in random single sections: mean PSD lengths were 0.236 μm for *cbln1*$^{-/-}$ versus 0.228 μm for wildtype mice. In addition, the incidence of perforated axospinous PSDs did not differ across genotypes (χ^2=0.129; NS).

Alterations in PF neurons and striatal dopamine. In order to begin to examine possible mechanisms that could account for the change in dendrite, we examined whether the number of PF neurons was altered in the *cbln1*-null mice relative to their wildtype littermates. Stereological assessment revealed that the number of Nissl-stained PF cells did not differ significantly across genotypes (Fig. 25). Consistent with this observation, immunoblot methods did not uncover any differences in striatal VGluT2 levels between *cbln1* knockout and wildtype mice (t_5 = 1.14; NS; Fig. 25). We did not observe a change in striatal dopamine concentration in the *cbln1* knockout mice relative to wildtype mice (t_{10} = .28; NS; see Fig. 26).

A

PF Neurons

B
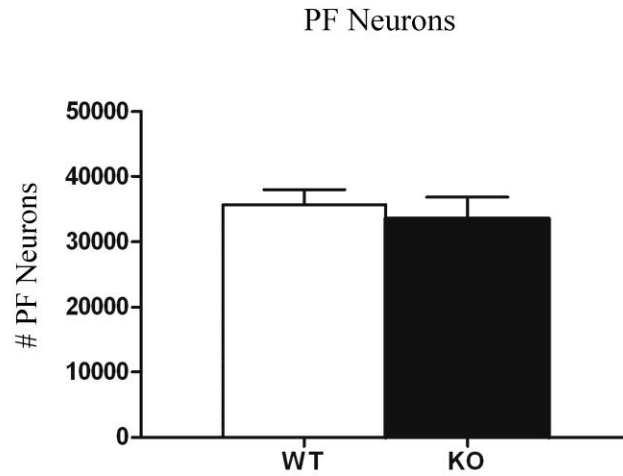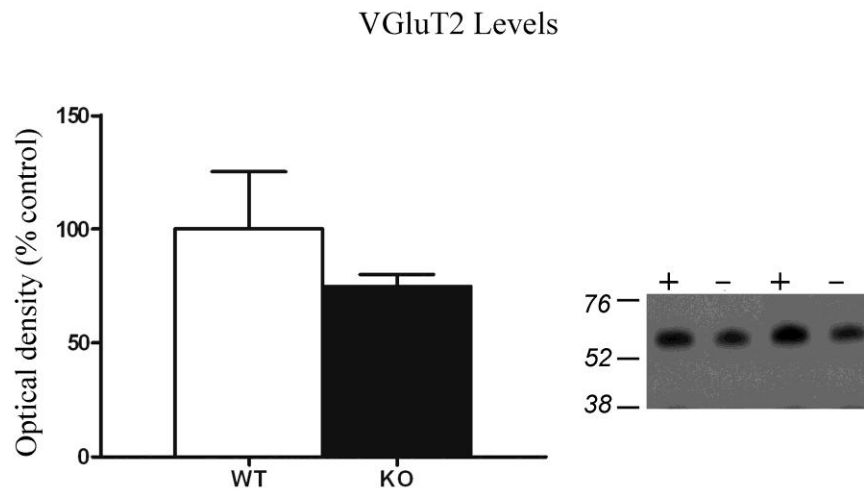
VGluT2 Levels

Figure 25. The number of PF neurons and striatal VGluT2 levels are unaltered in the *cbln1*^{-/-} mice. ***A)*** There is no difference in the number of PF neurons in *cbln1* knockout (KO) and wildtype (WT) mice, as revealed by sterological assessment. ***B)*** Striatal VGluT2 levels, as revealed by a single band at ~65 kDa on immunoblots, are not significantly different in *cbln1* KO (−) and WT (+) mice.
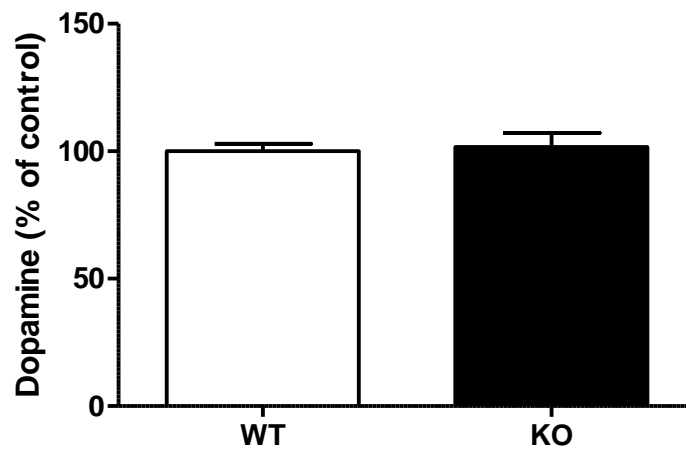
Figure 26. Striatal dopamine concentrations were unaltered in *cbln1* knockout mice (KO) relative to their wildtype (WT) littermates.

<u>Discussion</u>

Genetic deletion of *cbln1* increased the density of MSN dendritic spines, with a corresponding increase in the frequency of axospinous synapses on MSNs. These findings offer the first demonstration of extra-cerebellar actions of Cbln1 and indicate that the actions of Cbln1 differ markedly across brain regions.

We observed a marked increase in the density of MSN dendritic spines in $cbln1^{-/-}$ mice. Because lateral striatal afferents from sources other than the PF do not express Cbln1, it appears that the increased number of dendritic spines in the $cbln1^{-/-}$ mouse is due to the loss of Cbln1 in thalamostriatal neurons.

The increased number of dendritic spines was not attributable to an increase in the number of filopodia, immature spines that are longer than mature spines. Thus, mean spine length and the frequency distributions of spine length were virtually identical across *cbln1* knockout and wildtype mice. In addition, the observation that the proportion of total spines of different morphological classes was the same across genotypes further suggests that the spines that are present on striatal MSNs are mature. At the ultrastructural level we observed no change in the length of the postsynaptic density, consistent with a normal synaptic organization with an increased frequency of synaptic contacts.

In addition to Cbln1, PF neurons also express Cbln2 and Cbln4 mRNA (Miura et al., 2006). We did not observe a change in MSN dendritic spine density of the $cbln2^{-/-}$ or $cbln4^{-/-}$ mice relative to their wildtype littermates. Thus, it appears that Cbln2 and Cbln4 do not play an essential role in regulating MSN synapses.

The increased density of dendritic spines and frequency of axospinous asymmetric synapses in *cbln1*$^{-/-}$ mice is the opposite of changes reported in the cerebellar cortex of *cbln1* knockout mice, where there is a reduction in the number of granule cell-Purkinje cell synapses and the majority of existing dendritic spines lack a presynaptic partner (Hirai et al., 2005; Ito-Ishida et al., 2008). In addition, while there is no change in PSD length in the supernumerary MSN spines of *cbln1*$^{-/-}$ mice, PSDs are enlarged at the granule cell-Purkinje cell synapses of these mutant mice. The contrasting regionally-specific changes between the striatum and cerebellar cortex of *cbln1* null mutant mice raises the possibility that different Cbln1 receptors or intracellular signaling cascades may subserve different effects on postsynaptic neurons.

The mechanism through which loss of Cbln1 causes an increase in MSN spine density and axospinous synapses is unclear. Our stereological data indicate that the number of PF neurons is not changed in the *cbln1* knockout mouse, and striatal levels of VGluT2 are unchanged in total homogenates of the striatum, consistent with an intact glutamatergic projection of the PF to the striatum in the *cbln1*$^{-/-}$ mouse.

Studying the function of other C1q family members may give clues about how Cbln1 regulates synapses. The function of Cbln1 is similar to that of C1q in the visual system. Stevens and colleagues (2007) recently showed that C1q triggers synapse elimination in retinal ganglion cells. The expression of C1q in the visual system peaks during activity-dependent remodeling (Stevens et al. 2007). Retinal ganglion cells send ipsilateral and contralateral projections to the lateral geniculate nucleus. During development, these synapses are refined so that the contralateral projection is denser than the ipsilateral projection. Astrocytes are thought to induce C1q expression in retinal

ganglion cells. Once produced, C1q is released and binds to the postsynaptic surface, where it is thought to "tag" the synapse for removal through activation of the complement cascade. In the striatum, Cbln1 may similarly mark certain synapses for destruction, and thus, the loss of Cbln1 would result in an increase in spine density.

Cbln1 receptors have yet to be identified, although a recent study indicates that Cbln1 released from cerebellar granule cells binds to PC dendrites (Matsuda et al., 2009). Because glutamate signaling is a key regulator of spine development and maintenance (McKinney et al., 1999; Shi et al., 1999; Lippman and Dunaevsky, 2005; Richards et al, 2005; Alvarez and Sabatini, 2007) and thalamostriatal neurons are glutamatergic, it is possible that Cbln1 signals through a glutamate receptor to change the dendritic structure of MSNs. Hirai et al. (2005) found that the cerebellar phenotype of mice lacking the orphan glutamate receptor *grid2* is similar to that of the *cbln1*$^{-/-}$ mouse, including loss of granule cell-Purkinje cell synapses, and proposed that Cbln1 and grid2 are part of the same signaling pathway. Although grid2 does not bind recombinant Cbln1 (Jim Morgan, unpublished observations), the two are co-clustered at the granule cell-Purkinje cell synapse (Miura et al., 2009), leaving open the possibility that grid2 is a subunit of the Cbln1 receptor. However, neither grid2 nor its interacting protein are expressed in the PF or striatum (Gong et al., 2003), suggesting that Cbln1 may signal through unidentified receptor(s) on MSNs to increase spine density. Alternatively, Cbln1 that is released from PF axons and then incorporated into MSNs directly or in association with the internalization of a receptor (such as a G protein-coupled receptor) may modify the structures of MSNs.

Neuronal pentraxins have been shown to bind to C1q and have been proposed as a potential candidate receptor by which C1q mediates synaptic elimination in the visual system (see Stevens et al., 2007). Similar deficits in eye-specific segregation are seen in mice lacking NP1 and neuronal-regulated pentraxin (NARP; Bjartmar et al., 2006). Interestingly, pentraxins have been shown to tether members both directly and by co-assembling with NARP. An interaction between Cbln1 and members of the pentraxin family has not yet been demonstrated.

It is possible that the loss of Cbln1 modifies striatal dopamine tone and thereby increases dendritic spine density. Changes in striatal dopaminergic tone are known to alter spine density, with increases in striatal dopamine resulting in more spines and depletion of striatal dopamine eliciting spine loss (Li et al., 2003; Day et al., 2006; Deutch et al., 2007; Meyer et al., 2008). Interestingly, the cerebellin hexadecapeptide has been shown to elicit catecholamine release both *in vitro* and in perfused adrenal glands *in situ* (Mazzocchi et al., 1999; Albertin et al., 2000). The PF has been reported to send a small projection to the SN (Marini et al., 1999). However, we found little Cbln1-ir in the SN, with some Cbln1-ir axons in the pars lateralis. Thus, it is unlikely that there is a direct effect of Cbln1 on nigrostriatal dopamine neurons. Moreover, we did not observe a change in striatal dopamine concentration in the *cbln1*$^{-/-}$ mice relative to their wildtype littermates.

In Parkinson's disease, the number of neurons in the PF and CM is decreased by almost half (Henderson et al., 2000). Our observation that loss of Cbln1 leads to increased numbers of MSN dendritic spines (which is the opposite of the change seen in

PD) suggests that modulating thalamostriatal Cbln1 may be a novel means of improving

symptoms or slowing progression in PD. We will discuss this further in the next chapter.

CHAPTER VII

DISCUSSION AND FUTURE DIRECTIONS

We focused on the role of the PF and its relationship to the nigrostriatal system because of the observation that CM-PF thalamostriatal neurons degenerate in idiopathic PD (Henderson et al., 2000). Thalamostriatal neurons are glutamatergic and synapse on the dendrites of striatal MSNs (see Smith et al., 2004). Our lab discovered that corticostriatal glutamatergic neurons modulate striatal function and in particular are a critical factor in determining the loss of MSN dendritic spines in animal models of parkinsonism (Neely et al., 2007; Garcia et al., 2010). In light of these findings, we were intrigued by the possibility that the loss of CM-PF neurons could alter striatal function in PD.

Transsynaptic degeneration of PF neurons

A number of recent studies have illustrated the presence of a dopaminergic innervation of the thalamus that had hitherto been unappreciated (Sánchez-González et al., 2005; García-Cabezas et al., 2007; García-Cabezas et al., 2009). This dopaminergic projection originates from several areas, including the ventral mesencephalic dopamine cell groups (Freeman et al., 2001; Sánchez-González et al., 2005). It is particularly enriched in primate species but is also seen in the rodent (Freeman et al., 2001; Sánchez-González et al., 2005; García-Cabezas et al., 2009). The distribution of dopamine fibers across thalamic nuclei is heterogeneous. Some nuclei, such as the VA/VL, receive a

relatively dense dopamine innervation, and other nuclei, such as the primary sensory relay nuclei, receive scant or no dopamine fibers (Sánchez-González et al., 2005). Freeman and colleagues (2001) found that in the rat some nigrostriatal dopamine axons collateralize to innervate the thalamus as well as the striatum. Their findings focused on the motor thalamus and did not present data for such collateralization to other thalamic nuclei.

Aymerich and colleagues (2006) reported that nigrostriatal dopamine depletion causes a reduction in the number of retrogradely-labeled PF thalamostriatal neurons. Unfortunately, this has been interpreted by many to indicate degeneration of the PF neurons. In order to assess if there is indeed a degeneration of PF neurons secondary to a loss of nigrostriatal neurons, as has been suggested to occur in PD, we first examined the anatomical organization of the dopamine innervation of the PF and then determined if disruption of nigrostriatal dopamine neurons caused overt PF cell loss.

Using a number of different techniques, we failed to find any evidence of even a modest dopamine innervation. Moreover, we found that lesions of the dopamine cells of the SN did not cause a loss of PF cells as assessed stereologically nor did they decrease the number of retrogradely-labeled PF thalamostriatal neurons, as reported by Aymerich et al., 2006.

We hypothesized that the loss in retrograde labeling observed in the previous study was due to the inadvertent disruption of the noradrergic projection to the PF. However, in animals with lesions of the noradrergic neurons that project to the forebrain, we did not observe a change in the number of PF neurons or a significant effect on the retrograde labeling of PF neurons.

It remains unclear why the previous study found a change in retrograde labeling secondary to 6-OHDA MFB lesions. Our data, however, demonstrate that these changes are not caused by the degeneration of catecholaminergic neurons, and are unlikely to occur as a consequence of PF degeneration.

Regulation of striatal MSN dendrites by Cbln1

We therefore focused our efforts on the regulation of striatal MSN dendrites by PF thalamostriatal neurons. Parafascicular neurons are glutamatergic, but it is now clear that they also express Cbln1. Because Cbln1 had been shown to play a role in synapse development and maintenance in the cerebellar cortex, we reasoned that it might play a similar role in the terminals of the PF neurons, i.e. on MSN synapses.

Cerebellin was discovered over twenty-five years ago by Slemmon and colleagues (1984), but its function remained an enigma until only recently. In the intervening time, studies focused on the identification of the gene that encodes cerebellin, which was found to be Cbln1, and the proteolytic processing of Cbln1 (Urade et al., 1994; Bao et al., 2005). Initially, Cbln1 expression was thought to be restricted to the cerebellum, but over the last last four years, it has become evident that Cbln1 is widely expressed in the brain (Miura et al., 2006; Wei et al., 2007).

Our studies demonstrate that nearly all PF neurons express Cbln1 and that the PF axons are the exclusive source of Cbln1 to the lateral striatum. In addition, our studies provide the first demonstration of an extracerebellar action of Cbln1. We had predicted that the loss of Cbln1 would result in a decrease in striatal synapses based on its function in the cerebellum. However, we observed that the genetic deletion of *cbln1* causes

increased MSN dendritic spine density and a corresponding increase in the number of axospinous synapses in the striatum. These findings indicate that the actions of Cbln1 differ markedly across brain regions.

Enhanced excitatory input onto MSN dendrites of the *cbln1* null mouse

Excitatory synaptic inputs to the striatum mainly arise from the cortex and the PF, both of which are glutamatergic. Because Cbln1 is not expressed in cortical regions except for the retrosplenial cortex, which does not project to the dorsolateral striatum, the most parsimonious explanation for the increase in MSN synapses of the *cbln1* null mouse would be due to an increased number of PF neurons or an increased branching of their axons in the striatum.

Our stereological data indicated that there was no difference in the number of PF neurons, which suggests that the increase in MSN dendritic spines of the *cbln1* null mouse is due to an increased terminal arborization of PF axons. Because PF neurons are glutamatergic, one would suspect that an increase in the terminal arbor of PF neurons would be accompanied by a corresponding increase in VGluT2. Using immunoblots to assess VGluT2, we found no evidence of a change in levels of the transporter across genotypes. This suggests that the glutamatergic phenotype of the PF projection to the striatum is not altered in *cbln1* null mutants. However, immunoblot methods may lack the sensitivity to detect relatively small changes in levels of a protein. We observed a 22% increase in the density of axospinous synapses. Future studies will have to determine if the number of VGluT2-ir puncta apposed to MSN dendritic spines and dendritic shafts is altered. Finally, although the number of axospinous synapses was

increased in the *cbln1* null mutant, we observed no change in the number of perforated synapses, a marker of increased glutamatergic drive onto spines. This suggests there is no increase in glutamate release from PF neurons.

<p style="text-align:center">Secretion of Cbln1 from PF axons</p>

We were surprised to find Cbln1 in the dendritic shafts and spine heads of striatal MSNs in adult *cbln1* null mice because our light microscopic studies indicated that Cbln1 was not expressed in NeuN-ir neurons of the striatum. Miura et al. (2006) showed that Cbln1 mRNA was transiently expressed in the striatum at very low levels at postnatal day 1 (P1) but was absent in the adult striatum of mice. Recent studies indicate that Cbln1 is transsynaptically transported (both anterogradely and retrogradely) across cerebellar synapses (Wei et al., 2009). In light of our observations, we predict that PF axons secrete Cbln1 and that upon secretion, Cbln1 is transported across PF thalamostriatal synapses.

Because Cbln1 has been reported to be released from cerebellar granule cells (Hirai et al., 2005), it is reasonable to suppose that Cbln1 is secreted from PF neurons. However, we have not evaluated directly if Cbln1 is released from PF axons. One way to assess whether Cbln1 is secreted is to develop organotypic slice co-cultures of the thalamus (including the PF) and the striatum and then evaluate the presence of Cbln1 in the media.

How might PF neurons secrete Cbln1? In axon terminals, Cbln1 is not localized to synaptic vesicles. Wei et al. (2007) found that Cbln1-ir is localized to lysosomes and late-stage endosomes. Although this pattern of localization is typical of proteins targeted

for degradation, there are reports of neuronal secretory lysosomes (Arantes & Andrews, 2006; Coggins et al., 2007).

No studies to date have evaluated whether the release of Cbln1 is activity-dependent. However, the release of cerebellin (which is produced from a series of proteolytic cleavage events from Cbln1) has been shown to be activity-dependent in the cerebellum: cerebellin is released in a calcium-dependent manner by high potassium concentrations (Burnet et al. 1988; Urade et al. 1994).

<div align="center">Transsynaptic trafficking of Cbln1</div>

Cbln1 is anterogradely transported across cerebellar synapses (Wei et al., 2009). Given the lack of *cbln1* mRNA in the adult striatum (Miura et al., 2006) and the observation that Cbln1-ir is expressed in dendritic spines and shafts apposed to Cbln1-ir axon terminals, we propose that the postsynaptic expression of Cbln1 is the result of transsynaptic trafficking across thalamostriatal synapses.

To determine whether Cbln1 is capable of being accumulated by striatal neurons, one could prepare organotypic slice co-cultures of the cortex, striatum, and caudomedial thalamus (including the PF) from *cbln1* null mice. Once the cultures mature they could be treated with Cbln1, and ultrastructural methods could be used to evaluate sites of Cbln1 immunoreactivity.

Let us assume that the Cbln1 in striatal dendrites is transsynaptically accumulated across PF thalamostriatal synapses. How could this happen? Cbln1 should not diffuse through the membrane because it is not lipid-soluble. One possibility is that PF axons release Cbln1 and that Cbln1 then acts on a receptor, such as a G-protein coupled receptor (GPCR), at MSN dendrites, and that the binding of Cbln1 to its receptor results

in internalization of the receptor-ligand complex (Fig. 27). A second possibility is that Cbln1 enters the cell through a transporter-mediated process (Fig. 27). This seems unlikely because Cbln1 has a mass of ~20 kDa.

Our ultrastructural studies showed that Cbln1 was often seen near the plasma membrane of MSN spines. It is likely that Cbln1 is anchored in this region through interactions with other proteins. One could identify such interacting proteins by using the method described by Baucum and colleagues (2010): Cbln1 is immunoprecipitated from striatal extracts, and after tryptic digestion, mass spectrometry is used to identify proteins that bind to Cbln1. This could also serve as the first step in identifying a Cbln1 receptor. The internalization of GPCRs is mediated through β-arrestins (see Wolfe and Trejo, 2007). If the receptor for Cbln1 is found to be a GPCR, one could initially determine whether Cbln1 expression in MSN dendrites is altered in β-arrestin null mice.

In the cerebellum, Cbln1 binds to an unidentified postsynaptic receptor when it is secreted as a hexameric structure (Pang et al., 2000; Bao et al., 2005, 2006; Miura et al., 2009). Is hexameric assembly of Cbln1 required for receptor binding in the striatum? It has been shown that Cbln1 can form both homomeric and heteromeric complexes with other Cbln family members (Bao et al., 2005, 2006). In addition to expressing Cbln1, the PF expresses Cbln2 and Cbln4 mRNA (Miura et al., 2006). However, our finding that dendritic spine density is unaltered in *cbln2*$^{-/-}$ and *cbln4*$^{-/-}$ mice, suggests that Cbln2 and Cbln4 do not have an essential role in regulating striatal synapses.

We have not determined if Cbln1 is expressed in corticostriatal axon terminals. Interestingly, our EM studies showed that only 5.5% of Cbln1-ir axons terminate onto dendritic shafts, with the remainder contacting dendritic spine heads. This was surprising
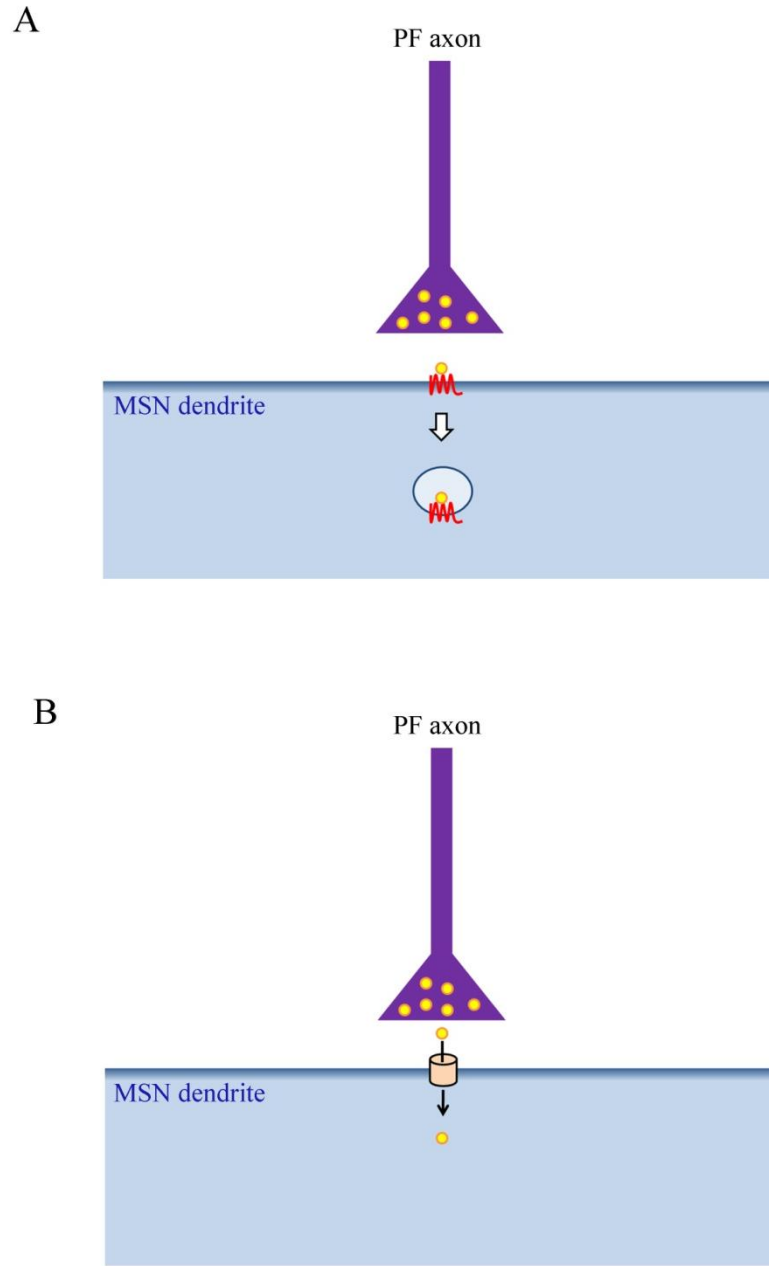
Figure 27. Illustration of two potential mechanisms by which Cbln1 is transsynaptically accumulated across parafascicular (PF) thalamostriatal synapses. *A)* A PF axon secretes Cbln1 (yellow circles), which binds to a receptor (indicated in red) residing on the membrane of an MSN dendrite. The binding of Cbln1 to the receptor causes the endocytosis of the Cbln1-receptor complex. *B)* Cbln1 accumulates in MSN dendrites by passing through a transporter (indicated in peach) on the dendritic surface of MSNs.

because Lacey et al. (2007) reported that ~63% of PF axons synapse on MSN dendritic shafts. As we previously noted, cortical neurons do not express Cbln1 except for the retrosplenial cortex.

Thus, we see no evidence of Cbln1-ir neurons in the cortex nor has Cbln1 mRNA been shown in the cortex of the mouse or rat (Miura et al., 2006; Wei et al., 2007), although in primate species, there is significant cortical expression (Murray et al., 2007). Does Cbln1 also get taken up into corticostriatal axons and then regulate corticostriatal synapses? To assess this possibility, one could label corticostriatal axons with vGluT1 and determine whether these terminals also co-expressed Cbln1.

Cbln1 regulation of striatal spine formation

We found that the genetic deletion of Cbln1 increases dendritic spine density, with a corresponding increase in axospinous synapses. As noted above, this might occur if the loss of Cbln1 causes the collateralization of PF axons that subsequently synapse onto dendritic spines (Fig. 28). Thus, we would predict that the *presence* of Cbln1 constrains collateralization of PF axons, which would in turn prevent the formation of excess striatal synapses. In this scenario, glutamate release from PF axons may be the primary factor regulating spine formation. A second possibility is that the loss of Cbln1 alters the ability of PF axons to form axodendritic synapses and causes them to instead preferentially form axospinous synapses (Fig. 28).

Let us assume that the function of Cbln1 is to prevent these extra axosynaptic synapses from forming. We envision three scenarios that may describe Cbln1 action in the striatum. One possibility is that the postsynaptic accumulation of Cbln1, independent

103

A

$cbln1^{+/+}$

PF axon

MSN dendrite

B

$cbln1^{-/-}$

or
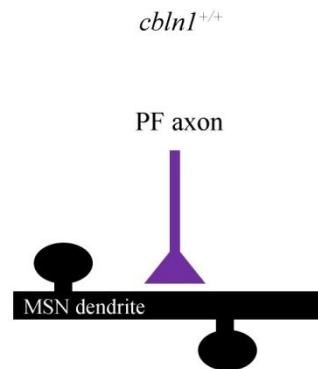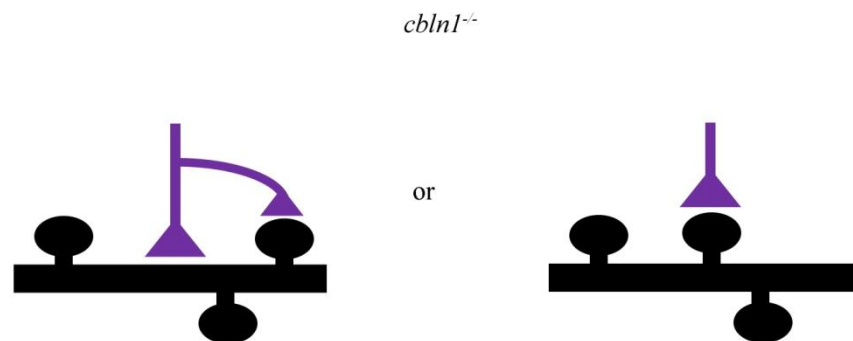
Figure 28. Schematic depiction of a parafascicular (PF) axon synapsing onto a striatal medium spiny neuron dendrite (MSN) in the $cbln1^{+/+}$ (**A**) and $cbln1^{-/-}$ mouse (**B**). **A)** A PF axon is seen synapsing onto the dendritic shaft of a MSN dendrite. **B)** There are two possible ways in which loss of Cbln1 could cause an increase in PF axospinous terminations in the $cbln1^{-/-}$ mouse. One is by causing increased collateralization of PF axons, and a subsequent increase in the number of axospinous synaptic terminations *(left)*. A second possibility is that the loss of Cbln1 alters the ability of PF axons to form axodendritic synapses, and that these PF terminals now must synapse onto dendritic spine heads *(right)*.

of receptor binding, regulates spine formation. A second is that Cbln1 binding to a receptor, which causes internalization of the receptor-ligand complex, is necessary to regulate spine formation. A third possibility is that Cbln1 binds to a receptor on the post-synaptic membrane target and activates an intracellular signaling cascade that ultimately regulates spine formation.

Are the effects of the genetic deletion of Cbln1 developmental in nature?

One limitation of our findings is that we used a constitutive *cbln1* knockout. Thus, it is unclear if the effects of Cbln1 are developmental in nature or whether Cbln1 also alters synapses late in adulthood. We have not examined the effects of suppression of Cbln1 that is restricted to the adult period. One approach is to generate conditional *cbln1* knockout mice and assess the time-dependence of the alterations in MSN dendritic spine density (our collaborator Jim Morgan is currently generating these mice). A second approach is to knockdown Cbln1 expression in the PF using siRNA. One could also acutely manipulate Cbln1 signaling in the striatum using a strategy such as immunoneutralization.

Because exogenous Cbln1 reverses synaptic deficits in the cerebellum of *cbln1* null mice (Ito-Ishida et al., 2008), it is reasonable to speculate that a similar rescue of the striatal synaptic changes would be seen. However, in the study which showed that exogeneous Cbln1 could restore synapses in the cerebellum, the protein was infused into the subarachnoid space and therefore bathed the cerebellar cortex directly (Ito-Ishida et al., 2008). Intrastriatal infusion of Cbln1 is likely to cause mechanical disruption and is therefore not a favored approach. Alternatively, one could infuse Cbln1 into the lateral

ventricle, assuming that this would result in the diffusion of the protein across significant distances to accumulate in the striatum.

It would be very useful to have a suitable *in vitro* model to investigate the mechanism. Ito-Ishida and colleagues (2008) showed that recombinant Cbln1 restored synapses in dissociated Purkinje cell cultures from *cbln1* null mice. Dissociated striatal cultures, however, would disrupt thalamostriatal and corticostriatal projections to MSNs. We have developed and used organotypic slice co-cultures with considerable success (Neely et al., 2007; Garcia et al., 2010). These cultures show appropriate anatomical organization and establishment of connections, and MSNs of the cultures display spontaneous and cortically-evoked activity (Plenz and Kitai, 1998; Snyder-Keller et al., 2008).

In particular, we have generated cultures containing the cortex, striatum, ventral midbrain, and the globus pallidus. We have shown in this system that dopamine depletion leads to a decrease in MSN dendritic spine density (Neely et al., 2007). One could therefore generate organotypic slice co-cultures containing the cortex, caudomedial thalamus, striatum, and substantia nigra from *cbln1$^{-/-}$* mice or their wildtype littermates. In this case, one would anticipate that the application of exogenous Cbln1 would reduce spine density of MSNs in cultures derived from *cbln1* null mutants.

Cbln1 and Behavior

In future studies, it will be necessary to determine how the loss of Cbln1 alters behavior. Because the *cbln1$^{-/-}$* mice have a cerebellar ataxia, which will confound the interpretation of most behavioral tests of interest, it will be necessary to specifically

suppress or eliminate Cbln1 expression in the PF and then assess its effects on behavior. This could be accomplished using siRNA. Given the reported lack of motor deficits (as assessed by evaluating postural asymmetries, sensory deficits on the contralateral side to the lesion, and apomorphine-induced rotational asymmetry) seen in PF-lesioned rodents (Henderson et al., 2005), it is unlikely that loss of Cbln1 from PF neurons will result in overt motor impairments in the basal condition, although more subtle impairments may become evident with appropriate testing.

<u>Is the loss of Cbln1 protective against spine loss in PD?</u>

We examined Cbln1 function in the striatum because of our interest in determining the significance of the loss of CM-PF neurons in PD. In idiopathic Parkinson's disease, striatal MSNs undergo a loss of dendritic spines (McNeill et al., 1988; Stephens et al., 2005; Zaja-Milatovic et al., 2005). Nigrostriatal dopamine depletion-induced changes in spine density are progressive (Ingham et al. 1993). Our finding that genetic deletion of Cbln1 causes an increase in MSN dendritic spines suggests that a study to determine if loss of PF Cbln1 prevents spine loss or slows progressive spine loss is warranted.

We have begun to analyze the effects of MPTP treatment on MSN dendrites in $cbln1^{-/-}$ and $cbln1^{+/+}$ mice. Because there is an increase in spine density in the $cbln1^{-/-}$ mouse and a decrease in spine density in the MPTP mouse, we predict that spine density will be normalized in the $cbln1^{-/-}$ mice that receive MPTP. We have found that striatal dopamine concentrations in $cbln1^{-/-}$ MPTP-treated mice are not different from $cbln1^{+/+}$

MPTP-treated mice (data not shown). Because spine loss, once established, appears to be independent of dopamine function, this is not a surprising observation.

These studies will inform us if the increased number of MSN spines seen in the *cbln1*^{-/-} mice is reduced to normal levels by MPTP, but they will not be of use in determining the effects of removal of PF inputs, as would occur with the loss of PF cells seen in PD. In order to untangle the relative contributions of Cbln1, glutamate, and other signaling molecules in the PF neurons, it will be useful to determine if PF lesions have the same effect as Cbln1 deletion.

Unfortunately, the geometry of the PF in the rodent makes it impossible to selectively lesion the nucleus without causing damage to neighboring nuclei. To circumvent this problem, one could use a transgenic mouse model of PF degeneration. This could be achieved by generating mice in which the Cbln1 promoter drives expression of the diphtheria or tetanus toxin receptor (Saito et al., 2001; Luquet et al., 2005). By this method, infusion of either diphtheria or tetanus toxin would selectively lesion neurons that express Cbln1. Within the thalamus, Cbln1 expression is primarily confined to the PF and is not expressed in adjacent thalamic nuclei. However, because Cbln1 is expressed in the habenula, the amount of diphtheria or tetanus toxin infused into the PF would have to be carefully titrated to avoid lesioning the habenula. Thus, it may be better to find another protein that is enriched in PF neurons in order to create discrete PF lesions. One such protein is Frizzled 5, whose expression is primarily restricted to the PF, hypothalamus, and retina (Liu et al. 2008). Deletion of Frizzled 5 in the adult mouse causes the degeneration of PF neurons (Liu et al. 2008).

Is the loss of CM-PF neurons protective in PD?

Caparros-Lefebvre et al. (1994), in an evaluation of the effects of deep brain stimulation (DBS) of the motor thalamus on PD symptoms, suggested that electrode placements that involved the CM-PF yielded the best responses. Since then, several small clinical trials of CM-PF DBS in PD have concluded that DBS of the the CM-PF improves the motor deficits of PD and decreases levodopa-induced abnormal involuntary movements (Caparros-Lefebvre et al., 1999; Peppe et al., 2008; Benabid, 2009; Stefani et al., 2009). This is consistent with experimental animal data suggesting that disruption of thalamostriatal projections reverses dopamine depletion-induced changes in preproenkephalin and GAD67 mRNA in striatal MSNs (Bacci et al., 2004). While the mechanism of action of DBS of the PF is completely unknown, a functional inhibition of the stimulated site is one hypothesis.

Until recently, we have been unable to assess the behavioral significance of MSN spine loss. A major advance towards determining the functional impact of spine loss was the finding that interventions that reduce corticostriatal glutamate drive onto MSNs reverse the loss of dendritic spines seen after nigrostriatal dopamine depletion (Garcia et al. 2010). Thus, one can establish spine loss and conduct behavioral studies and then reverse spine loss with the appropriate treatment and examine behavior in animals with the same tasks. We have hypothesized that the reduction in levodopa responsiveness that occurs over time in Parkinson's disease is a consequence of the loss of dendritic spines. Thus, we predict that spine restoration would prolong the full motor benefit of levodopa-treatment in PD and suggest that modulating thalamostriatal Cbln1 may be a novel treatment strategy for slowing the progression of PD.

Conclusion

This work has resolved the controversy over whether loss of nigrostriatal dopamine neurons determines the survival of PF neurons. Through multiple lines of evidence, we have demonstrated that the loss of nigrostriatal dopamine neurons does not cause PF cell death. In addition, our work has uncovered a protein, Cbln1, that is enriched in PF neurons and regulates MSN synapses in a manner opposite to that of dopamine depletion. The study of Cbln1 function is still in its infancy, but promises to be an exciting opportunity for future research.

REFERENCES

Albertin G, Malendowicz LK, Macchi C, Markowska A, Nussdorfer GG. 2000. Cerebellin stimulates the secretory activity of the rat adrenal gland: in vitro and in vivo studies. Neuropeptides 34:7-11.

Aldridge GM, Podrebarac DM, Greenough WT, Weiler IJ. 2008. The use of total protein stains as loading controls: an alternative to high-abundance single-protein controls in semi-quantitative immunoblotting. J Neurosci Methods 172:250-4.

Alvarez VA, Sabatini BL. 2007. Anatomical and physiological plasticity of dendritic spines. Ann Rev Neurosci 30:79-97.

Anglade P, Mouatt-Prigent A, Agid Y, Hirsch E. 1996. Synaptic plasticity in the caudate nucleus of patients with Parkinson's disease. Neurodegeneration. 5:121-8.

Arantes RM, Andrews NW. 2006. A role for synaptotagmin VII-regulated exoctyosis of lysosomes in neurite outgrowth from primary sympathetic neurons. J Neurosci 26:4630-7.

Aymerich MS, Barroso-Chinea P, Perez-Manso M, Munoz-Patino AM, Moreno-Igoa M, Gonzalez-Hernandez T, Lanciego JL. 2006. Consequences of unilateral nigrostriatal denervation on the thalamostriatal pathway in rats. Eur J Neurosci 23:2099-108.

Bacci JJ, Kachidian P, Kerkerian-Le Goff L, Salin P. 2004. Intralaminar thalamic nuclei lesions: widespread impact on dopamine denervation-mediated cellular defects in the rat basal ganglia. J Neuropathol Exp Neurol 63:20-31.

Bamford NS, Robinson S, Palmiter RD, Joyce JA, Moore C, Meshul CK. 2004. Dopamine modulates release from corticostriatal terminals. J Neurosci 24:9541-9552.

Bao D, Pang Z, Morgan JI. 2005. The structure and proteolytic processing of Cbln1 complexes. J Neurochem 95:618-29.

Bao D, Pang Z, Morgan MA, Parris J, Rong Y, Li L, Morgan JI. 2006. Cbln1 is essential for interaction-dependent secretion of Cbln3. Mol Cell Biol 26:9327-37.

Baucum AJ 2nd, Jalan-Sakrikar N, Jiao Y, Gustin RM, Carmody LC, Tabb DL, Ham AJ, Colbran RJ. 2010. Identification and validation of novel spinophilin-associated proteins in rodent striatum using an enhanced ex vivo shotgun proteomics approach. Mol Cell Proteomics.

Beckstead RM, Domesick VB, Nauta WJH. 1979. Efferent connections of the substantia nigra and ventral tegmental area in the rat. Brain Res 175:191–217.

Benabid AL. 2009. Targeting the caudal intralaminar nuclei for functional neurosurgery of movement disorders. Brain Res Bull 78:109-112.

Bennett BD, Bolam JP. 1993. Characterization of calretinin-immunoreactive structures in the striatum of the rat. Brain Res 609:137-48.

Bennett BD, Wilson CJ. 1999. Spontaneous activity of neostriatal cholinergic interneurons in vitro. J Neurosci 19:5586-96.

Berendse HW, Groenewegen HJ. 1990. Organization of the thalamostriatal projections in the rat, with special emphasis on the ventral striatum. J Comp Neurol 299:187-228.

Berendse HW, Groenewegen HJ. 1991. Restricted cortical termination fields of the midline and intralaminar thalamic nuclei in the rat. Neuroscience. 42:73-102.

Bergson C, Mrzljak L, Smiley JF, Pappy M, Levenson R, Goldman-Rakic PS. 1995. Regional, cellular, and subcellular variations in the distribution of D1 and D5 dopamine receptors in primate brain. J Neurosci 15:7821-7836.

Berlanga ML, Simpson TK, Alcantara AA. 2005. Dopamine D5 receptor localization on cholinergic neurons of the rat forebrain and diencephalon: a potential neuroanatomical substrate involved in mediating dopaminergic influences on acetylcholine release. J Comp Neurol. 492:34-49.

Bertorelli R, Consolo S. 1990. D1 and D2 dopaminergic regulation of acetylcholine release from striata of freely moving rats. J Neurochem 54:2145-2148.

Bjartmar L, Huberman AD, Ullian EM, Rentería RC, Liu X, Xu W, Prezioso J, Susman MW, Stellwagen D, Stokes CC, Cho R, Worley P, Malenka RC, Ball S, Peachey NS, Copenhagen D, Chapman B, Nakamoto M, Barres BA, Perin MS. Neuronal pentraxins mediate synaptic refinement in the developing visual system. 2006. J Neurosci 26:6269-81.

Bouyer JJ, Park DH, Joh TH, Pickel VM. 1984. Chemical and structural analysis of the relation between cortical inputs and tyrosine hydroxylase-containing terminals in rat neostriatum. Brain Res 302:267-75.

Bracci E, Centonze D, Bernardi G, Calabresi P. 2002. Dopamine excites fast-spiking interneurons in the striatum. J Neurophysiol 87:2190-2194.

Braak H, Del Tredici K, Bratzke H, Hamm-Clement J, Sandmann-Keil D, Rüb U. 2002. Staging of the intracerebral inclusion body pathology associated with idiopathic

Parkinson's disease (preclinical and clinical stages). J Neurol 249 Suppl 3:III/1-5.

Braak H, Del Tredici K, Rüb U, de Vos RA, Jansen Steur EN, Braak E. 2003. Staging of brain pathology related to sporadic Parkinson's disease. Neurobiol Aging. 24:197-211.

Brooks D, Halliday GM. 2009. Intralaminar nuclei of the thalamus in Lewy body diseases. Brain Res Bull 78:97-104.

Bubser M, Scruggs JL, Young CD, Deutch AY. 2000. The distribution and origin of the calretinin-containing innervation of the nucleus accumbens of the rat. Eur J Neurosci 12:1591-1598.

Burnet PW, Bretherton-Watt D, Ghatei MA, Bloom SR. 1988. Cerebellin-like peptide: tissue distribution in rat and guinea-pig and its release from rat cerebellum, hypothalamus and cerebellar synaptosomes in vitro. Neurosci 25:605-12.

Caparros-Lefebvre D, Ruchoux MM, Blond S, Petit H, Percheron G. 1994. Long-term thalamic stimulation in Parkinson's disease: postmortem anatomoclinical study. Neurology 44:1856-1860.

Caparros-Lefebvre D, Blond S, Feltin MP, Pollak P, Benabid AL. 1999. Improvement of levodopa induced dyskinesias by thalamic deep brain stimulation is related to slight variation in electrode placement: possible involvement of the centre median and parafascicularis complex. J Neurol Neurosurg Psychiatry 67:308-314.

Castle M, Aymerich MS, Sanchez-Escobar C, Gonzalo N, Obeso JA, Lanciego JL. 2005. Thalamic innervation of the direct and indirect basal ganglia pathways in the rat: Ipsi- and contralateral projections. J Comp Neurol 483:143-53.

Castren E, Thoenen H, Lindholm D. 1995. Brain-derived neurotrophic factor messenger RNA is expressed in the septum, hypothalamus and in adrenergic brain stem nuclei of adult rat brain and is increased by osmotic stimulation in the paraventricular nucleus, Neuroscience 64:71–80.

Centonze D, Bracci E, Pisani A, Gubellini P, Bernardi G, Calabresi P. 2002. Activation of dopamine D1-like receptors excites LTS interneurons of the striatum. Eur J Neurosci 15:2049-2052.

Centonze D, Grande C, Usiello A, Gubellini P, Erbs E, Martin AB, Pisani A, Tognazzi N, Bernardi G, Moratalla R, Borrelli E, Calabresi P. 2003. Receptor subtypes involved in the presynaptic and postsynaptic actions of dopamine on striatal interneurons. J Neurosci 23:6245-6254.

Cepeda C, Hurst RS, Altemus KL, Flores-Hernández J, Calvert CR, Jokel ES, Grandy DK, Low MJ, Rubinstein M, Ariano MA, Levine MS. 2001. Facilitated

glutamatergic transmission in the striatum of D2 dopamine receptor-deficient mice. J Neurophysiol 85:659-670.

Chagnaud JL, Mons N, Tuffet S, Grandier-Vazeilles X, Geffard M. 1987. Monoclonal antibodies against glutaraldehyde-conjugated dopamine. J Neurochem 49:487-94.

Chang HT, Wilson CJ, Kitai ST. 1981. Single neostriatal efferent axons in the globus pallidus: a light and electron microscopic study. Science 213:915-8.

Chang HT, Wilson CJ, Kitai ST. 1982. A Golgi study of rat neostriatal neurons: light microscopic analysis. J Comp Neurol 208:107-26.

Cheatwood JL, Corwin JV, Reep RL. 2005. Overlap and interdigitation of cortical and thalamic afferents to dorsocentral striatum in the rat. Brain Res 1036:90-100.

Chung JW, Hassler R, Wagner A. 1977. Degeneration of two of nine types of synapses in the putamen after center median coagulation in the cat. Exp Brain Res 28:345-61.

Clissold BG, McColl CD, Reardon KR, Shiff M, Kempster PA. 2006. Longitudinal study of the motor response to levodopa in Parkinson's disease. Mov Disord 21:2116-21.

Coggins MR, Grabner CP, Almers W, Zenisek D. 2007. Stimulated exocytosis of endosomes in goldfish retinal bipolar neurons. J Physiol 584(Pt 3):853-65.

Conner JM, Lauterborn JC, Yan Q, Gall CM, Varon S. 1997. Distribution of brain-derived neurotrophic factor (BDNF) protein and mRNA in the normal adult rat CNS: evidence for anterograde axonal transport. J Neurosci 17:2295–2313.

Cornwall J, Phillipson OT. 1988. Afferent projections to the parafascicular thalamic nucleus of the rat, as shown by the retrograde transport of wheat germ agglutinin. Brain Res Bull 20:139-50.

Cowan WM, Powell TP. 1956. A study of thalamo-striate relations in the monkey. Brain 79:364-90.

Day M, Wang Z, Ding J, An X, Ingham CA, Shering AF, Wokosin D, Ilijic E, Sun Z, Sampson AR, Mugnaini E, Deutch AY, Sesack SR, Arbuthnott GW, Surmeier DJ. 2006. Selective elimination of glutamatergic synapses on striatopallidal neurons in Parkinson disease models. Nat Neurosci 9:251-9.

Deschênes M, Bourassa J, Doan VD, Parent A. 1996. A single-cell study of the axonal projections arising from the posterior intralaminar thalamic nuclei in the rat. Eur J Neurosci 8:329-43.

114

Deschênes M, Bourassa J, Parent A. 1995. Two different types of thalamic fibers innervate the rat striatum. Brain Res 701:288-92.

Deutch AY. 2006. Striatal plasticity in parkinsonism: dystrophic changes in medium spiny neurons and progression in Parkinson's disease. J Neural Transm Suppl. 70:67-70.

Deutch AY, Cameron DS. 1992. Pharmacological characterization of dopamine systems in the nucleus accumbens core and shell. Neurosci 46:49-56.

Deutch AY, Colbran RJ, Winder DJ. 2007. Striatal plasticity and medium spiny neuron dendritic remodeling in parkinsonism. Parkinsonism Relat Disord 13:S251-8.

Deutch AY, Zahm DS. 1992. The current status of neurotensin-dopamine interactions: issues and speculations. Ann N Acad Sci 668:232-252.

Ding J, Peterson JD, Surmeier DJ. 2008. Corticostriatal and thalamostriatal synapses have distinctive properties. J Neurosci 28:6483-92.

Dubé L, Smith AD, Bolam JP. 1988. Identification of synaptic terminals of thalamic or cortical origin in contact with distinct medium-size spiny neurons in the rat neostriatum. J Comp Neurol 267:455-71.

Elena Erro M, Lanciego JL, Gimenez-Amaya JM. 2002. Re-examination of the thalamostriatal projections in the rat with retrograde tracers. Neurosci Res 42:45-55.

Fahn S. 2003. Description of Parkinson's disease as a clinical syndrome. Ann N Y Acad Sci 991:1-14.

Finley JC, Maderdrut JL, Petrusz P. 1981. The immunocytochemical localization of enkephalin in the central nervous system of the rat. J Comp Neurol 198:541-65.

Florio T, Di Loreto S, Cerrito F, Scarnati E. 1993. Influence of prelimbic and sensorimotor cortices on striatal neurons in the rat: electrophysiological evidence for converging inputs and the effects of 6-OHDA-induced degeneration of the substantia nigra. Brain Res 619:180-188.

François C, Tande D, Yelnik J, Hirsch EC. 2002. Distribution and morphology of nigral axons projecting to the thalamus in primates. J Comp Neurol 447:249-60.

Freeman A, Ciliax B, Bakay R, Daley J, Miller RD, Keating G, Levey A, Rye D. 2001. Nigrostriatal collaterals to thalamus degenerate in parkinsonian animal models. Ann Neurol 50:321-9.

Freund TF, Powell JF, Smith AD. 1984. Tyrosine hydroxylase-immunoreactive boutons

in synaptic contact with identified striatonigral neurons, with particular reference to dendritic spines. Neuroscience. 13:1189-215.

Freyaldenhoven, TE, Ali SF, Schmued LC. 1997. Systemic administration of MPTP induces thalamic neuronal degeneration in mice. Brain Res 759:9-17.

Garcia BG, Neely MD, Deutch AY. 2010. Cortical Regulation of Striatal Medium Spiny Neuron Dendritic Remodeling in Parkinsonism: Modulation of Glutamate Release Reverses Dopamine Depletion-Induced Dendritic Spine Loss. Cereb Cortex.

García-Cabezas MA, Martínez-Sánchez P, Sánchez-González MA, Garzón M, Cavada C. 2009. Dopamine innervation in the thalamus: monkey versus rat. Cereb Cortex 19:424-34.

García-Cabezas MA, Rico B, Sánchez-González MA, Cavada C. 2007. Distribution of the dopamine innervation in the macaque and human thalamus. Neuroimage 34:965-84.

Gauthier J, Parent M, Levesque M, Parent A. 1999. The axonal arborization of single nigrostriatal neurons in rats. Brain Res 834:228-32.

Geffard M, Buijs RM, Seguela P, Pool CW, Le Moal M. 1984. First demonstration of highly specific and sensitive antibodies against dopamine. Brain Res 294:161-5.

Gerfen CR. 1992. The neostriatal mosaic: multiple levels of compartmental organization. Trends Neurosci 15:133-9.

Gerfen CR. 2000. Molecular effects of dopamine on striatal-projection pathways. Trends Neurosci 23:S64-70.

Gerfen CR, Engber TM, Mahan LC, Susel Z, Chase TN, Monsma FJ Jr, Sibley DR. 1990. D1 and D2 dopamine receptor-regulated gene expression of striatonigral and striatopallidal neurons. Science 250:1429-32

Gerfen CR, Young WS 3rd. 1988. Distribution of striatonigral and striatopallidal peptidergic neurons in both patch and matrix compartments: an in situ hybridization histochemistry and fluorescent retrograde tracing study. Brain Res 460:161-7.

German DC, Manaye KF, White CL 3rd, Woodward DJ, McIntire DD, Smith WK, Kalaria RN, Mann DM. 1992. Disease-specific patterns of locus coeruleus cell loss. Ann Neurol 32:667-76.

Ghorayeb I, Fernagut PO, Hervier L, Labattu B, Bioulac B, Tison F. 2002. A 'single toxin-double lesion' rat model of striatonigral degeneration by intrastriatal 1-methyl-4-phenylpyridinium ion injection: a motor behavioural analysis. Neurosci

115:533-46.

Giménez-Amaya JM, de las Heras S, Erro E, Mengual E, Lanciego JL. 2000.
    Considerations on the thalamostriatal system with some functional implications.
    Histol Histopathol 15:1285-92.

Gong S, Zheng C, Doughty ML, Losos K, Didkovsky N, Schambra UB, Nowak NJ,
    Joyner A, Leblanc G, Hatten ME, Heintz N. 2003. A gene expression atlas of the
    central nervous system based on bacterial artificial chromosomes. Nature
    425:917-25.

Graybiel AM. 1984. Correspondence between the dopamine islands and striosomes of
    the mammalian striatum. Neurosci 13:1157-87.

Graybiel AM, Ragsdale CW Jr. 1978. Histochemically distinct compartments in the
    striatum of human, monkeys, and cat demonstrated by acetylthiocholinesterase
    staining. Proc Natl Acad Sci U S A. 75:5723-6.

Groenewegen HJ. 1988. Organization of the afferent connections of the mediodorsal
    thalamic nucleus in the rat, related to the mediodorsal-prefrontal topography.
    Neurosci 24:379-431.

Grofová I. 1975. The identification of striatal and pallidal neurons projecting to
    substantia nigra. An experimental study by means of retrograde axonal transport
    of horseradish peroxidase. Brain Res 91:286-91

Gurevich EV, Joyce JN. 1999. Distribution of dopamine D3 receptor expressing neurons
    in the human forebrain: comparison with D2 receptor expressing neurons.
    Neuropsychopharmacology 20:60-80.

Halliday GM. 2009. Thalamic changes in Parkinson's disease. Parkinsonism Relat
    Disord 15 Suppl 3:S152-5.

Halliday GM, Macdonald V, Henderson JM. 2005. A comparison of degeneration in
    motor thalamus and cortex between progressive supranuclear palsy and
    Parkinson's disease. Brain 128:2272-80.

Henderson JM, Carpenter K, Cartwright H, Halliday GM. 2000. Degeneration of the
    centre median-parafascicular complex in Parkinson's disease. Ann Neurol 47:345-
    352.
Henderson JM, Schleimer SB, Allbutt H, Dabholkar V, Abela D, Jovic J, Quinlivan M.
    2005. Behavioural effects of parafascicular thalamic lesions in an animal model
    of parkinsonism. Behav Brain Res 162:222-32.

Hersi AI, Kitaichi K, Srivastava LK, Gaudreau P, Quirion R. 2000. Dopamine D-5
    receptor modulates hippocampal acetylcholine release. Brain Res Mol Brain Res

76: 336-340.

Hirai H, Pang Z, Bao D, Miyazaki T, Li L, Miura E, Parris J, Rong Y, Watanabe M, Yuzaki M, Morgan JI. 2005. Cbln1 is essential for synaptic integrity and plasticity in the cerebellum. Nat Neurosci 8:1534-41.

Hong JS, Yang HY, Racagni G, Costa E. 1977. Projections of substance P containing neurons from neostriatum to substantia nigra. Brain Res 122:541-4.

Ingham CA, Hood SH, Arbuthnott GW. 1989. Spine density on neostriatal neurones changes with 6-hydroxydopamine lesions and with age. Brain Res 503:334-8.

Ingham CA, Hood SH, van Maldegem B, Weenink A, Arbuthnott GW. 1993. Morphological changes in the rat neostriatum after unilateral 6-hydroxydopamine injections into the nigrostriatal pathway. Exp Brain Res 93:17-27.

Ito-Ishida A, Miura E, Emi K, Matsuda K, Iijima T, Kondo T,Kohda K, Watanabe M, Yuzaki. 2008. Cbln1 regulates rapid formation and maintenance of excitatory synapses in mature cerebellar Purkinje cells in vitro and in vivo. J Neurosci 28:5920-30.

Jankovic J. 2005. Motor fluctuations and dyskinesias in Parkinson's disease: clinical manifestations. Mov Disord 20 Suppl 11:S11-6.

Jones EG. 1999. Making brain connections: neuroanatomy and the work of TPS Powell, 1923-1996. Annu Rev Neurosci 22:49-103.

Jones EG. 2007a. Neuroanatomy: Cajal and after Cajal. Brain Res Rev 55:248-55.

Jones EG. 2007b. The Thalamus. New York: Cambridge University Press.

Kawaguchi Y. 1993. Physiological, morphological, and histochemical characterization of three classes of interneurons in rat neostriatum. J Neurosci 13:4908–4923.

Kawaguchi Y. 1997. Neostriatal cell subtypes and their functional roles. Neurosci Res 27:1-8.

Kawaguchi Y, Wilson CJ, Augood SJ, Emson PC. 1995. Striatal interneurones: chemical, physiological and morphological characterization. Trends Neursoci 18:527-35.

Kelley JJ, Gao XM, Tamminga CA, Roberts RC. 1997. The effect of chronic haloperidol treatment on dendritic spines in the rat striatum. 146:471-8.

Kemp JM. Observations on the caudate nucleus of the cat impregnated with the Golgi method. Brain Res 11:467-70.

Kemp JM, Powell TP. 1971. The site of termination of afferent fibres in the caudate nucleus. Philos Trans R Soc Lond B Biol Sci 262:413-27.

Kerkerian-Le Goff L, Bacci JJ, Jouve L, Melon C, Salin P. 2009. Impact of surgery targeting the caudal intralaminar thalamic nuclei on the pathophysiological functioning of basal ganglia in a rat model of Parkinson's disease. Brain Res Bull 78:80-84.

Kilpatrick IC, Jones MW, Pycock CJ, Riches I, Phillipson OT. 1986. Thalamic control of dopaminergic functions in the caudate-putamen of the rat--III. The effects of lesions in the parafascicular-intralaminar nuclei on D2 dopamine receptors and high affinity dopamine uptake. Neurosci 19:991-1005.

Krout KE, Belzer RE, Loewy AD. 2002. Brainstem projections to midline and intralaminar thalamic nuclei of the rat. J Comp Neurol 448:53-101.

Lacey CJ, Bolam JP, Magill PJ. 2007. Novel and distinct operational principles of intralaminar thalamic neurons and their striatal projections. J Neurosci 27:4374-84.

Lanciego JL, Gonzalo N, Castle M, Sanchez-Escobar C, Aymerich MS, Obeso JA (2004) Thalamic innervation of striatal and subthalamic neurons projecting to the rat entopeduncular nucleus. Eur J Neurosci 19:1267-77.

Lanciego JL, López IP, Rico AJ, Aymerich MS, Pérez-Manso M, Conte L, Combarro C, Roda E, Molina C, Gonzalo N, Castle M, Tuñón T, Erro E, Barroso-Chinea P. 2009. The search for a role of the caudal intralaminar nuclei in the pathophysiology of Parkinson's disease. Brain Res Bull 78:55-9.

Lapper SR, Bolam JP. 1992. Input from the frontal cortex and the parafascicular nucleus to cholinergic interneurons in the dorsal striatum of the rat. Neurosci 51:533-45.

Le Moine C, Bloch B. 1995. D1 and D2 dopamine receptor gene expression in the rat striatum: sensitive cRNA probes demonstrate prominent segregation of D1 and D2 mRNAs in distinct neuronal populations of the dorsal and ventral striatum. J Comp Neurol 355:418-26.

Lévesque M, Parent A. 2005. The striatofugal fiber system in primates: a reevaluation of its organization based on single-axon tracing studies. Proc Natl Acad Sci U S A 102:11888-93.

Li Y, Kolb B, Robinson TE. 2003. The location of persistent amphetamine-induced changes in the density of dendritic spines on medium spiny neurons in the nucleus accumbens and caudate-putamen. Neuropsychopharmacol 28:1082-5.

Lippman J, Dunaevsky A. 2005. Dendritic spine morphogenesis and plasticity. J Neurobiol 64:47-57.

Liu C, Wang Y, Smallwood PM, Nathans J. 2008. An essential role for Frizzled5 in neuronal survival in the parafascicular nucleus of the thalamus. J Neurosci 28:5641-53.

Luquet S, Perez FA, Hnasko TS, Palmiter RD. 2005. NPY/AgRP neurons are essential for feeding in adult mice but can be ablated in neonates. Science 310:683-5.

Mann DM, Yates PO. 1983. Pathological basis for neurotransmitter changes in Parkinson's disease. Neuropathol Appl Neurobiol 9:3-19.

Marini G, Pianica L, Tredici G. 1999. Descending projections arising from the parafascicular nucleus in rats: trajectory of fibers, projection pattern and mapping of terminations. Somatosens Mot Res 16:207-22.

Marsden CD, Parkes JD. 1977. Success and problems of long-term levodopa therapy in Parkinson's disease. Lancet 1:345-9.

Matsuda K, Kondo T, Iijima T, Matsuda S, Watanabe M, Yuzaki M. 2009. Cbln1 binds to specific postsynaptic sites at parallel fiber-Purkinje cell synapses in the cerebellum. Eur J Neurosci 29:707-717.

Matsumoto N, Minamimoto T, Graybiel AM, Kimura M. 2001. Neurons in the thalamic CM-Pf complex supply striatal neurons with information about behaviorally significant sensory events. J Neurophysiol 85:960-76.

Mazzocchi G, Andreis PG, De Caro R, Aragona F, Gottardo L, Nussdorfer GG. 1999. Cerebellin enhances in vitro secretory activity of human adrenal gland. J Clin Endocrinol Metab 84:632-5.

McFarland NR, Haber SN. 2000. Convergent inputs from thalamic motor nuclei and frontal cortical areas to the dorsal striatum in the primate. J Neurosci 20:3798-813.

McGeorge AJ, Faull RL. 1989. The organization of the projection from the cerebral cortex to the striatum in the rat. Neurosci 29:503-37.

McKinney RA, Capogna M, Dürr R, Gähwiler BH, Thompson SM. 1999. Miniature synaptic events maintain dendritic spines via AMPA receptor activation. Nat Neurosci 2:44-9.

McNeill TH, Brown SA, Rafols JA, Shoulson I. 1988. Atrophy of medium spiny I striatal dendrites in advanced Parkinson's disease. Brain Res 455:148-52.

McRae-Degueurce A, Geffard M. 1986. One perfusion mixture for immunocytochemical detection of noradrenaline, dopamine, serotonin and acetylcholine in the same rat brain. Brain Res 376:217-9.

Meador-Woodruff JH, Mansour A, Grandy DK, Damask SP, Civelli O, Watson SJ Jr. 1992. Distribution of D5 dopamine receptor mRNA in rat brain. Neurosci Lett 145:209-12.

Meador-Woodruff JH, Mansour A, Healy DJ, Kuehn R, Zhou QY, Bunzow JR, Akil H, Civelli O, Watson SJ Jr. 1991. Comparison of the distributions of D1 and D2 dopamine receptor mRNAs in rat brain. Neuropsychopharmacology 5:231-42.

Meshul CK, Emre N, Nakamura CM, Allen C, Donohue MK, Buckman JF. 1999. Time-dependent changes in striatal glutamate synapses following a 6-hydroxydopamine lesion. Neurosci 88:1-16.

Meyer DA, Richer E, Benkovic SA, Hayashi K, Kansy JW, Hale CF, Moy LY, Kim Y, O'Callaghan JP, Tsai LH, Greengard P, Nairn AC, Cowan CW, Miller DB, Antich P, Bibb JA. 2008. Striatal dysregulation of Cdk5 alters locomotor responses to cocaine, motor learning, and dendritic morphology. Proc Natl Acad Sci USA 105:18561-6.

Minamimoto T, Hori Y, Kimura M. 2009. Roles of the thalamic CM-PF complex-Basal ganglia circuit in externally driven rebias of action. Brain Res Bull 78:75-9.

Minamimoto T, Kimura M. 2002. Participation of the thalamic CM-Pf complex in attentional orienting. J Neurophysiol 87:3090-101.

Miura E, Iijima T, Yuzaki M, Watanabe M. 2006. Distinct expression of Cbln family mRNAs in developing and adult mouse brains. Eur J Neurosci. 24:750-60.

Miura E, Matsuda K, Morgan JI, Yuzaki M, Watanabe M. 2009. Cbln1 accumulates and colocalizes with Cbln3 and GluRdelta2 at parallel fiber-Purkinje cell synapses in the mouse cerebellum. Eur J Neurosci 29:693-706.

Moore RY, Bloom FE. 1979. Central catecholamine neuron systems: anatomy and physiology of the norepinephrine and epinephrine systems. Annu Rev Neurosci 2:113-68.

Mugnaini E, Morgan JI. 1987. The neuropeptide cerebellin is a marker for two similar neuronal circuits in rat brain. Proc Natl Acad Sci U S A 84:8692-6.

Mullen RJ, Buck CR, Smith AM. 1992. NeuN, a neuronal specific nuclear protein in vertebrates. Development 116:201-11.

Muly EC, Maddox M, Smith Y. 2003. Distribution of mGluR1alpha and mGluR5

immunolabeling in primate prefrontal cortex. J Comp Neurol 467:521-35.

Murray KD, Choudary PV, Jones EG. 2007. Nucleus- and cell-specific gene expression in monkey thalamus. Proc Natl Acad Sci USA 104:1989-94.

Neely MD, Schmidt DE, Deutch AY. 2007. Cortical regulation of dopamine depletion-induced dendritic spine loss in striatal medium spiny neurons. Neuroscience 149:457-64.

Ni ZG, Gao DM, Benabid AL, Benazzouz A. 2000. Unilateral lesion of the nigrostriatal pathway induces a transient decrease of firing rate with no change in the firing pattern of neurons of the parafascicular nucleus in the rat. Neurosci 101:993-9.

Olson L, Seiger A, Fuxe K. 1972. Heterogeneity of striatal and limbic dopamine innervation: highly fluorescent islands in developing and adult rats. Brain Res 44:283-8.

Pakan JM, Graham DJ, Iwaniuk AN, Wylie DR. 2008. Differential projections from the vestibular nuclei to the flocculus and uvula-nodulus in pigeons (Columba livia). J Comp Neurol 508: 402-17.

Pang Z, Zuo J, Morgan JI. 2000. Cbln3, a novel member of the precerebellin family that binds specifically to Cbln1. J Neurosci 20:6333-9.

Parent M, Parent A. 2005. Single-axon tracing and three-dimensional reconstruction of centre median-parafascicular thalamic neurons in primates. J Comp Neurol 481:127-44.

Parr-Brownlie LC, Poloskey SL, Bergstrom DA, Walters JR. 2009. Parafascicular thalamic nucleus activity in a rat model of Parkinson's disease. Exp Neurol 217:269-81.

Penny GR, Wilson CJ, Kitai ST. 1988. Relationship of the axonal and dendritic geometry of spiny projection neurons to the compartmental organization of the neostriatum. J Comp Neurol 269:275-89.

Peppe A, Gasbarra A, Stefani A, Chiavalon C, Pierantozzi M, Fermi E, Stanzione P, Caltagirone C, Mazzone P. 2008. Deep brain stimulation of CM/PF of thalamus could be the new elective target for tremor in advanced Parkinson's Disease? Parkinsonism Relat Disord 14:501-504.

Peters A, Kaiserman-Abramof IR. 1970. The small pyramidal neuron of the rat cerebral cortex. The perikaryon, dendrites and spines. Am J Anat 127:321-55.

Plenz D, Kitai ST. 1998. Up and down states in striatal medium spiny neurons simultaneously recorded with spontaneous activity in fast-spiking interneurons

studied in cortex-striatum-substantia nigra organotypic cultures. J Neurosci 18:266–283.

Powell TP, Cowan WM. 1954. The connexions of the midline and intralaminar nuclei of the thalamus of the rat. J Anat 88:307-19.

Preston RJ, Bishop GA, Kitai ST. 1980. Medium spiny neuron projection from the rat striatum: an intracellular horseradish peroxidase study. Brain Res. 183:253-63.

Raju DV, Ahern TH, Shah DJ, Wright TM, Standaert DG, Hall RA, Smith Y. 2008. Differential synaptic plasticity of the corticostriatal and thalamostriatal systems in an MPTP-treated monkey model of parkinsonism. Eur J Neurosci 27:1647-58.

Raju DV, Shah DJ, Wright TM, Hall RA, Smith Y. 2006. Differential synaptology of vGluT2-containing thalamostriatal afferents between the patch and matrix compartments in rats. J Comp Neurol 499:231-43.

Reynolds JN, Wickens JR. 2004. The corticostriatal input to giant aspiny interneurons in the rat: a candidate pathway for synchronising the response to reward-related cues. Brain Res 1011:115-28.

Richards DA, Mateos JM, Hugel S, de Paola V, Caroni P, Gähwiler BH, McKinney RA. 2005. Glutamate induces the rapid formation of spine head protrusions in hippocampal slice cultures. Proc Natl Acad Sci USA 102:6166-71.

Rieck RW, Ansari MS, Whetsell, Jr. WO, Deutch AY, Kessler RM. 2004. Distribution of dopamine D2-like receptors in the human thalamus: autoradiographic and PET studies. Neuropsychopharmacology 29:362-72.

Rinne UK. 1981. Treatment of Parkinson's disease: problems with a progressing disease. J Neural Transm 51:161-74.

Rivera A, Alberti I, Martin AB, Narvaez JA, de la Calle A, Moratalla R. 2002. Molecular phenotype of rat striatal neurons expressing the dopamine D5 receptor subtype. 2002. Eur J Neurosci 16:2049-2058.

Rommelfanger KS, Weinshenker D. 2007. Norepinephrine: The redheaded stepchild of Parkinson's disease. Biochem Pharmacol 74:177-90.

Rub U, Del Tredici K, Schultz C, Ghebremedhin E, de Vos RA, Jansen Steur E, Braak H. 2002. Parkinson's disease: the thalamic components of the limbic loop are severely impaired by alpha-synuclein immunopositive inclusion body pathology. Neurobiol Aging 23:245-54.

Rudkin TM, Sadikot AF. 1999. Thalamic input to parvalbumin-immunoreactive GABAergic interneurons: organization in normal striatum and effect of neonatal

decortication. Neurosci 88:1165-75.

Sadikot AF, Parent A, Smith Y, Bolam JP. 1992. Efferent connections of the centromedian and parafascicular thalamic nuclei in the squirrel monkey: a light and electron microscopic study of the thalamostriatal projection in relation to striatal heterogeneity. J Comp Neurol 320:228-42.

Saito M, Iwawaki T, Taya C, Yonekawa H, Noda M, Inui Y, Mekada E, Kimata Y, Tsuru A, Kohno K. 2001. Diphtheria toxin receptor-mediated conditional and targeted cell ablation in transgenic mice. Nat Biotechnol 19:746-50.

Sánchez-González MA, García-Cabezas MA, Rico B, Cavada C. 2005. The primate thalamus is a key target for brain dopamine. J Neurosci 25:6076-83.

Sarikcioglu L, Altun U, Suzen B, Oguz N. 2008. The evolution of the terminology of the basal ganglia, or are they nuclei? J Hist Neurosci 17:226-9.

Schapira AH, Emre M, Jenner P, Poewe W. 2009. Levodopa in the treatment of Parkinson's disease. Eur J Neurol 16: 982-9.

Scheinin M, Lomasney JW, Hayden-Hixson DM, Schambra UB, Caron MG, Lefkowitz RJ, Fremeau RT Jr. 1994. Distribution of alpha 2-adrenergic receptor subtype gene expression in rat brain. Brain Res Mol Brain Res 21:133-49.

Schmued LC, Albertson C, Slikker W Jr. 1997. Fluoro-Jade: a novel fluorochrome for the sensitive and reliable histochemical localization of neuronal degeneration. Brain Res 751:37-46.

Schmued LC, Stowers CC, Scallet AC, Xu L. 2005. Fluoro-Jade C results in ultra high resolution and contrast labeling of degenerating neurons. Brain Res 1035:24-31.

Schneider JS, Rothblat DS. 1996. Alterations in intralaminar and motor thalamic physiology following nigrostriatal dopamine depletion. Brain Res 742:25-33.

Sedaghat K, Finkelstein DI, Gundlach AL. 2009. Effect of unilateral lesion of the nigrostriatal dopamine pathway on survival and neurochemistry of parafascicular nucleus neurons in the rat--evaluation of time-course and LGR8 expression. Brain Res 1271:83-94.

Shi SH, Hayashi Y, Petralia RS, Zaman SH, Wenthold RJ, Svoboda K, Malinow R. 1999. Rapid spine delivery and redistribution of AMPA receptors after synaptic NMDA receptor activation. Science 284:1811-6.

Sidibé M, Paré JF, Smith Y. 2002. Nigral and pallidal inputs to functionally segregated thalamostriatal neurons in the centromedian/parafascicular intralaminar nuclear complex in monkey. J Comp Neurol 447:286-99.

Sidibé M, Smith Y. 1996. Differential synaptic innervation of striatofugal neurones projecting to the internal or external segments of the globus pallidus by thalamic afferents in the squirrel monkey. J Comp Neurol 365:445-65.

Sidibé M, Smith Y. 1999. Thalamic inputs to striatal interneurons in monkeys: synaptic organization and co-localization of calcium binding proteins. Neurosci 89:1189-208.

Slemmon JR, Blacher R, Danho W, Hempstead JL, Morgan JI. 1984. Isolation and sequencing of two cerebellum-specific peptides. Proc Natl Acad Sci U S A 81:6866-6870.

Smeal RM, Keefe KA, Wilcox KS. 2008. Differences in excitatory transmission between thalamic and cortical afferents to single spiny efferent neurons of rat dorsal striatum. Eur J Neurosci 28:2041-52.

Smith Y, Bennett BD, Bolam JP, Parent A, Sadikot AF. 1994. Synaptic relationships between dopaminergic afferents and cortical or thalamic input in the sensorimotor territory of the striatum in monkey. J Comp Neurol 344(1):1-19.

Smith Y, Raju D, Nanda B, Pare JF, Galvan A, Wichmann T. 2009. The thalamostriatal systems: anatomical and functional organization in normal and parkinsonian states. Brain Res Bull 78:60-8.

Smith Y, Raju DV, Pare JF, Sidibé M. 2004. The thalamostriatal system: a highly specific network of the basal ganglia circuitry. Trends Neurosci 27:520-7.

Snyder-Keller A, Tseng KY, Lyng GD, Graber DJ, O'Donnell P. 2008. Afferent influences on striatal development in organotypic cocultures. Synapse 62:487–500.

Somogyi P, Smith AD. 1979. Projection of neostriatal spiny neurons to the substantia nigra. Application of a combined Golgi-staining and horseradish peroxidase transport procedure at both light and electron microscopic levels. Brain Res 178:3-15.

Stefani A, Peppe A, Pierantozzi M, Galati S, Moschella V, Stanzione P, Mazzone P. 2009. Multi-target strategy for Parkinsonian patients: the role of deep brain stimulation in the centromedian-parafascicularis complex. Brain Res Bull 78:113-118.

Stephens B, Mueller AJ, Shering AF, Hood SH, Taggart P, Arbuthnott GW, Bell JE, Kilford L, Kingsbury AE, Daniel SE, Ingham CA. 2005. Evidence of a breakdown of corticostriatal connections in Parkinson's disease. Neuroscience 132:741-754.

Stevens B, Allen NJ, Vazquez LE, Howell GR, Christopherson KS, Nouri N, Micheva KD, Mehalow AK, Huberman AD, Stafford B, Sher A, Litke AM, Lambris JD, Smith SJ, John SW, Barres BA. 2007. The classical complement cascade mediates CNS synapse elimination. Cell 131:1164-78.

Stocker SD, Simmons JR, Stornetta RL, Toney GM, Guyenet PG. 2006. Water deprivation activates a glutamatergic projection from the hypothalamic paraventricular nucleus to the rostral ventrolateral medulla. J Comp Neurol 494:673-685.

Surmeier DJ, Ding J, Day M, Wang Z, Shen W. 2007. D1 and D2 dopamine-receptor modulation of striatal glutamatergic signaling in striatal medium spiny neurons. Trends Neurosci 30:228-35.

Surmeier DJ, Song WJ, Yan Z. 1996. Coordinated expression of dopamine receptors in neostriatal medium spiny neurons. J Neurosci 16:6579-6591.

Tepper JM, Abercrombie ED, Bolam JP. 2007. Basal ganglia macrocircuits. Prog Brain Res 160:3-7.

Tepper JM, Bolam JP. 2004. Functional diversity and specificity of neostriatal interneurons. Curr Opin Neurobiol 14:685-92.

Testa CM, Friberg IK, Weiss SW, Standaert DG. 1998. Immunohistochemical localization of metabotropic glutamate receptors mGluR1a and mGluR2/3 in the rat basal ganglia. J Comp Neurol 390:5-19.

Tsumori T, Yokota S, Ono K, Yasui Y. 2002. Synaptic organization of GABAergic projections from the substantia nigra pars reticulata and the reticular thalamic nucleus to the parafascicular thalamic nucleus in the rat. Brain Res 957:231-41.

Tunstall MJ, Oorschot DE, Kean A, Wickens JR. 2002. Inhibitory interactions between spiny projection neurons in the rat striatum. J Neurophysiol 88:1263-9.

Urade Y, Oberdick J, Molinar-Rode R, Morgan JI. 1991. Precerebellin is a cerebellum-specific protein with similarity to the globular domain of complement C1q B chain. Proc Natl Acad Sci USA 88:1069-73.

Villalba RM, Lee H, Smith Y. 2009. Dopaminergic denervation and spine loss in the striatum of MPTP-treated monkeys. Exp Neurol 215:220-7.

Voorn P, Vanderschuren LJ, Groenewegen HJ, Robbins TW, Pennartz CM. 2004. Putting a spin on the dorsal-ventral divide of the striatum. Trends Neurosci 27:468-74.

Wang Z, Kai L, Day M, Ronesi J, Yin HH, Ding J, Tkatch T, Lovinger DM, Surmeier DJ. 2006. Dopaminergic control of corticostriatal long-term synaptic depression in medium spiny neurons is mediated by cholinergic interneurons. Neuron 50:443-52.

Wei P, Smeyne RJ, Bao D, Parris J, Morgan JI. 2007. Mapping of Cbln1-like immunoreactivity in adult and developing mouse brain and its localization to the endolysosomal compartment of neurons. Eur J Neurosci 26(10):2962-78.

Wei P, Rong Y, Li L, Bao D, Morgan JI. 2009. Characterization of trans-neuronal trafficking of Cbln1. Mol Cell Neurosci 41:258-73.

Wilson CJ. 1993. The generation of natural firing patterns in neostriatal neurons. Prog Brain Res 99:277-97.

Wilson CJ, Chang HT, Kitai ST. 1990. Firing patterns and synaptic potentials of identified giant aspiny interneurons in the rat neostriatum. J Neurosci 10: 508-19.

Wilson CJ, Groves PM. 1980. Fine structure and synaptic connections of the common spiny neuron of the rat neostriatum: a study employing intracellular inject of horseradish peroxidase. J Comp Neurol 194:599-615.

Wolfe BJ, Trejo J. 2007. Clathrin-dependent mechanisms of G protein-coupled receptor endocytosis. Traffic 8:462-70.

Wu Y, Richard S, Parent A. 2000. The organization of the striatal output system: a single-cell juxtacellular labeling study in the rat. Neurosci Res 38:49-62.

Xu ZQ, Shi TJ, T Hokfelt T. 1998. Galanin/GMAP- and NPY-like immunoreactivities in locus coeruleus and noradrenergic nerve terminals in the hippocampal formation and cortex with notes on the galanin-R1 and -R2 receptors. J Comp Neurol 392:227-251.

Zackheim J, Abercrombie ED. 2005. Thalamic regulation of striatal acetylcholine efflux is both direct and indirect and qualitatively altered in the dopamine-depleted striatum. Neuroscience 131:423-36.

Zaja-Milatovic S, Milatovic D, Schantz AM, Zhang J, Montine KS, Samii A, Deutch AY, Montine TJ. 2005. Dendritic degeneration in neostriatal medium spiny neurons in Parkinson disease. Neurology 64:545-547.